TECHNICAL TRANSACTIONS

CZASOPISMO TECHNICZNE

CHEMISTRY

CHEMIA

ISSUE
1-Ch (1)

ZESZYT
1-Ch (1)

YEAR
2013 (110)

ROK
2013 (110)

WYDAWNICTWO
POLITECHNIKI
KRAKOWSKIEJ

TECHNICAL TRANSACTIONS | CZASOPISMO TECHNICZNE

CHEMISTRY | CHEMIA

ISSUE 1-Ch (1) | ZESZYT 1-Ch (1)
YEAR 2013 (110) | ROK 2013 (110)

Chairman of the Cracow University of Technology Press Editorial Board	**Jan Kazior**	Przewodniczący Kolegium Redakcyjnego Wydawnictwa Politechniki Krakowskiej
Chairman of the Editorial Board	**Józef Gawlik**	Przewodniczący Kolegium Redakcyjnego Wydawnictw Naukowych
Scientific Council	**Jan Błachut** **Tadeusz Burczyński** **Leszek Demkowicz** **Joseph El Hayek** **Zbigniew Florjańczyk** **Józef Gawlik** **Marian Giżejowski** **Sławomir Gzell** **Allan N. Hayhurst** **Maria Kusnierova** **Krzysztof Magnucki** **Herbert Mang** **Arthur E. McGarity** **Antonio Monestiroli** **Günter Wozny** **Roman Zarzycki**	Rada Naukowa
Chemistry	**Krzysztof Pielichowski**	Redaktor Serii Chemia
Section Editor	**Dorota Sapek**	Sekretarz Sekcji
Editorial Compilation	**Aleksandra Urzędowska**	Opracowanie redakcyjne
Typesetting	**Anna Pawlik**	Skład i łamanie
Cover Design	**Michał Graffstein**	Projekt okładki

Pierwotną wersją każdego Czasopisma Technicznego jest wersja on-line
www.czasopismotechniczne.pl www.technicaltransactions.com

© Politechnika Krakowska
Kraków 2013

Polskie Towarzystwo Reologii Technicznej
Instytut Inżynierii Chemicznej i Procesowej Politechniki Krakowskiej
EKMA

RHEOLOGY

REOLOGIA

zeszyt pod redakcją naukową
prof. Barbary Tal-Figiel

book edited by
prof. Barbara Tal-Figiel

Kraków 2013

TECHNICAL TRANSACTIONS | CZASOPISMO TECHNICZNE
CHEMISTRY | CHEMIA
1-Ch/2013

RENATA CICHA-SZOT, SŁAWOMIR FALKOWICZ*

PROCEDURE OF PREPARATION BRITTLE GEL SAMPLE FOR RHEOLOGICAL MEASUREMENT IN PLATE-PLATE SYSTEM

PPROCEDURA PRZYGOTOWANIA KRUCHYCH PRÓBEK ŻELI DO POMIARÓW OSCYLACYJNYCH ZA POMOCĄ UKŁADU PŁYTKA-PŁYTKA

Abstract

New way of preparation brittle gel samples for determining gel strength during oscillatory measurements in plate-plate system was presented in this paper. Presented procedure of sample preparation greatly decrease a cost of selection proper additive for improving gel strength and enable to obtain more reliable evaluation of gel's mechanical properties. Moreover, by external preparation of corrosive samples (e.g. silicate gelling systems) gel's aging time can be prolonged without the impact on sensor's lifetime

Keywords: *determining of the gel strength*, *silicate gels*, *sample preparation*, *brittle gels*

Streszczenie

W artykule przedstawiono nowy sposób przygotowania próbek kruchych żeli do pomiarów oscylacyjnych w układzie płytka-płytka. Przedstawiona procedura przygotowania próbki w znacznym stopniu ogranicza koszty doboru modyfikatorów żeli oraz pozwala na bardziej precyzyjne określenie właściwości mechanicznych żelu. Ponadto przygotowanie próbki (np. silnie alkalicznych lub kwasowych cieczy na bazie krzemianów) poza elementem pomiarowym reometru pozwala na wydłużenie czasu starzenia żelu bez wpływu na żywotność elementu pomiarowego.

Słowa kluczowe: *określenie wytrzymałości żelu*, *żele krzemianowe*, *przygotowanie próbki*, *żele kruche*

* Mgr inż. Renata Cicha-Szot, dr inż. Sławomir Falkowicz, Instytut Nafty i Gazu w Krakowie, Zakład Inżynierii Naftowej.

1. Introduction

Determining the consistency of gelling system is of great practical interest [1]. Among the techniques, which characterize polymers and polymer like solutions, rheology is considered the most complete [2, 3]. Presently three methods are accepted for rheological study of crosslinking polymers. In the first method the polymer in a liquid state is exposed to shear flow. The measured viscosity increases with increasing extent of reactions until the material break or until stress reaches the limits of instrument [4, 5–7]. In the second method sample is subjected to small amplitude oscillatory shear mode. The measurement has to be done within the linear viscoelastic region (LVR). Conducting rheological tests in this manner avoid to overstrain the sample which may cause destruction of elastic structure. The measured components of the complex modulus (storage moduli and loss moduli) during the crosslinking process show viscoelastic behavior of the gelling system [2, 5, 6]. The third method, based on small vibrations of fork rheometer, is used for better understanding and complete characterization of sol-gel transition. This method provide additional information on complexity of coagulation and gelation process, which is not monotone and single direction. In some polymer systems after initiation of gelation, a transient process starts and the viscosity of system is fluctuating between wide limits (Fig. 1) [8].

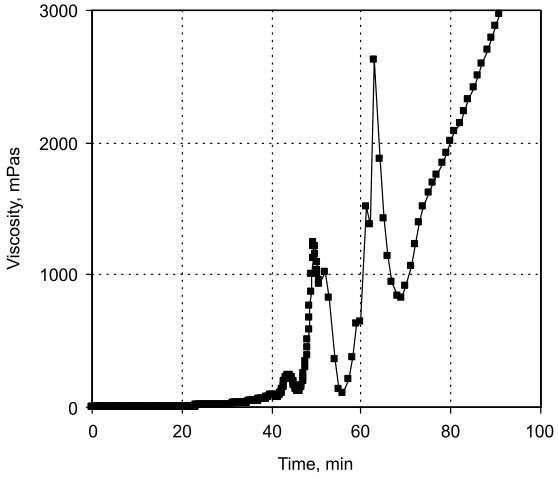

Fig. 1. Transient, induction period of gelation in modified silicate systems [8]

Rys. 1. Krótkotrwałe zmiany lepkości podczas żelowania modyfikowanego krzemianu sodu [8]

Viscoelastic behavior of the gel sample is responsible of the gel consistency at different temperature, time and pH [2]. That is why for complete characterization of the gelling system second method is the most recommended. The most used sensors for dynamic evaluation of the gelling system is plate-plate geometry. Using that sensor the gelling system has been characterized by imposing defined oscillatory strain at a fixed stress rate. Therefore in phase (elastic component – storage modulus G') and out phase (viscous component – loss modulus G'') response of the gel is measured. This two moduli are the components of complex modulus

G^* which represents the total resistance of the substance against the maximum applied strain what indicate gel strength [2, 9].

2. Silicate gelling system

Silicate gelling systems, which are the current state-of-the-art method for porous rock permeability modification in petroleum industry, display a pH-dependent transition between a soluble form and gel form. A gel network is formed after exceed critical pH, and beyond gel point it firmness continues to increase with increasing cross linking density. One of the main problem during determination viscoelastic properties of silicate gelling system is brief or very slow sol-gel transition time and specific properties of silicate gel such as brittleness, shrinking/syneresis [10]. Moreover, modification or destruction of the building tridimensional structures in gel network, that might occur at shear rate and oscillation has to be taken into consideration. Above mentioned disadvantages impede measurement accuracy and make impossible to determine gel strength of such a challenging samples.

In regard to cost effectiveness and measurement accuracy, existing procedures are not proper for determining gel strength of the biocatalysed gelling systems or to match the additives to improve its properties.

3. New procedure of sample preparation

To avoid all mentioned above disadvantages and decrease a cost of sample preparation in Polish Oil and Gas Institute (POGI) new stand and procedure of preparation modified silicate based gel samples was invented. Invention was registered by Polish Patent Office No 119464.

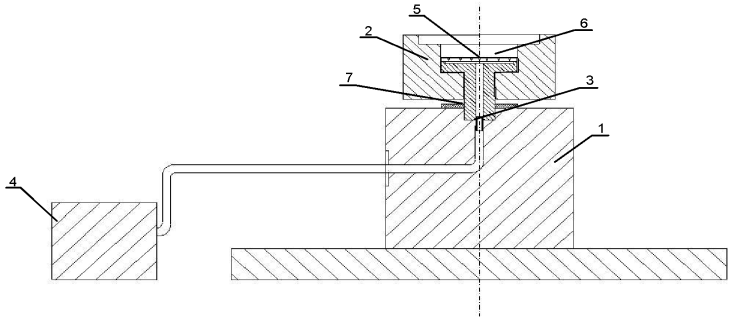

Fig. 1. Lab stand to prepare samples to evaluation viscoelastic properties of brittle gels: 1 – support stand, 2 – chamber, 3 – butt-coupling, 4 – vacuum pump, 5 – perforation, 6 – membrane, 7 – piston

Rys. 1. Przyrząd do wykonywania próbek do pomiaru wiskoelastycznych właściwości kruchych żeli: 1 – statyw, 2 – naczynie, 3 – króciec, 4 – pompa próżniowa, 5 – perforacja, 6 – membrana, 7 – tłok

To perform oscillatory measurement using plate-plate sensor there is a need to prepare cylindrical sample in dimension of plate sensor (e.g. 50mm) and precisely place on the bottom plate of rheometer. Invented lab stand to prepare such a sample consist of cylindrical chamber (2), support stand (1) and vacuum pump (4) (Fig. 1.).

Plastic membrane at the bottom of the sample chamber is placed (6) to separate the gel and the chamber walls and prevent gel adhesion to the bottom of the chamber. Membrane is kept hermetically at the bottom of the chamber by supply through perforation (5) negative pressure which is produced by the vacuum pump [11].

Using graduated pipette relevant amount of the previously prepared silicate sol is placed in the chamber. After the sol-gel transition negative pressure is disconnected and gel can be placed at the sensor's bottom plate. Sample is placed precisely at the center of the bottom plate by the piston and the measurement can be carried out

4. Conclusions

To evaluate with required accuracy rheological properties of brittle silicate gels new stand and procedure of sample preparing was invented. Using special chamber sample can be prepared at required atmosphere (inert, CO_2, oxygen) what enable of gel networking via homogeneous and heterogeneous catalysis as well as biocatalysis.

This technique allows to test substantial number of silicate gel modifiers and strongly decrease number of time consuming tests on samples of porous rocks. Moreover, by external preparation of corrosive samples (e.g. silicate gelling systems) we can prolong the gels ageing time without the impact on sensor's lifetime.

References

[1] Michon C., Cuvelier G., Launay B., *ConcentrationDependence of the Critical Viscoleastic Properties Of Gelatin at Gel Point*, Rheological Acta, 32, 94, 1993.

[2] Kakadjian S., Rauseo O., Mejias F., *Dynamic Rheology as a Method for Quantify Gel Strength of Water Shutoff Systems*, SPE 50751, 1999.

[3] Winter H., Chambon F., *Analisys of linear viscoelasticity of a crosslinking polymer at the Gel Point*, Journal of Rheology, 30 (2), 367, 1986.

[4] Castro J., Macosko C., Perry S., *Urethane Polymerization with Phase Separation*, Polym. Com., 25, 82, 1984.

[5] Farris R., Lee C., *Rheological Behaviour of a Commercial TGDDM-DDS Based Epoxy Matrix During the Isothermal Curve*, Polymers Engineering and Science, 23, 586, 1983.

[6] Chambon G., Winter H., *Stopping Of Crosslinking Reaction in a PDMS Polymer at Gel Point*, Polymers Bull., 13, 499, 1985.

[7] Lukah G., Sun S.T., *Gelled Aqueous composition*, Patent USA 4604217, 1986.

[8] Lakatos I., Medic B., Jovicic D., Basic I., Lakatos-Szabo J., *Prevention of Vertical Gas Flow in a Collapsed Well Using Silicate/Polymer/Urea Method*, SPE 121045, 2009.

[9] Schramm G., *A Practical Approach to Rheology and Rheometry*, HAAKE, 1997.

[10] Falkowicz S., Cicha-Szot R., Dubiel S., Bailey S., *Biocatalized silicate gels in oil and geothermal industry*, Gospodarka Surowcami Mineralnymi, Tom 25, Zeszyt 4, 2009.

[11] Falkowicz S., Cicha-Szot R., *Przyrząd do przygotowania próbek żeli*, WU. No 119464, 15, 11, 2010.

TECHNICAL TRANSACTIONS | CZASOPISMO TECHNICZNE
CHEMISTRY | CHEMIA
1-Ch/2013

MARCEL KRZAN*

RHEOLOGY OF THE WET SURFACTANT FOAMS AND BIOFOMAS – A REVIEW

WŁAŚCIWOŚCI REOLOGICZNE PIAN CIEKŁYCH WYTWARZANYCH NA BAZIE SYNTETYCZNYCH SURFAKTANTÓW ORAZ BIOSURFAKTANTÓW – PRZEGLĄD

Abstract

The rheology of foams is a difficult subject due to the complexity of their structure and the nature of their components. It's influenced by multiple factors including: liquid bulk properties, gas properties, air phase volume, liquid volume fraction, solution viscosity, interfacial thin film visco-elasticity, bubble size distribution, and bubble shape. A nature of the adsorbed surfactants or biosurfactants and state of adsorption layer also modified the properties of the thin liquid film. The physical measurements of foam rheological properties are also complicated by its inherently unstable nature. Therefore, this review is focused on rheological studies and comparisons between various surfactant based foams and biofoams having well-characterized and different properties.

Keywords: *rheology*, *foams*, *surfactants*, *biosurfactants*, *proteins*, *viscoelasticity*, *yielding*

Streszczenie

Reologia układów pianowych jest skomplikowanym zagadnieniem badawczym ze względu na ich złożoną strukturę. Wpływają na nią wielorakie czynniki, takie jak: właściwości fazy ciekłej i gazowej, objętości fazy gazowej i ciekłej, lepkość roztworu, lepkoelastyczność cienkiego filmu pianowego, rozmiar i rozkład pęcherzyków gazowych. Właściwości powierzchniowo-aktywne surfaktanta lub biosurfaktanta i ich stopień adsorpcji również modyfikują parametry otrzymywanego cienkiego filmu pianowego. Fizyczny pomiar właściwości reologicznych pian jest również rzeczą skomplikowaną ze względu na ich niestabilną naturę. Z tego powodu tematem tego artykułu jest przegląd i porównanie różnych reologicznych badań dotyczących pian surfaktantowych oraz biosurfaktanowych o różnych, dobrze scharakteryzowanych właściwościach

Słowa kluczowe: *reologia*, *piany*, *surfaktanty*, *biosurfaktanty*, *proteiny*, *lepkoelastyczność*, *plastyczność*

* PhD. Marcel Krzan, J. Haber Institute of Catalysis and Surface Chemistry, Polish Academy of Science.

1. Introduction

The applications of foams are based on the large specific surface, the small specific weight and mechanical properties, depending on the applied stress. Foams exhibit linear viscoelastic behaviour when they are subjected to small shear stresses while they flow like viscous liquids when the applied shear stress is large enough to trigger bubble rearrangements [1–7]. The origin of foam elasticity comes from the deformation of bubbles from a perfectly spherical shape, in order to increase their packing density. The energy stored during the deformation increasing the surface energy and is also responsible for the viscoelastic properties of foams, their specific geometry of films, Plateau borders and vertices in the limit of dry foams.

All of these features are important in applications where foams are used to transport particles [3], i.e. in various kinds of froth flotation, in oil industry where foams are used as drilling fluids or in technology of hydraulic fracturing technology of shale gas extraction. In this context, as well as from a fundamental point of view, it is important to develop a constitutive rheological law, predicting the relation between macroscopic stress, strain and strain history. Moreover, the rheological study of the interface in foams can determine how the dispersed phase resists to deformation, or even coalescence.

The biofoams could be used in those applications in place on surfactants based foams [8–10]. Recently published papers clearly present that foams can also be stabilized by nano-particles, without surfactant or by proteins or other surface-active bioplymers. Proteins or polysaccharides received a special attention from scientific, technological and environmental points of view. Since proteins are known to form films with high interfacial elasticity and viscosity, via various forms of cross-linking that can occur between the adsorbed molecules, it might be expected that proteins would be the ideal candidates for preventing foam disproportionation thought the interfacial elastic mechanism.

In order to fully characterize the foam to allow the comparison with the theoretical models descriptions, the bubble diameter, liquid volume fraction and the solution surface tension have to be known [2, 4, 6, 7]. It is necessary to understand how the foam rheology (elasticity, viscosity and yielding) depends on the foam components (surfactants, liquid and gas) and on the parameters describing the surfactant adsorption on the thin liquid film layer. Changing the surfactants has an impact not only on the surface tension, but also modifies the properties of the lamellae thin liquid film via the variation of the degree of surfactant adsorption on the interface. The solution viscosity may also have influence on the shear rate dependence. It is still not clear how the viscoelastic properties depend on the chemical formulation (surfactants, mixtures with polymers, etc). Literature of subject report experimental results for very limited surfactant and a few proteins based systems. The importance of the nature of gas used for foaming should be also mention here. Gases soluble in water, like air or N_2 give less stable foams then less soluble gases, like C_2F_6 because the air or nitrogen diffusion through the lamellae film is faster.

2. Foam structure – drainage, coarsening and disproportionation

Foam is an extremely complex system with a cellular internal structure, in which the polydispersed bubbles are separated by thin, plane-parallel liquid films, stabilized by surfactant adsorption layers [1–4]. To produce foam the gas phase needs to be dispersed in liquid phase into bubbles. The structure and geometry of dry foam was first described by the 19th century scientist Joseph Plateau [1, 11]. It was experimentally shown that the lamellae thin films in dry foam always meet at edge (Plateau border) at angle of 120 degrees. The four borders of those lamellae films meet in a symmetrical tetrahedral vertex at angle 109.47 degrees.

Foam formation occurs always under dynamic conditions so the equilibrium adsorption coverage is rather not attained there. It can strongly affect the magnitude of the forces stabilizing the foam films. Therefore foams are inherently difficult to study systems because they are transient and the study is essentially restricted to the observations of dynamic system evolution. Owing to the size of the bubbles, which varies from fractions of a millimetre to several centimetres, foams are classified as coarse dispersion systems. In European Union foam is classified as a soft matter, while in United Stated is included for complex fluids. Production of foams involves the generation of a liquid thin film surrounding the gas bubble and a packing of gas bubbles into an overall structure. The generated foam may persist for a reasonable length of time without collapsing into separate constituent phases. However, from a thermodynamic viewpoint, foams are unstable dispersions by their very nature and should break into individual component phases in the direction of decreasing total surface free energy. The effects of the disjoining pressure, of surface elasticity and viscoelasticity, structural forces and possible effects of steric repulsions are the main parameters to be responsible for the foamability and foam stability. Foams irreversible evolve with time (ageing process).

The main processes taking places in wet foams are a free drainage from lamellae and Plateau borders, coalescence and disproportionation [1–4]. By drainage, we are referring to the irreversible flow of liquid through the foam, induced by the influence of gravitational acceleration, viscous force and pressure exceeded between the adjacent bubbles. As a result the liquid accumulate at the bottom part of foam and a global liquid content decrease within the foam. In the upper part of the foam the "dry foam" is formed with the polyhedral bubbles with thin edges. While the bubbles in the bottom part of the foams are still spherical.

When the liquid films between the bubbles are very thin, they may eventually break. The merging of two bubbles as a result of the rupture of the film between them is known as coalescence. Larger bubbles appear in the foam and the number of bubbles decreases. If this continues, the whole foam collapses.

Disproportionation (known also as a coarsening or an Oswald ripening) is described as inter-bubble gas diffusion. As a result of gas diffusion larger bubbles grow at the expense of smaller bubbles. Smaller bubbles shrink and may finally disappear. The driving force is the Laplace pressure, which for a spherical bubble is inversely proportional to its radius: $\Delta P = 2\sigma_T/r$, where σ_T is the interfacial tension and r is the bubble radius. As a result of foam ageing, the average bubble diameter was found to grow with the time elapsed since foam production following a parabolic law. The characteristic coarsening time was described [12]

as a function of the bubble deformation, gas diffusivity and solubility constants, function of the liquid content, thin film thickness, bubble initial diameter and the solution surface tension.

It is clear that all destabilization (ageing) mechanisms are occurring simultaneously (see Fig. 1). Therefore the various methods, such as a conductivity or fluid drainage rate, are used for qualitative description of each of those processes. All these coupled ageing processes affected the elasticity properties as they respectively changed the distribution of the liquid and gas phase (liquid and gas volume fraction) and bubble size. The increases in the gas fraction due to drainage tend to raise the yield stress, whereas increases in the bubble size (coarsening) leads to a reduction in the yield stress [2]. Therefore they alter seriously the macroscopic (textural and rheological) properties of foams.

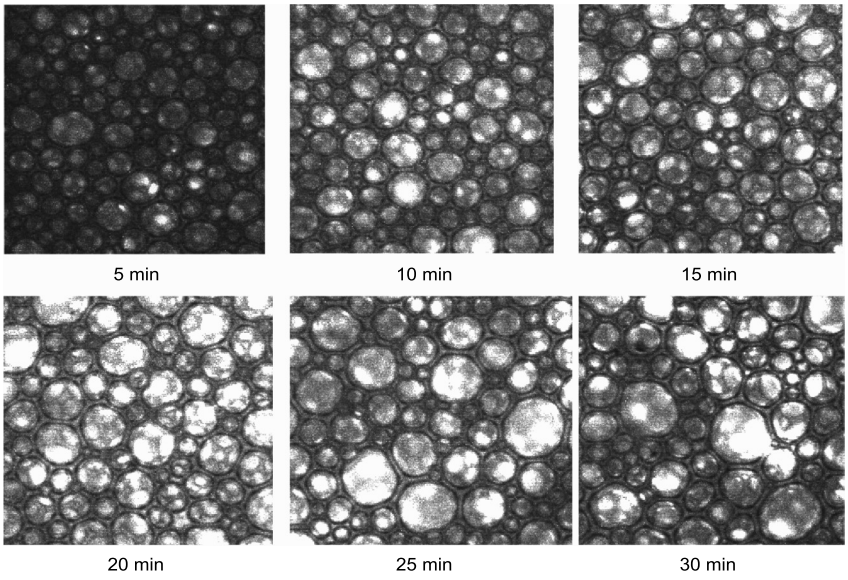

Fig. 1. Process of ageing in Nivea commercial shaving cream

Rys. 1. Proces stężenia się piany otrzymanej z komercyjnej pianki do golenia Nivea

3. Surfactant and biopolymer foams – the various ways of thin film layer stabilizations

It is generally accepted that the presence of surfactant is necessary for foam formation and stability. There is a minimum concentration of surface-active molecules necessary for foam generation. In the case of detergents, this concentration is associated with a surface coverage of the bubbles and corresponds to the inflection point on the adsorption isotherm curve [2–4].

However, there were recently published papers showing that foams can also be stabilized by nano-particles, without surfactant or by proteins or other surface-active biopolymers.

Proteins or polysaccharides received a special attention from scientific, technological and environmental points of view. Proteins are complex molecules with unique properties, which determine the life in our planet. From their easy biodegradation and natural recycling, proteins raise a motivation for using them in various industrial applications.

The relatively non-specific foaming of denatured proteins is commonplace and widely exploited in food technology [8, 13–15], the simplest examples are whipped cream and foam with whites eggs. Proteins are the most ubiquitous surface active polymers in nature. The spontaneous adsorption of proteins from solution to the air/aqueous interface is a central importance to their foaming performance [16–18]. Surface active biological macromolecules like proteins and polysaccharides can adsorb at the almost every interface and they form highly stable films contributing to stability of membranes, foams, emulsions and dispersions in general. Since proteins are known to form films with high interfacial elasticity and viscosity, via various forms of cross-linking that can occur between the adsorbed molecules, it might be expected that proteins would be the ideal candidates for preventing disproportionation via the interfacial elastic mechanism.

During foam formation proteins diffuse from the aqueous phase and adsorb at the air-water interface due to the compatibility of their hydrophobic groups with the hydrophobic character of the interfaces [13, 19]. During adsorption, protein molecules can unfold to a certain degree and reorient at the interface with polar groups exposed towards water phase and the non-polar groups towards the air phase. Protein adsorption is thermodynamically favourable due to the simultaneous dehydration of the hydrophobic portions of the protein. Hydrophobic patches of proteins surface initially drive this process, and surface hydrophobicity has been correlated with improved foaming properties. Once contacts are made with the interface, natural flexibility within the molecules can expose previously hidden hydrophobic part to the interface, potentially leading to interfacial denaturisation of the molecules. This in turn, leads to the decrease of the interfacial tension and to the formation of more or less stable interfacial protein films. The casein molecules adsorb at the gas/solution interfaces, and form elastic and rigid film with average thickness of the order of a few hundreds of nanometers. The protein molecules aggregated in a jellified matrix, making the film quite non-uniform in texture and thickness. The adsorption rate of proteins, as the most important factor for foam formation, depends on the protein concentration, the molecular weight and the structure of the proteins used. Foaming properties of proteins are influenced by a large number of parameters including thermal or chemical pre-processing conditions, method of foaming, whipping time and the physical and chemical properties of the proteins as well as the environmental factors like ionic strength or pH [20, 21]. The effect of pH on proteins is usually explained by the net charge of the molecules and the protein conformation. The final protein conformation results not only from internal interactions between the amino acids side chains, but also from their interactions with water molecules. It was shown that the Bovine Serum Albumin foam apparent poor foamability is counterbalanced by relatively large stability in 2D system of Hele-Shaw cell [22]. The foam was almost solidified. Even as a continuously thinning of the foam films was observed, the bubbles kept the nearly same shape and size on photos recorded immediately after stop of the flipping procedure and 5 minutes later (Fig. 2) [23]. The size and shape of the foam bubbles were stable as far as the foam exists. The foam collapsed only due to the film leaking. The effect was probably

caused by network of adsorbed and denaturised proteins in the foam film, which solidified the cell structure, not prevent the film drainage.

One must distinguish polysaccharides that are not surface active, which includes most natural ones, from chemically modified polysaccharides that are surface active. The polysaccharides foams exist in the literature of subject mostly as a solidified foam gel materials (produced as a gas dispersion from the hydrogel) [24, 25], a resin foams [25], a polymerised foams or a dry foams [26] (foams frozen or dried). Once dispersed in water polysaccharides they have the property to increase bulk viscosity and improve stability against coalescence. The most common polysaccharides used for confectionary products are guar gum, xanthan gum and k-carrageenan [27–29].

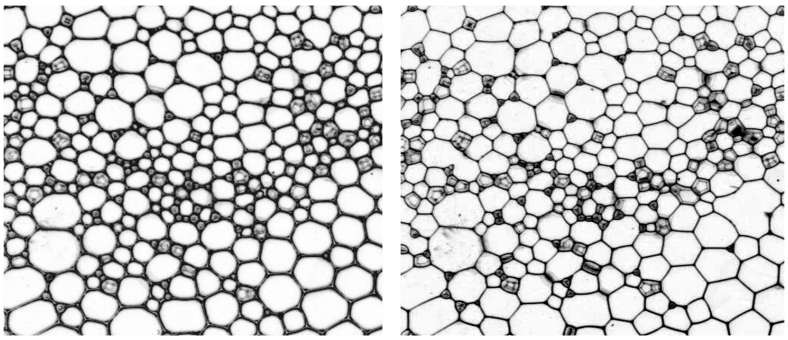

Fig. 2. Photos of Bovine Serum Albumine foams freely ageing foam in Hele-Shaw cell. Snapshots of a foam taken just after foam formation (left photo) and after long term drainage (5min – right photo) [23]

Rys. 2. Zdjęcia piany otrzymanej z roztworu Bovine Serum Albumine starzejącej się w celi Hele-Shaw. Klatki pokazują pianę od razu po wytworzeniu (lewe zdjęcie) oraz po długim czasie wyciekania (5min – prawe zdjęcie) [23]

Relatively little is known about what happens when both surface active biopolymers (proteins and polysaccharides) will be present together [29, 30]. Any lipids or other low molecular-weight surfactants present will probably adsorb to the polysaccharides nanoparticles and change their contact angle and adsorption characteristics. Proteins will adsorb to almost any type of surface, often with high affinity, and may therefore do the same. In addition, the interfacial coverage is likely to be dominated by the proteins or low molecular-weight surfactants, since the particles will adsorb more slowly due to their slower mass transport. Mixed protein - polysaccharide multilayer films may have improved properties in terms of colloidal stabilization, encapsulation and controlled release in food and pharmaceutical applications. The presence of a polysaccharide in the foaming solution can modify the interfacial and foaming properties of the protein and impart desired characteristics to a product. In particular, if there is a synergistic interaction between protein and polysaccharide, drainage and disproportionate may thus be further retarded. In addition, if the continuous phase of the protein stabilized foam could gel, interesting characteristics related to foam stability and texture properties should arise.

4. Foam generation

Foams properties varied with the method and equipment using for their preparation [2–4, 31–34]. Aqueous foams with controlled and reproducible properties are not easy to produce, especially in terms of bubble diameter, liquid volume fraction, and foam uniformity (meaning no initial gradients, holes, etc). Despite this till today exists a lack of general methodology for foam generation. Foam fraction are generated in various ways. The most familiar is simply to vigorously shake a closed container partially filled with surfactant solution. The other commonly used automatic foaming methods are: i) gas aeration in the foam column, where the gas is blowing by the porous membrane, ii) mechanical flipping, shaking or vibrating in various closed containers (i.e. in Hele-Shaw cell), iii) using various kind of mixing devices (homogenizers, turax, etc.) or iv) in special apparatus, via turbulent mixing of gas with a narrow jet of a surfactant solution inside a delivery tube. The cross-linking comparison of the methods validity is almost impossible. Let's short describe positive and negative points of those methods.

Foam in the column starts to form when the numbers of bubbles arriving to the solution surface exceed the number of rupturing bubbles [31]. The lifetime of the single bubble is determined by the composition of the solution (surface activity and concentration of the detergent) and by state of adsorption layers in the thin film in upper part of the bubble. Similar process of the gas dispersing into bubbles is hard to control because there are different interdependent interactions between the bubbles, which were formed under dynamic conditions and rising in chaotic stream under the buoyancy force. The bubbling method is slow, what leading the significant change of the liquid content along the foam height. The foam fraction is drier at top and wetter at bottom. Drainage may also cause the variations of the adsorption equilibrium coverages in the foam films. During similar dynamic measurements, the variation of the height of the foam and the solution level with the time were recorded. The foam power (foamability) is determined from the height of the foam just after the generation, while foam stability is described by measuring rate of foam volume decreasing (or/and solution recovery rate) with the time.

As it was already mentioned foam can be also created in some closed cells partially filled with the surfactant solutions, like Hele-Shaw cell, using special mechanisms such as flipping, shaking or vibrating [22, 32, 33]. Due to wetting on the cell walls, thin liquid films are created during each flip or shake cycle. Starting with a large bubble over a liquid pool, it is clearly shown that successive cycles lead to the formation of foam composed of many bubbles. This foam obeys statistical laws that are highly reproducible. Similar method is really good for characterising the foaming power and foam stability. Differentiation of the foaming agents could be there done using few, relative simple parameters, as an evolution ratio of the number of bubbles composing the foam and foam homogeneity (which can be expressed in terms of bubble size distribution or spatial organization).

From the rheology measurements point of view, both described above methods have one major disadvantage. Samples created in the foam column or in Hele-Shaw cell couldn't be removed from the "generator" and injected to the rheometer measuring geometry.

Mechanical homogenizers such as mixers (blenders, handheld homogenizers => rotor--stator or turax devices) work by shearing which is created by a tangential force being applied

to the sample [34]. They can foaming large samples quickly and are easy to use. Laboratory blenders or rotor-stator devices are available in stainless steel which allows fast and easy decontamination or sterilization. Rotor-stators are designed with an outer stationary tube (stator) and an inner turning shaft (rotor) which is connected to a motor. At the bottom of the rotor-stator are slots on both the tube and shaft. When running at 5000–30000 rpm, samples pressed into the slots of the rotor-stator are efficiently sheared. However, what is important from our point of view, the high speed homogenization created heat and vortexes, which can cause a significant protein denaturation. Despite this similar devices are commonly used for the food foaming experiments [35–41].

To avoid the experimental problems describing above, a simple apparatus based on fire fighting technology have been constructed for reproducible foam generation [42]. The center of the apparatus is a cylindrical brass mixing chamber into which both gas and solution are metered at steady rate. To force surfactant solution into the chamber, the high pressure in a reservoir is raised by a bottle of compressed N_2. This produces a powerful jet of liquid through a tiny hole in the center of the chamber. To produce foam, gas is simply fed into the jet-side of the chamber. This method allows producing large volumes of uniform foam rapidly, with a liquid content that is easily varied.

5. Foam rheology – introduction

Foams rheology is a difficult subject due to the complexity of their structure and the nature of their components (gas, liquid, surfactants, surface-active biopolymers or particles) [2, 5–7, 11, 43–49]. Moreover, as others foam ageing processes, the rheology is also interdependent. The slow creep below the yield stress can caused the changing of foam structure and coarsening. Therefore it could be counted as a fourth dynamic process occurring in the foam fraction (after drainage, coarsening and collapse). Multiple factors influenced the rheology of foams, including: liquid bulk properties, gas properties, air phase volume, liquid volume fraction, solution viscosity, interfacial thin film visco-elasticity, bubble size distribution, and bubble shape. A nature of the adsorbed surfactant or biopolymer and state of adsorption layer also modified the properties of the thin liquid film which separate the bubbles.

As is generally known rheology give us information how the materials respond to applied forces and deformations. The rheological evaluation is basing on simple concepts of stress (force per area) and strain (deformation per length). Stress (σ) is always a measurement of force per unit of surface area and is expressed in units of Pascals (Pa). The storage moduli G' gives us information of the deformation energy stored in the sample during the shear process, describing the elasticity properties.

$$G = \phi_{gas}(\phi_{gas} - \phi_c)\frac{T}{r} \tag{1}$$

Where the ϕ_{gas}, ϕ_c, T and r are gas volume fraction, critical gas volume fraction, surface tension and bubble radius, respectively. Beyond the critical gas volume fraction the foam cells (spheres) come apart and the foam loses it mechanical stability and becomes a bubbly liquid. This loss of foam stability is also known as the rigidity loss transition point. In te case of aqueous foams the critical points is equal ca. 64% ($\phi_c = 0.64$).

The loss moduli G'', which present the viscous properties of the sample, shown deformation energy used to the shear and lost to the sample.

$$\sigma_{yield} = (\phi_{gas} - \phi_c)^2 \frac{T}{r} \tag{2}$$

When flow occurs in foam, the bubbles must slide past each other. If the stress is progressively increased, the structure yields and plastic flow sets in. During the deformation, when the bubbles are strained, the osmotic pressure is exerted and bubbles store surface energy. Hence, foams exhibit linear viscoelastic behaviour when they are subjected to small shear stresses while they flow like viscous liquids when the applied shear stress is large enough to trigger bubble rearrangements. This behaviour is related to the foam structure on the bubble scale. It therefore has a yield stress, and belongs to that category of complex materials that may be termed "Bingham fluids", with a viscosity inversely proportional to shear rate. The scale of the shear moduli as well as the yield stress in this situation is set by the Laplace pressure of the bubbles.

In the linear regime the static shear moduli is governed by well-known Princen law as a function of liquid fraction, average bubble size and surface tension [7, 42]. However, as it was already mentioned, foam is a dynamic and non-equilibrium system. In reality the truly static elastic behaviour hasn't existed there [48]. Even if drainage and bubble coalescence could be suppressed, the foam is ageing due to process of Oswald ripening. Upon a ripening induced rearrangement, the bubble packing locally settles into a new configuration of minimal energy, so that the elastic strain induced by the applied macroscopic stress is at least partly converted into an irreversible strain. The local elastic stress existing prior to the rearrangement is thus relaxed [2, 46, 47].

For strain beyond yield strain, packing of the bubbles undergoes irreversible topological changes and non-Newtonian liquid-like behaviour occur [2]. Yielding typically occurs at strains of the order of 0.1–1, sufficiently large so that nonlinear elastic behaviour may be expected before the onset of significant plastic flow. However, the passage between these two types of mechanical behaviour is not yet well understood. When an elastic material is subjected to shear strains that are large but insufficient to induce significant plastic flow or yielding, the induced shear stress is accompanied by unequal normal stresses. This nonlinear phenomenon, known as the Poynting effect [50, 51], is governed by a universal relation between shear strain and first normal stresses difference, valid for nondissipative isotropic elastic materials. It was experimentally shown that the similar effect exists also in aqueous foams [52]. The viscoelastic linear properties and yield stress are strongly dependent on the liquid fraction, and for a low molecular weight surfactant, providing "fluid-like" interfaces, a universal behavior was recovered [53].

It was also shown that transient relaxation region, between the initial elastic responses and finally a steady state foam flow exists [54]. The effect was explained as a consequence of intermittent temporary loss of elasticity upon coarsening-induced structural rearrangements on the bubble scale.

6. Foam rheology – experimental problems

The physical measurements of foam rheological properties are complicated by its inherently unstable nature, foam ageing and by the presence of a liquid film slip layer at the wall. Traditional rheometer geometries, such as parallel plates, cone-plate or Couette tend to experience wall slip and could cause foam structure destruction during sample loading. Till today no general and uniform methodology for foam rheology measurements were developed. Therefore the direct comparison of various experimental data is complicated and often impossible.

The liquid film layer generated at the flat wall could easy slip during the experiments, what affect the accuracy of measurement [55, 56]. Some techniques could be applied for the minimize wall slip, like:

i) an additional hydrophobization of the walls,
ii) sandblasting (roughening) of the flat stainless steel or acrylic geometries (cone or plate),
iii) covering of cone and plates by polydisperse sand grains,
iv) specially grooved, cross-hatched of serrated geometries or
v) vane tool. It is hard to qualify which geometry is the best for the foam rheology experiments.

However, few general marks could be pointed. Despite the geometry choose, the both measuring parts of the device (parallel plates, cone and plate, Couette cup and bob or the vane toll and cup) must be prepared to prevent foam slipping. Without it, the wall slip will happen on the flat or smooth surface and the experimental data will be unreliable.

The parallel plates (serrated, cross-hatched or covered by sand grains) are the most adequate experimental tool in the order to measure foam rheology. However plate-plate geometry has a limitation and is insufficient in the case of transient foams. In similar foams, where collapse of the foam reduces the sample height, the disengaging of the foam from the upper plate happens.

Some author suggests that the foam compression during the sample loading into plate-plate geometry, and connected with this some distortion of foam structure, could cause the rheological properties of the material [57]. However, together with the letter author own experiences basing on the experiments with Gillete foam cream [58], in the linear regime the results are independent of gap width (plate-plate => gap variation 2–5mm, cone-plate => gap 0.15 mm) and consistent for cone-plate and plate-plate geometries, excluding artifacts due to wall slip or finite size of the gap compared to bubble structures.

Yield stress of foams depends strongly on gas volume fraction, bubble radius and surface tension. Therefore it is important to characterize these foam parameters throughout the full duration of the experiment. Thus, the bubble size should be measured using some digital camera. Images will be there captured at certain time intervals during the foam drainage process to give details on how the bubble size changed with time during the experiments.

The gas volume fraction in the foam could be measure by various methods. However, almost none of them could be coupled with the rheological test in rheometer. The only “in situ” method is a study of the local structural rearrangements rate in ageing foam

using diffusing-wave spectroscopy DWS. The samples should be there injected between the transparent glass plates of the rheometer [54].

The other method for gas volume fraction ϕ_{gas} verification is a simultaneously experiment in Hele-Shaw cell [32, 33]. The measurements is basing on the series of following snapsots of the foam fraction. On the foam pictures, the drainage effect can be monitored by measuring the light intensity transmitted through the bubble edges. In so doing, the liquid fraction φ that is actually measured on the Hele-Shaw walls slightly differs from the 'bulk' liquid fraction φ. Nevertheless, φ gives the relevant information about the liquid flows inside the bubble edges [22, 32, 33].

The air volume fraction could be also measured by the gravimetrically method [59]. A syringe with known volume is there filled with foam and weighed. The air volume fraction in the foam is determined from the relation $\phi_{gas} = 1 - m_F/(V_F\rho)$, where m_F is the mass of the foam in the syringe, V_F is the respective foam volume, and ρ is the mass density of the foaming solution.

The serious problem is connected with the water evaporation from the measured wet foams samples. It is clear that the evaporation is equal with the destruction of foam structure due to faster coarsening. To prevent the evaporation, the air in contact with the foam should be saturated. The samples should be therefore closed during the viscoelastic measurements in special, additional humidity cell. All the experiments must be carried out at constant temperature.

The coarsening of the foam could be suppressed by the using of hexafluoroethane C_2F_6, which has much lower diffusion and solubility constants then air or N_2 [49]. Similar effect could be done by mixing of nitrogen saturated with perfluorohexane vapor and special surfactant solution formulation [60].

7. Foam rheology – measurements methodology

The measurements of the foam rheological properties and for detecting the occurrence of nonlinearities and yielding could be done in various ways [2, 49–54]. Two types of oscillatory experiments can be performed: amplitude sweep at fixed frequency or frequency sweep at fixed amplitude. However, the foam ageing (drainage and coarsening) mostly do not allow low frequency experiments. So therefore in the case of wet foam the amplitude sweep measurements are used (oscillations at a fixed frequency $\omega = 1$ rad s^{-1} and with a strain amplitude γ varied from 10^{-4} to 1). It allow to measure storage and loss moduli (G' and G''), and to determine linear and non-linear responses (yielding) of foam fraction. The creep experiments could also be performed, where the foam is subjected to a constant stress Σ. In such experiment the resulting strain γ and compliance J ($J = \gamma/\Sigma$) [2, 42, 61] are measured versus time.

Fig. 3 and 4 present a typical result of strain-sweeps for shaving foam at a fixed liquid volume fraction. This sweep procedure consists in the application of a strain g varying from 0.001 up to 10, at a constant frequency of 1 Hz. The storage G' and the loss G'' moduli are classically obtained from those measurements. For all wet foams, the amplitude sweep curves keep the same classical shape with only variations for the plateau values G_0.

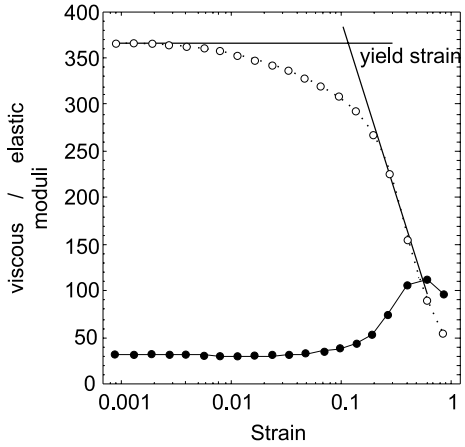

Fig. 3. (left) Evolution of the elastic and loss moduli with the applied stress amplitude. The intersection presents the foam yield strain. (Measurement was done by Bohlin Gemini II rheometer, equipped with serrated parallel plates, 4 mm gap)

Rys. 3. (po lewej) Zmiany modułów zachowawczego i stratnego w funkcji amplitudy naprężenia. Punkt przecięcia prostych prezentuje granicę plastyczności w funkcji naprężenia. (Eksperymenty wykonane przy pomocy reometru Bohlin Gemini II, wyposażonego w układ podwójnych, nacinanych płytek, odstęp między płytkami 4 mm)

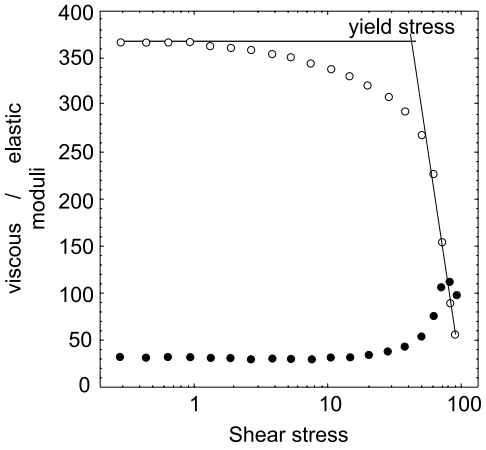

Fig. 4. (right) Evolution of the elastic and loss moduli with the applied strain amplitude for Nivea shaving cream. The intersection presents the foam yield strain

Rys. 4. (po prawej) Zmiany modułów zachowawczego i stratnego w funkcji amplitudy ścinania – dla pianki do golenia Nivea. Punkt przecięcia prostych prezentuje granicę plastyczności w funkcji ścinania

Yield strain and yield stress also could be determined from oscillatory data. A possibility consists in representing G' versus stress amplitude σ (or strain amplitude γ) in a log–log plot (Fig. 3). The behavior well above and well below the yield stress is well described by power laws corresponding to straight lines in such a plot. Their intersection provides an empirical definition of a yield stress σ_y. It can be used the parallel analysis to determine the yield strain γ_y using a log–log plot of G' versus strain amplitude γ (Fig. 4).

8. Foam rheology – surfactants and proteins foams

The liquid foam rheology has been studied extensively during last twenty years. However it can be easy noticed, that the numbers of surfactant foams systems (solutions and foams compositions) described by reliable rheological experiments are a very limited. The surfactant or polymer foams described below were formed mostly under high pressure is some variations of turbulent mixing devices [42].

Khan et al. used the polymer-surfactant aqueous solution as a foaming liquid [62] (parallel plate geometry with discs covered by the sandy paper). Politova et al. present the effect of two commercial cationic polymers (Jaguar C13c and Merquat 100) on the foam rheological properties (also using parallel plate geometry covered by the sandy paper) [59].

Cohen-Addad et al. [48, 54, 58, 63], Höhler et al; [64], Krishan et al. [65], Rouyer et al. [60, 66] and Labiausse et al. [67, 68] studied extensively the foam stability and rheological properties in various surfactant based systems, like:

i) Gillette shaving cream [48, 54, 60, 63–65],
ii) tetradecyltrimethylammonium bromide TTAB [60] (TTAB 0.936%, g/g, dodecanol 6.24×10^{-4}%, g/g and glycerol 50%, g/g),
iii) sodium dodecyl sulfate SDS [66] (SDS, polyethylene oxide PEO, dodecanol, and butanol),
iv) polymer-surfactants [48, 67, 68] based aqueous solution contained sodium α-olefin sulfonate AOK, polyethylene-oxide and dodecanol (concentrations: 1:5% g = g, 0:4% g = g, and 0:2% g = g, respectively),
v) Sodium Lauryl-dioxyethylene Sulfate SLES [65, 69] (SLES 0.33% g/g, Cocoamido-propyl 0.17% g/g and Glycerol 99.5%).

The Couette grooved geometry, grooved cone – serrated plate or serrated parallel plates were used in mentioned experiments. The rigidity of the particle-laden Gillette foams was also evaluated (grooved cone-serrated plate tools) [58].

Saint-James and coworkers [70] present the rheological study of foam generated from a mixture of surfactants α-olefin sulfonate AOS, polyacrylic acid polymer CARBOPOL 941, and cosurfactants dodecanol in solvent mixture butanol/water (two different measurement devices were used,

i) Couette cell, where the walls of both cylinders have been covered with sand paper,
ii) sandblasted cone-plate device made of transparent acrylic).

The influence of the doped colloidal Laponite on the SDS foam stability and rheology were measured in the same geometrical system [71]. Recently, Salonen et al. [72] provide the data describing the rheology of foams generated basing on cationic ammonium bromide surfactants;

i) monomers dodecylTAB (DTAB),
ii) tetradedylTAB (TTAB) and
iii) oligomers of DTAB with the degree of polymerization x varied from 2 to 4 and the spacer length s equal to 3 or 6 (plate-plate configuration with the gap was 2 or 3 mm).

In the case of biopolymer based foams the literature of subject is even more limited. Only the rheology of foams generated from various egg, white egg or whey proteins were studied using the vane tool or serrated parallel plate geometries. However, all described below tests were performed on the foam samples generated by various mixing devices with different methodology.

The Pernell with co-workers measured the yield stress of foams based on egg white and whey protein isolate (homemade vane tool) [57, 73]. Luck et al. [37] and Davies et al. [38, 39] described the factors determining yield stress in the whey protein foams (vane geometry). Mleko with coworkers [35] measured the rheological properties of foams based on egg albumin after pH treatment using cross-hatched parallel plates. The same geometry was used by Nastaj and Mleko [36] and Nastaj [40] during evaluation of calcium chloride concentrations [36] or pH effects [40] on rheological properties and stability of foams obtained from different whey protein propagates.

Together with the best knowledge of the author letter in the whole literature of subject exist only one set of experiments, where the rheological properties of surfactant (SDS) and protein (casein) foams were compared in well defined and controlled conditions. Marze and his coworkers [49, 74, 75] carefully studied the influence of:
i) surfactant solution composition,
ii) gas volume fraction,
iii) bubble size,
iv) foam age,
v) bulk viscosity,
vi) gas diffusion rate and,
vii) wall slip conditions – on the foam stability and rheology properties.

The foams were produced by using a turbulent mixer apparatus [42], which was mentioned above in the section “foam generation”. The foam liquid volume fraction, controlled by adjusting the gas and liquid flow rates in the foam generator, was varied from 0.05 up to 0.25. For the gas, the use of nitrogen N_2 and perfluoroethane C_2F_6 allowed to control the rate of coarsening and drainage of the foams. The three types of foaming chemicals were used;
i) sodium dodecyl sulfate SDS, an anionic surfactant;
ii) casein CAS, a mixture of milk proteins; and
iii) Amilite GCK-12 GCK, a commercial name for an anionic surfactant made of a fatty acid residue from coconut oil.

The rheological parameters of the foams were studied using the homemade cone-plate geometries in transparent Plexiglass coupled with transmission diffusing wave spectroscopy (DWS).

It was shown that the normalised storage moduli $G_0/(\sigma/R)$ turns out to be almost constant and independent of the chemicals used [49] at 85% gas volume fraction. No big differences were found between protein (casein) and surfactant (SDS) foams, what is in opposition

to results for emulsions. The main reason for this was probably too high surface tensions always present in foams. Surface tension is always much bigger than any interfacial elasticities. In contrary authors observed the huge differences in the behaviours of the loss moduli G_0'''', which was about 4–5 times higher for the casein foams than for the SDS ones. It could be estimated that some extra dissipation occurs in the casein foam due to the solution viscosity or/and from the thick structure and texture of protein lamellae foam film.

The influence of the solution bulk viscosity on the foam properties is still not clear. Some authors claims that the increasing of the bulk viscosity improved the foam stability [27]. While the others [49] shown that with 300% increasing of the bulk viscosity caused only minor variations of the storage and loss moduli. It suggests that the foam linear viscoelastic properties are almost independent from the bulk viscosity [49].

It was also proved that the foam viscoelastic linear properties and yield stress were strongly dependent on the liquid fraction. The storage and loss moduli and yield stress values decreases with the gas volume fraction decreasing (5–30%) [75]. Foam becomes less elastic as the liquid fraction increases, since the bubbles are less and less packed. For low molecular weight surfactant foams, which have the "fluid-like" interfaces, and universal behavior was recovered. In the case of protein foams the discrepancies was connected with interface and thin film properties.

The variations of the storage and loss moduli with the foam age were clearly described as a result of foam drainage and coalescence [49, 74, 75]. The ageing evolution of the foam was changed by the selection of the gas with the proper diffusion and solubility conditions (C_2F_6). Thanks for it the foam almost no coarsening occur and foam age only due to the drainage process. In the result the bubbles get more packed with the foam age and the storage (elastic) moduli is increasing with the time. In opposite cases, where the coarsening dominates over the drainage, the storage moduli is decrease with the time. The crucial role of coarsening in the long time liquid foam ageing was also confirmed [49].

9. Concluding remarks

Foam rheology is still a quite new area of scientific research. The numbers of various foams systems (different surfactants or biosurfactants solutions and/or foams compositions), which are described by proper viscoelastic experiments, are still relatively limited. Many of existing measurements are valid only under the experimental conditions described by the authors. The various methods of foam generation and the different rheological examination methodology lead the additional problems. The foam samples were studied by cone-plates, parallel plates (with various gap width), Couette cups, vane tools and others geometries Therefore the analysis and comparison of the data are really complicated. Some additional experimental errors, caused by the foam ageing, wall slip or other sources have also the strong influence on the obtained data.

It must be say, that there have been many important advances in the field of aqueous foams rheology during recent years. It was clearly shown that the foam stability and its rheological properties are controlled by various parameters, like:

i) the conditions of the surface layer that protect the air-water lamellae interfaces,
ii) surfactant solution composition,

iii) gas volume fraction,
iv) bubble size,
v) foam age,
vi) gas diffusion rate and,
vii) wall slip conditions.

However, the additional tests with other foams systems under other conditions (new chemical compositions and other foams parameters) should be done. Without it the further progress in the investigation of foam behavior seems to be impossible.

This paper was partially financially supported by Polish National Science Center, contract no. UMO-2011/01/B/ST8/03717.

References

[1] Plateau J.A.F., *Statique Experimentale et Theorique des Liquides Soumis aux Seules Forces Moleculaires*, Gauthier-Villar, Paris 1873.
[2] Weaire D., Hutzler S., *The Physics of Foams*, Clarendon Press, Oxford 1999.
[3] Nguyen A.V., Schulze J., *Colloidal Science of Flotation*, Marcel Dekker, New York 2004.
[4] Exerowa D., Kruglyakov P.M., *Foam and Foam Film Theory, experiment, applications*, Elsevier, Amsterdam, Holland 1998.
[5] Prud'homme R.K., Khan S., ed., *Foams: Theory, Measurements and Applications*, Marcel Dekker, New York 1996.
[6] Princen H.M., Kiss A.D., *Rheology of foams and highly concentrated emulsions: III. Static shear modulus*, J. Colloid Interf. Sci., 112, 1986, 427.
[7] Princen H.M., Kiss A.D., *Rheology of foams and highly concentratedemulsions. IV. An experimental study of the shear viscosity and yield stress of concentrated emulasions*, J. Colloid Interf. Sci., 128, 1989, 176.
[8] Cooper A., Kennedy M.W., *Biofoams and natural protein surfactants*, Biophys Chem. 151, 2010, 96-104.
[9] Rahman P.K.S.M., Gakpe E., *Productions, Cherecterisation and Applications of Biosurfactants – review*, Biotechnology 7, 2008, 360.
[10] Muthusamy K., Gopalakrishnan S., Ravi T.K., Sivachidambaram P., *Biosurfactants: Properties, commercial production and application*, Current Science, 94, 2008, 736.
[11] Weaire D, Hutzler S., Drenckhan W., Saugey A., Cox S.J., *The Rheology of Foams*, Progr. Colloid Polym. Sci.,133,2006, 100.
[12] Hilgenfeldt S.H., Koehler S.A., Stone H.A., *Dynamics of coarsening foams: Accelerated and self-limiting drainage*, Phys. Rev. Lett. 86, 2001, 4704.
[13] Allen Foegeding E., Luck P.J., Davis J.P., *Factor determining the physical property of protein foams*, Food Hydrocolloids, 20, 2006, 284.
[14] Murray B.S., Ettelaie R., *Foam stability: proteins and nanoparticles*, Curr. Opin. Colloid Interface Sci., 9, 2004, 314.
[15] Murray B.S., *Rheological propertiesof protein films*, Curr. Opin. Colloid Interface Sci, 16, 2011, 27.
[16] Yampolskaya G., Platikanov D., *Proteins at fluid interfaces: Adsorption layer and thin liquid film*, Adv. Colloid Interface Sci., 128–130, 2006, 159.

[17] Makievski A.V., Loglio G., Kralgel J., Miller R., Fainerman V.B., Neumann A.W., *Adsorption of Protein Layers at the Water/Air Interface As Studied by Axisymmetric Drop and Bubble Shape Analysis*, J. Phys. Chem. B 103, 1999, 9557.
[18] Fainerman V.B., Lucassen-Reynders E.H., Miller R., *Adsorption of surfactants and proteins at fluid interfaces*, Colloid Surf. A,143, 1998, 141.
[19] Wierenga P.A., Gruppen H., *New views on foams from protein solutions*, Curr. Opin. Colloid Interface Sci, 15, 2010, 365.
[20] Pezennec S., Gauthier F., Alonso C., Graner F., Croguennec T., Brule G., Renault A., *The protein net electric charge determines the surface rheological properties of ovalbumin adsorbed at the air–water interface*, Food Hydrocolloids, 14, 2000, 463.
[21] Niño M.R.R., Sánchez C.C., Fernández M.C., Patino J.M.R., *Protein and Lipid Films At Equilibrium At Air-Water Interface*, JAOCS, 78, 2001, 873.
[22] Caps H., Krzan M., Vandewalle N., *High stability of the Bovine Serum Albumine foams evidenced in Hele-Shaw cell*, Colloid Surf. A, 2012, in preparation.
[23] Caps H., Krzan M., Vandewalle N., 2012, unpublished data.
[24] Salam B.A., Pawlak J.J., Vendetti R.A., El-tahlawy K., *Synthesis and characterization of starch citrate-chitosan foam with superior water and saline absorbance properties*, Biomacromolecules, 14, 2010, 1453-9.
[25] *Method of producing polysaccharide foams*, United States Patent 5840777, 1998.
[26] *Biodegradable foam*, USPTO Patent Application 20070254016, 2007.
[27] Lennox S., *Gelatin alternatives in gummi confections*, Manufacturing Confectioner, 82, 2002, 65.
[28] Wei Y.P., Wang C.S., Wu J.S.B., *Flow properties of fruit fillings*, Food Res. Intern., 34, 2001, 377.
[29] Miquelim J.N., Lannes S.C.S., Mezzenga R., Food Hydrocolloids, 24, 2010, 398.
[30] Dickinson E., Izgi E., *Foam stabilization by protein-polysaccharide complexes*, Colloid Surf. A, 113, 1996, 191.
[31] Malysa K., Lunkenheimer K., *Foams under dynamic conditions*, Curr. Opin. Colloid Interface Sci., 13, 2008, 150.
[32] Caps H., Vandewalle N., Broze G., *Foaming dynamics in Hele-Shaw cells*, Phys. Rev. E, 73, 2006, 065301.
[33] Caps H., Vandewalle N., Broze G., Zocchi G., *Foamability and strucure analysis of foams in Hele-Shaw cell*, Appl. Phys. Lett., 90, 2007, 214101.
[34] Hanselmanna W., Windhabh E., *Flow characteristics and modeling of foam generation in a continous rotor/stator mixer*, J. Food Eng., 38, 1999, 393-405.
[35] Mleko S., Kristinsson H.G., Liang Y., Gustaw W., *Rheological properties of foams generated from egg albumin after pH treatment*, LWT 40, 2007, 908.
[36] Nastaj M., *Wpływ pH na właściwości reologiczne pian uzyskanych z albuminy wysokopiennej*, rozdział 3 w „Żywność projektowana", monografia pod red. Marii Walczyckiej i in., ISBN 978-83-932389-7-2, pp. 33-45.
[37] Luck P.J., Bray N., Foegeding E.A., *Factors determining yield stress and overrun of whey protein foams*, J. Food Sci., 67, 2002, 1667.
[38] Davis P.J., Foegeding E.A., *Foaming and interfacial properties of polymerized whey protein isolate*, J. Food Sci., 69, 2004, 404.
[39] Davis P.J., Foegeding E.A., Hansen K., *Electrostatic effects on the yield stress of whey protein isolate foam*s, Colloid. Surf. B, 34, 2004, 13.
[40] Nastaj M., Mleko S., *The effect of calcium chloride on rheological properties and stability of foams obtained from different whey protein preparates*, Milchwissenschaft, in press.

[41] Nastaj M., *Wpływ karagenu na właściwości reologiczne pian otrzymanych z preparatów białek serwatkowych*, http://www.e-wydawnictwo.eu/Document/DocumentPreview/2368, E-wydawnictwo 2012.
[42] Saint-Jalmes A., Vera M.U., Durian D.J., *Uniform foam production by turbulent mixing: new results on free drainage vs. liquid content*, Eur. Phys. J. B 12, 1999, 67.
[43] Princen H.M., *Rheology of foams and highly concentrated emulsions, I. Elastic properties and yield stress of a cylindrical model system*, J. Colloid Interface Sci., 91, 1983, 160.
[44] Khan S.A., Armstrong R.C., *Rheology of foams: I. Theory of dry foams*, Journal of Non-Newtonian Fluid Mechanics, 22, 1986, l.
[45] Kraynik A.M., *Foam flows*, Annu. Rev. Fluid Mech., 20, 1988, 325.
[46] Höhler R., Cohen-Addad S., *Rheology of liquid foam*, J. Phys. Condens. Matter, 17, 2005, R1041.
[47] Weaire D., *The rheology of foams*, Curr. Opin. Colloid Interface Sci., 13, 2008, 171.
[48] Cohen-Addad S., Höhler R., Khidas Y., *Origin of the slow linear viscoelastic response of aqueous foams*, Physical Review letters, 93, 2004, 028302.
[49] Marze S.P.L., Saint-Jalmes A., Langevin D., *Protein and surfactant foams: linear rheology and dilatancy effect*, Colloid Surf. A, 263, 2005, 121.
[50] Mal A., Singh S., *Deformation of Elastic Solids*, Prentice-Hall, London 1991.
[51] Poynting J.H., *On pressure perpendicular to the shear planes in finite pure shears, and on the lengthening of wires when twisted*, Proc. R. Soc. London, Ser. A, 82, 1909, 546.
[52] Labiausse V., Höhler R., Cohen-Addad S., *Shear induced normal stress differences in aqueous foams*, Journal of Rheology, 51, 2007, 479.
[53] Marze S., Guillermic R.M., Saint-Jalmes A., *Oscillatory rheology of aqueous foams: surfactant, liquid fraction,experimental protocol and aging effects*, Soft Matter, 5, 2009, 1937.
[54] Cohen-Addad S., Höhler R., *Bubble dynamics relaxation in aqueous foam probed by multispeckle Diffusing-Wave Spectroscopy*, Physical Review Letters, 86, 2001, 4700.
[55] Wenzel H.G., Brungraber R.J., Stelson T.E., *The Viscosity of High Expansion Foam*, J. Mater., 5, 1970, 396.
[56] Gardiner B.S., Dlugogorski B.Z., Jameson G.J, *Yield stress measurements of aqueous foams in the dry limit*, J. Rheol., 42, 1998, 1437.
[57] Pernell C.W., Foegeding E.A., Daubert C.R., *Measurement of the yield stress of protein foams by vane rheometry*, J. Food Sci., 65, 2000, 110.
[58] Cohen-Addad S., Krzan M., Höhler R., Herzhaft B., *Rigidity Percolation in Particle-Laden Foams*, Phys. Rev. Lett., 99, 2007, 168001-4.
[59] Politova N., Tcholakova S., Golemanov K., Denkov N.D., Vethamuthu M., Ananthapadmanabhan K.P., *Effect of cationic polymers on foam rheological properties*, Langmuir, 28, 2012, 1115.
[60] Rouyer F., Cohen-Addad S., Höhler R., *Is the yield stress of aqueous foam a well-defined quantity*?, Colloid Surf. A, 263, 2005, 111.
[61] Barnes H.A., Hutton J.F., Walters K., *An Introduction to Rheology*, Elsevier, Amsterdam 1989.
[62] Khan S.A., Schnepper C.A., Armstrong R.C., *Foam Rheology. III. Measurement of shear flow properties*, J. Rheol, 32, 1988, 69.
[63] Cohen-Addad S., Hoballah H., Höhler R., *Viscoelastic response of a coarsening foam*, Phys. Rev. Lett., 57, 1998, 6897.
[64] Höhler R., Cohen-Addad S., Asnacios A., *Rheological memory effect in aqueous foam*, Europhys. Lett., 48, 1999, 93.

[65] Krishan K., Helal A., Höhler R., Cohen-Addad S., *Fast relaxations in foams*, Phys. Rev. E, 82, 2010, 011405.
[66] Rouyer F., Cohen-Addad S., Vignes-Adler M., Höhler R., *Dynamics of yielding observed in a three dimensional aqueous dry foam*, Phys Rev. E, 67, 2003, 021405.
[67] Labiausse V., Höhler R., Cohen-Addad S., *Shear induced normal stress differences in aqueous foams*, Mechanics of 21st Century – ICTAM04 Proceedings XXI ICTAM, 15–21 August 2004, Warsaw.
[68] Labiausse V., Höhler R., Cohen-Addad S., *Shear induced normal stress differences in aqueous foams*, *J. Rheol*., 51, 2007, 479.
[69] Ovarlez G., Krishan K., Cohen-Addad S., *Investigation of shear banding in foams*, Europhysics Lett., 91, 2010, 68005.
[70] Saint-Jalmes A., Durian D.J., *Vanishing elasticity for wet foams: Equivalence with emulsions and role of polydispersity*, J. Rheol., 43, 1999, 1411.
[71] Guillermic R.M., Salonen A., Emile J., Saint-Jalmes A., *Surfactant Foams Doped with Laponite: Unusual Behaviors Induced by Aging and Confinement*, Soft Matter, 5, 2009, 4975.
[72] Salonen A., In M., Emile J., Saint-Jalmes A., *Solutions of surfactant oligomers: a model system for tuning foam stability by the surfactant structure*, Soft Matter, 6, 2010, 2271.
[73] Pernell C.W., Foegeding E.A., Luck P.J., Davis J.P., *Properties of whey and egg white protein foams*, Colloid. Surf. A, 204, 2002, 9-21.
[74] Marze S., Langevin D., Saint-Jalmes A., *Aqueous foam slip and shear regimes determined by rheometry and multiple light scattering*, J. Rheol,. 52, 2008, 1091.
[75] Marze S., Guillermic R.M., Saint-Jalmes A., *Oscillatory rheology of aqueous foams: surfactant, liquid fraction,experimental protocol and aging effects*, Soft Matter, 5, 2009, 1937.

TECHNICAL TRANSACTIONS | CZASOPISMO TECHNICZNE
CHEMISTRY | CHEMIA
1-Ch/2013

ANGELIKA ŁUCZAK, BEATA FRYŹLEWICZ-KOZAK*

METHODS OF RESEARCH INTO HAIR CONDITIONERS STABILITY

METODY BADANIA STABILNOŚCI KONDYCJONERÓW DO WŁOSÓW

Abstract

The aim of this work was to produce emulsion hair conditioners, and then to study their stability and rheological properties. For preparing emulsions two recipes with different oil phases and various emulsifiers were used. The emulsification process was performed using a homogenizer. Obtained samples were analyzed to determine their stability. Under the microscope the size of dispersed phase droplets was identified. The samples were also subjected to visual observation. At the same time rheological tests were carried out, which aimed at observing changes in rheological properties of emulsions.

Keywords: *emulsion*, *emulsion stability*, *yield stress*

Streszczenie

Celem niniejszego artykułu było wytworzenie emulsyjnych odżywek do włosów, a następnie zbadanie ich stabilności i własności reologicznych. Do sporządzenia emulsji wykorzystano dwie receptury z różnymi fazami olejowymi oraz emulgatorami. Proces emulgowania wykonano przy użyciu homogenizatora. Stosując techniki mikroskopowe, analizowano strukturę wytworzonych układów. Badania stabilności prowadzono dwoma metodami, tj. metodą wizualną oraz metodą zmiany rozkładu wielkości kropel fazy rozproszonej podczas przechowywania.

Słowa kluczowe: *emulsje*, *stabilność emulsji*, *granica płynięcia*

* PhD. Eng. Beata Fryźlewicz-Kozak, Angelika Łuczak, student, Institute of Chemical and Process Engineering, Cracow University of Technology.

Notation

$\dot{\gamma}$ – shear rate [1/s]
τ – shear stress [Pa]
τ_0 – yield stress [Pa]
η – fluid viscosity [Pa·s]
d – droplet diameter [μm]

1. Introduction

The cosmetics industry is dominated by products which are multi-component heterophasic systems. The most valued form because of their properties are emulsions. Emulsions are defined as a heterogeneous system consisting of at least two mutually immiscible liquid phases, one of which is dispersed in the other in the form of droplets. The liquid that forms droplets is called a dispersed phase – internal, the liquid over which the droplets are scattered is a continuous phase – outer. Emulsions can be divided according to the number of phases into simple oil-in-water (O/W) emulsions and water-in-oil (W/O) emulsions, as well as into complex ones of the types O/W/O and W/O/W. The most popular in cosmetics are simple emulsions, in which additional components such as liposomes, antioxidants, fragrances or preservatives are dissolved in particular phases. For producing emulsions later used for hair cosmetics such as shampoos and conditioners mainly emulsions O/W are used because of their nutritional values, where the dispersed phase content is 10–30%.

One of the factors affecting consumers' assessment are application properties and the consistency of a product. Due to viscosity emulsions are divided into creams, lotions or milks. A type and quantity of ingredients of the oil phase as well as the presence of components affecting consistency all have a significant influence on rheological properties of emulsions.

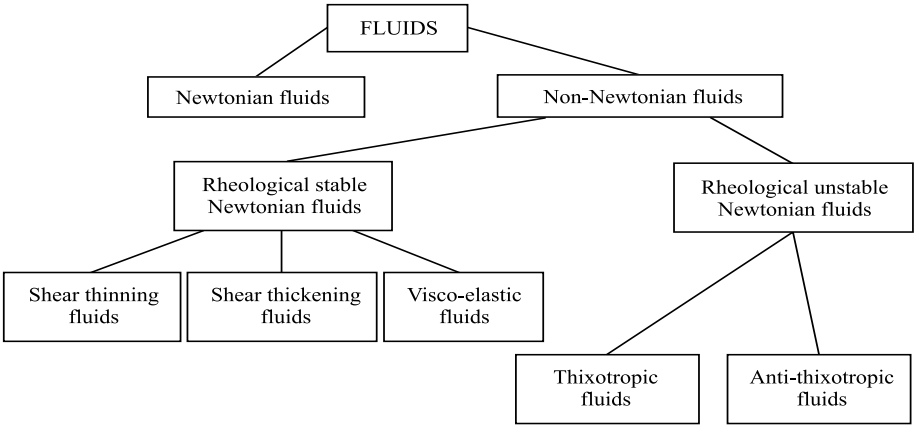

Chart 1. Fluids division due to their rheological properties
Schemat 1. Podział płynów ze względu na ich właściwości reologiczne

Rheology deals with issues related to the deformation and flow of materials. These phenomena are described by presenting the relationship between the occurring stresses and deformations or the rate of deformation formation. The basic rheological properties are viscosity, plasticity and elasticity.

Liquids having a complex internal structure, such as pastes, disperse systems, suspensions, polymers, emulsions, mortar and cement slurries exhibit non-Newtonian characteristics. Their structure is characterized by the presence of suspended particles or dispersed molecules that are larger than typical fluid particles. This results in the formation of long-range interactions between movements of these elements.

Depending on the reported rheological properties fluids can be classified according to Chart 1.

2. Emulsion stability

Emulsion systems are thermodynamically unstable. They embrace various processes that lead to the binding of particles and the violation of dispersed phase balance and ultimately to the destruction of the entire system. Their durability depends on many factors, such as the presence of substances lowering interfacial tension, emulsion particle size, viscosity, sphericity of droplets in dispersed phase, Brownian motion and temperature. Emulsion stability is highly influenced by an applied emulsifier which is absorbed on the interfacial surface, which lowers surface tension. It causes a decrease in cohesion forces between the dispersed liquid particles, which increases the degree of dispersion of one phase in the other.

Emulsion stability is a basic and very important property. The phenomenon of instability may relate to processes occurring simultaneously or sequentially, depending on conditions. Physicochemical mechanisms responsible for emulsion instability are the Stokes' law, Van der Waals forces, the phenomenon of Ostwald ripening and Brownian motion.

Instability phenomena can be divided into two groups – reversible and irreversible instabilities. There are two types of reversible instability, namely creaming and sedimentation. In both cases mixing causes restoration of the primary emulsion. Creaming is a process in which the dispersed phase particles migrate to the sample surface without changes in the droplets distribution. However, the sedimentation process involves movement of the dispersed phase drops under the influence of gravity force to the bottom of a vessel without changing their sizes.

Another type of reversible instability is flocculation. The mechanism of this phenomenon consists in concentrating the dispersed phase particles into larger aggregates with no tendency to accumulation at the top or bottom of the vessel. However, merging of these into larger droplets often occurs, which is the essence of the phenomenon of coalescence, i.e. irreversible instability. The coalescence process often leads to emulsion breaking, which is the process of complete phase separation into the organic phase and water phase. This effect is also irreversible.

3. Experimental part

Tested hair conditioner emulsions are silk and protein. They differ in the oil phase and an emulsifier used. In the cases of both silk and protein conditioner the oil phase was 11% whereas aqueous phase 89%. The composition is shown in Table 1.

Table 1

The composition of examined hair conditioners

PROTEIN CONDITIONER – B	
OIL PHASE 11%	AQUEOUS PHASE 89%
Avocado Oil	Keratin
Cottonseed oil	D-panthenol
SPL, HLB 11	Silk hydrolyzate
	FEOG
	Hydrolate – sweet almond water
SILK CONDITIONER – A	
OIL PHASE 11%	AQUEOUS PHASE 89%
Avocado Oil	Sorbitol
Refined coconut oil	D-panthenol
GSC, HLB 12	Silk hydrolyzate
	FEOG
	Hydrolate –Ylang Ylang flower water

3.1. Emulsion preparation

In industry emulsions are obtained with methods which are based mainly on mechanical stirring, homogenizing, ultrasonic energy, or shaking. Emulsion systems consist of two mutually immiscible liquids. After mixing they form drops, one of them becomes a continuous phase, the other one – a dispersed phase. The intensity and duration of the mixing process should be individualized for each emulsion. In order to receive the studied emulsions the homogenization method was used with a homogenizer MICCRA D-9. After initial tests the following parameters were established for the studied emulsion systems: emulsification time 480 seconds, revolutions frequency 350 s^{-1}.

In the case of emulsification with a homogenizer emulsions with almost the same dispersion degree may be obtained. In the initial phase of emulsification the decomposition of oil and water phases occurs; large droplets of one phase dispersed in the other are formed then. In subsequent stages these droplets are broken down into smaller ones. This phenomenon is dependent on two interacting forces: disintegration force generated by the homogenizer and surface tension forces that make drops stick together. Such obtained emulsions are more stable than emulsion systems which are not homogenized.

3.2. Emulsion preparation

The samples obtained in this way were subjected to stability tests. The tests were conducted at the following time intervals: immediately after preparing a sample, a day after, 7 days after, one month and 3 months after making the emulsion they were subjected to rheological testing with a rotational rheometer HAAKE RS 75 using a cone-plate system with a diameter of 35 mm and an angle of 1°. The research was carried out at a temperature of 293 K. Then emulsion stability tests were performed using a Mastersizer 2000 apparatus which measured particle size distribution. Photographs of the samples were taken using a microscope Morphologi G3.

4. Tests results

One of the factors affecting the stability of emulsion is the size of dispersed phase droplets. The formation of droplets in the emulsification process is static. Sizes of droplets depend on the method of emulsion preparation, when a homogenizer is applied particles of a relatively small size and of an approximate size are formed. The narrower size distribution of emulsion droplets the greater emulsion stability.

Figures 1 and 2 as well as Tables 2 and 3 show the droplet size distribution, the corresponding diameters d_{32}, d_{43}, d_{10}, d_{50}, $d_{90,}$ and microscopic images (Fig. 3) on the basis of which histograms of quantitative droplets distribution of dispersed phase were made.

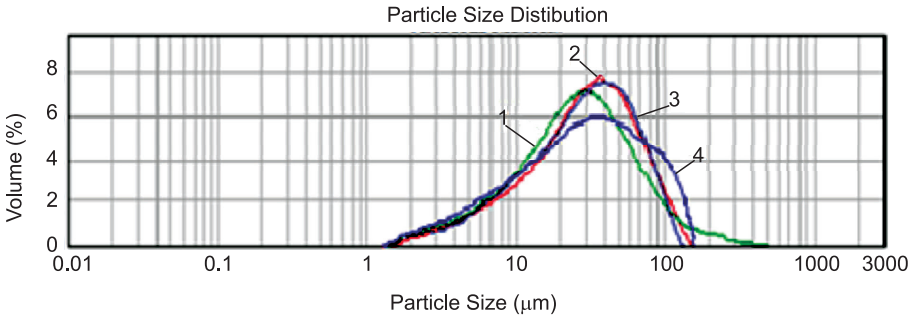

1 - protein conditioner - after 1 hours
2 - protein conditioner - after 1 day
3 - protein conditioner - after 7 days
4 - protein conditioner - after 1 month

Fig. 1. Comparison chart of particle size distribution of protein conditioner dispersed phase after a specified time

Rys. 1. Wykres porównawczy rozkładu wielkości cząstek fazy rozproszonej odżywki proteinowej po określonym czasie

Table 2

Change in average diameter sizes compared to the time of protein emulsion aging

Time of conducted study	Average diameters of dispersed phase droplets [μm]					SPAN
	d_{10}	d_{32}	d_{50}	d_{90}	d_{43}	
after 1hour	8.930	11.776	31.133	70.876	33.175	1.975
after 1 day	7.708	16.836	28.152	72.192	35.642	2.139
after 7 days	7.759	17.287	30.809	75.17	37.067	2.199
after 30 days	6.931	18.327	26.703	78.138	38.667	2.667

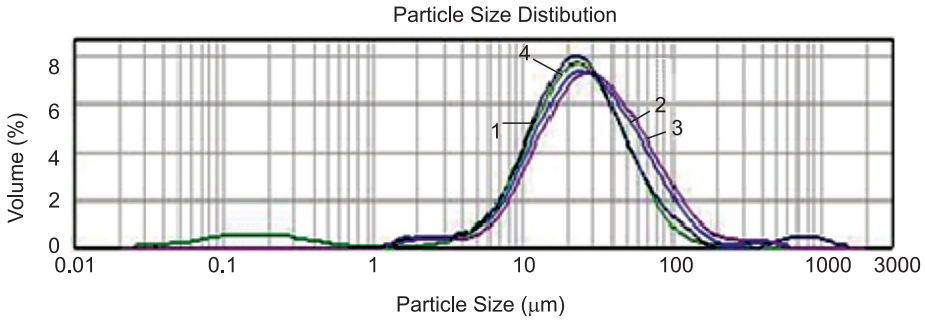

1 - silk conditioner - after 1 hours
2 - silk conditioner - after 1 day
3 - silk conditioner - after 7 days
4 - silk conditioner - after 1 month

Fig. 2. Comparison chart of particle size distribution of silk conditioner dispersed phase after a specified time

Rys. 2. Wykres rozkładu wielkości cząstek fazy rozproszonej odżywki jedwabnej po określonym czasie

Table 3

Change in average diameter sizes compared to the time of silk emulsion aging

Time of conducted study	Average diameters of dispersed phase droplets [μm]					SPAN
	d_{10}	d_{32}	d_{50}	d_{90}	d_{43}	
after 1 hour	0.261	0.903	16.356	38.539	18.442	2.339
after 1 day	4.224	1.173	21.417	56.780	27.701	2.454
after 7 days	9.044	17.095	26.673	78.679	38.248	2.611
after 30 days	10.456	19.926	29.980	91.140	44.697	2.691

Both charts present a shift towards larger droplets of the dispersed phase, which is associated with aging of the emulsion. Changes in the sample were observed 7 and 30 days after the emulsion was made.

Basing on the results from Table 1 and Table 2 it may be noted that the diameters of dispersed phase droplets d_{10}, d_{32}, d_{50}, d_{90}, d_{43} grow during the aging of the emulsion. The size of the diameter d_{32} of dispersed phase droplets of silk conditioner is 0.903 μm on the day when it is made. However, the measurement made after 30 days shows that the diameter increased and amounts to 19.926 μm for the same sample, which shows that there has been a reduction in the interface. For the protein emulsion the values were 11.776 μm on the day of sample obtaining and 18.327 μm after 30 days.

Using the visual method it was observed that the silk conditioner sample on the day of obtaining was a homogeneous emulsion. However, after 30 days a clear phase separation was observed. In the case of samples with protein conditioner changes could be observed as early as after 14 days. The phase separation gradually increased. Photomicrographs taken with Morphologi G3 also allow to observe changes taking place in the system. One may also observe how droplets diameters change.

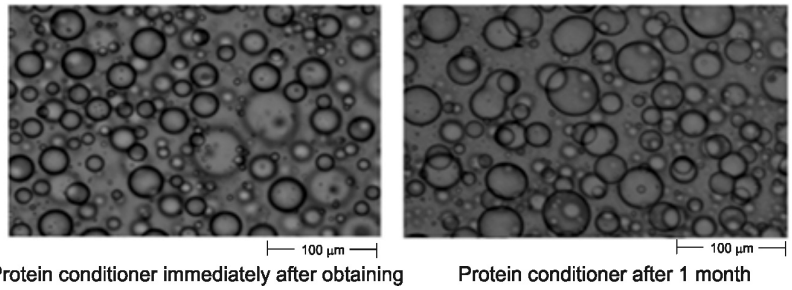

Fig. 3. Photomicrographs of protein conditioner taken with Morphologi G3

Rys. 3. Zdjęcia mikroskopowe odżywki proteinowej wykonane przy użyciu Morphologi G3

Comparing these two pictures one can clearly observe changes that take place in the aging process of the emulsion. Droplets lost their spherical shape, some of them mingled together to form larger droplets. This can indicate that there is a correlation between changes affecting the conditioner structure and their rheological properties. Thickening of the emulsion structure is associated with a change in its viscosity. In this way the rheometric measurement gives the opportunity to evaluate the quality of the emulsion.

Emulsion systems are classified as non-Newtonian fluids. The nature of the emulsion rheological test using a rheometer allows to investigate the relationship between shear velocity and tangential stress.

Non-Newtonian fluids require a greater number of parameters characterizing their rheological properties. Data describing the nature of a fluid is, among others, viscosity coefficient and the relation between shear rate and tangential stress, called the flow curve. Therefore, while conducting rheological research the fundamental test was to determine the flow curves of both conditioners. This curve is not a straight line, it often shifts along the y-axis, so in order to determine its course approximations in the form of equations are used. The results obtained using HAAKE rheometer RS 75 were then elaborated by regression of experimental points with equations listed in Table 4. HAAKE ReoWin – rheometer software was used for this purpose.

Table 4

Equations describing flow curves for visco-elastic fluids

AUTHOR	FLOW CURVE EQUATION
Herschel, Bulkley	$\tau = K\dot{\gamma}^n + \tau_0$
Casson	$\tau^{1/2} = \tau_0^{1/2} + (\eta_p \dot{\gamma})^{1/2}$
Tscheuschner	$\tau = \gamma \left(\eta_\infty + \frac{\tau_0}{\dot{\gamma}} + \frac{\eta_b}{\left(\frac{\dot{\gamma}}{\dot{\gamma}_b}\right)^n} \right)$

In systems of two-or multi-phase, where one or more phases are dispersed in the form of particles the so called yield stress also occurs. When we deal with a sufficiently high concentration of dispersion the interaction between the dispersed particles can cause a three-dimensional structure, to some degree resistant to the impact of shear stress. Below the boundary point the system behaves as an elastic solid. By contrast, we assume that above this value, the structure is completely destroyed and begins to behave like a viscous liquid – it flows. This limit value is called the yield point. Under the conditions of tangential stress greater than yield stress the rheological properties can be explained as a result of the characteristics of the continuous phase. It may therefore be assumed that the dispersion of particles in a dilute sheared fluid will be Herschel-Bulkley fluid.

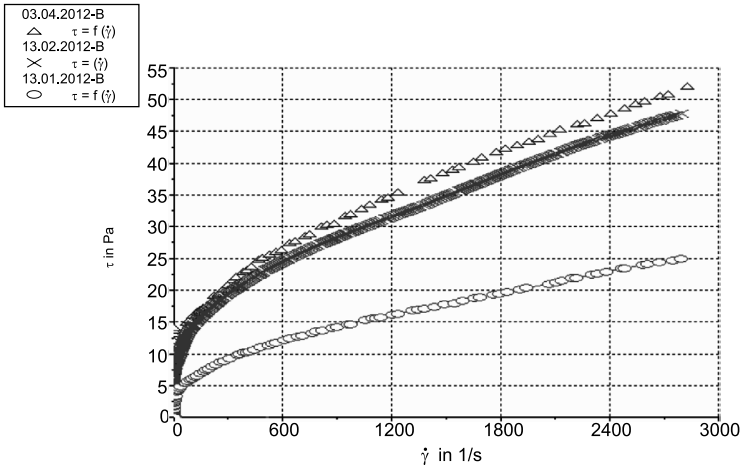

Fig. 4. Comparison chart of flow curves for protein conditioner

Rys. 4. Wykres porównawczy krzywych płynięcia dla odżywki proteinowej

The graph shows (Fig. 4) that with time the emulsion changes in viscosity, there is an increase in viscosity of the tested example, which results in a shift of flow curves. An increase in the yield point of both tested emulsions has been observed together with a decrease in quality.

The next step was to find an equation most accurately describing the obtained flow curves. Each of the equations presented in Table 4 allows to obtain the approximate correlation. It can be concluded that the rheological models by Tscheuschner and Herschel-Bulkley describe the flow accurately. Both give a very close approximation of the curve in the conformity test Ch2, however, the Herschel-Bulkley equation is easier to write, making it easier to grasp the sense of physical constants of the equation (Fig. 5).

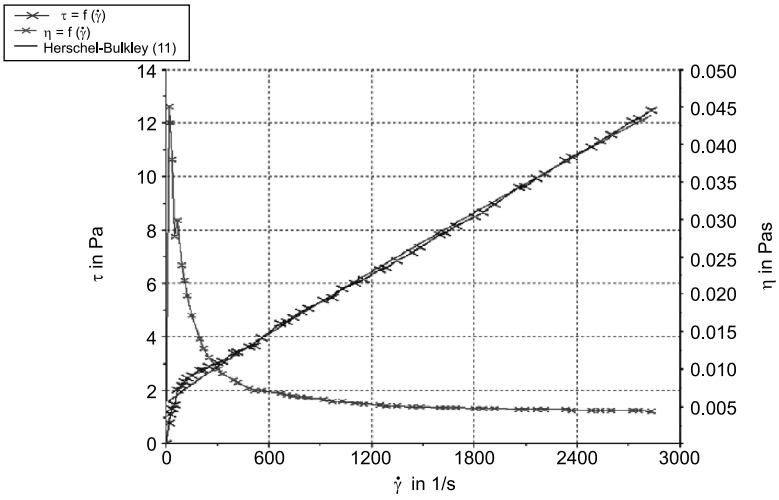

Fig. 5. Flow curve of silk conditioner at 293 K with tailored rheological model of Herschel-Bulkley

Rys. 5. Krzywa płynięcia odżywki jedwab w temperaturze 293 K z dopasowanym modelem reologicznym Herschel-Bulkley

5. Conclusions

In this study two types of conditioners were tested for their stability. The emulsion stability depends on numerous factors. The present research indicated that what matters is a method for obtaining the system, because the size of dispersed phase drops significantly affects the emulsion stability. The smaller the droplets the more stable the system. Emulsion systems, however, are thermodynamically unstable. After a longer period the system demonstrated merging of droplets, coalescence, which led to complete phase separation. The studies allowed to notice that there is a correlation between the values of rheological parameters, and sometimes the emulsion breakdown. The best description of experimental data allows to obtain the Herschel-Bulkey model.

References

[1] Sherman P., *Emulsion science*, Academic Press INC, LTD, London and New York 1968.
[2] Kiljański T., Dziubiński M., Sęk J., Antosik K., *Wykorzystanie parametrów właściwości reologicznych płynów w praktyce inżynierskiej*, EKMA Krzysztof Antosik, Warszawa 2009.
[3] Sherman P., *Rheology of emulsions*, Symposium Publications Division Pergamon Press, Oxford 1963.
[4] Ferguson J., Kembłowski Z., *Reologia stosowana płynów*, Wydawnictwo Marcus sc, Łódź 1995.
[5] Gilewicz J., *Emulsje*, Państwowe Wydawnictwo Naukowe, Warszawa 1957.
[6] McClements D.J., *Food Emulsions: Principles*, *Practice and Techniques*, CRC Press, London 2000.
[7] Myers D., *Surfaces Interfaces and Colloids*, Wilely-vch, Germany 1999.
[8] Binks B., *Modern aspects of emulsion science*, The Royal Society of Chemistry, UK 1998.
[9] Coussot P., *Rheometry of pastes, suspensions and granular materials*, Wiley, New Jersey 2005.
[10] Figiel W., Kwiecień M., *Właściwości reologiczne komponentów maści farmaceutycznych*, Czasopismo Techniczne, 10, 2010, 73-81.

TECHNICAL TRANSACTIONS | **CZASOPISMO TECHNICZNE**
CHEMISTRY | CHEMIA
1-Ch/2013

TOMASZ M. MAJKA, KRZYSZTOF PIELICHOWSKI, AGNIESZKA LESZCZYŃSKA*

COMPARISON OF THE RHEOLOGICAL PROPERTIES OF POLYAMIDE-6 AND ITS NANOCOMPOSITES WITH MONTMORILLONITE OBTAINED BY MELT INTERCALATION

PORÓWNANIE WŁAŚCIWOŚCI REOLOGICZNYCH POLIAMIDU-6 ORAZ JEGO NANOKOMPOZYTÓW Z MONTMORYLONITEM OTRZYMANYCH METODĄ DYSPERGOWANIA W STOPIE POLIMERU

Abstract

Each varying parameter which can contribute to the quality of final products plays an important role in the processing of polymer nanomaterials. Rheological properties are useful in proper formulation of new polyamide-6 (PA-6) based materials and selecting processing parameters. However, the measured rheological properties depend strongly on the sample preparation method, humidity regulation, and time-temperature history during the measurement and not least on the kind of rheometer being used. The results of the preliminary investigation show the changes in visco-elastic properties of two types of PA-6 and their nanocomposites with montmorilonite.

Keywords: *nanocomposite*, *polyamide*, *montmorillonite*, *rheology*

Streszczenie

W przetwórstwie nanomateriałów polimerowych istotną rolę odgrywa każdy zmienny parametr, który może przyczynić się do jakości otrzymanych produktów. Znajomość właściwości reologicznych polimeru może być potrzebna do poprawnego opracowania formuły kompozycji polimerowej oraz ustawienia parametrów przetwórstwa. Należy jednak podkreślić, że mierzone właściwości reologiczne zależą przede wszystkim od historii termicznej próbki, metody przygotowania, rozkładu wilgotności, temperatury oraz czasu, w jakim wykonywany jest pomiar, a także od rodzaju używanego reometru. W niniejszym artykule przedstawiono wyniki wstępnych badań właściwości lepko-sprężystych dwóch typów handlowego poliamidu-6 oraz ich nanokompozytów z montmorylonitem.

Słowa kluczowe: *nanokompozyt*, *poliamid*, *montmorylonit*, *reologia*

* MSc. Eng. Tomasz M. Majka, Prof. Krzysztof Pielichowski, PhD. Agnieszka Leszczyńska, Department of Chemistry and Technology of Polymers, Fsculty of Chemical Engineering and Technology, Cracow University of Technology.

1. Introduction

Polymer nanocomposites are nowadays the subject of intensive research efforts owing to their various unique properties [1–5]. In recent years, polymer/clay nanocomposites have attracted great attention both in industry and academia in achieving various excellent properties of nanocomposites compared to conventional ones. Polymer/clay nanocomposites have been obtained using different preparation methods such as melt mixing to get the intercalated or exfoliated structures in homopolymers [6].

Although polyamide-6/montmorillonite nanocomposites gathered industrial interest, only a few scientific papers on its rheological properties have been published [1–4]. In polymer processing, such an injection molding and extrusion, the rheological properties of the nanocomposites are of vital importance. A polymer network is generally visco-elastic with a complex shear modulus having both elastic and viscous components of similar magniture over a large range of frequencies. It is suggested that rheological measurements are performed at a humidity lower than 0.1% using relatively short measurement times. The rheological properties of polymer are changed by introducing the filler compound. Montmorillonite particles due to nanometric dimensions cause noticeable increase in viscosity at very low concentrations (below 5 wt%). Solid like behavior of polymer melt was reported at higher concentrations. Nanocomposite formulations generally requires high shearing and long dwell times. When producing new polymeric nanocomposite by direct melt mixing a thermomechanical degradation of polymer matrix should be considered as a cause of variation of rheological properties. In most of the scientific work on the thermal degradation of polyamide, the polymer was severely damaged at temperatures much above 300°C [5]. The solid end-product can hardly be called polyamide any more. Only a few papers describe investigations on the thermal degradation of polyamide-6 under milder conditions, i.e., at temperatures lower or not much higher than those at which the polymer is processed [4–5]. Other publications report studies at moderate temperatures, but with very long annealing times.

The purpose of the present investigation was to define the proper conditions of oscillatory measurements of PA-6/MMT nanocomposites and evaluate the effect of nanoparticles dispersed in polyamide-6 on its visco-elastic behavior.. Also it was the task of this study to find out whether processing conditions affect the rheological properties of polyamide-6 and nanocomposites with layered silicate, and whether these initial conditions are chosen appropriately.

2. Experimental

2.1. Materials

Polyamide-6 (PA-6) was purchased from Zaklady Azotowe w Tarnowie – Moscicach S.A. under the trade name Tarnamid® T27 and Tarnamid® T30.

Montmorillonite (DELLITE® 72T – trade name) was supplied by Laviosa Chimica SpA Mineraria. DELLITE® 72T is a nanoclay deriving from a naturally occurring montmorillonite

especially purified and modified with a quaternary ammonium salt (dimethyl dihydrogenated tallow ammonium).

2.2. Nanocomposite samples: preparation by melt compounding

Before the preparation of nanocomposites, materials were dried in a laboratory vacuum oven. Polyamide was dried at 80°C for 3 hours. Polyamide-6 and polyamide-6/montmorillonite nanocomposite samples were prepared using a mini process line (twin co-rotating screw extruder Thermo Scientific Rheomex PTW 16/25 XL, cooling tank of ZAMAK and granulator ZAMAK G-16/325). The materials were processed at the processing temperatures shown in Table 1, at 240 rpm rotation of the screws. The sample bars in shape of plates were made using a laboratory injection molding machine ZAMAK WT 12.

Table 1

Processing parameters of polyamide-6 and polyamide-6/montmorillonite nanocomposites obtained by melt intercalation

Twin co-rotating screw extruder								
Flow rate [%]	**Rotational speed [1/min]**	**Heating zones**						
		1	**2**	**3**	**4**	**5**	**6**	**Die**
0,3	240							
Temperature [°C]		245	245	245	250	255	250	260
Atmospheric venting		-------	-------	-------	-------	YES	-------	-------
Length of the zones [mm]		80	60	60	64	60	76	23
L/D		5,00	3,75	3,75	4,00	3,75	4,75	-------
Cooling tank								
Length of cooling surface [mm]		1500						
Tank volume [dm^3]		27						
Height of bath [mm]		1081						
Water temperature [°C]		18						
Granulator								
Size of pellets [mm]		1						
Rotational speed [1/s]		12						

2.3. Characterization techniques

The rheological investigations have been performed using modular advanced rheometer platform – HAAKE MARS III. The research were carried out with plate – plate sensor system. Diameter of plate was 20 mm. The plate-plate system is determined by the plate radius and the variable distance the stationary and the movable plate. This distance should be not be smaller than 0,5 mm and not larger than 3 mm as other measurements error, depending on the materials, could be experienced. In these tests, width of gap was 1,8 mm.

Nanomaterials based on plastics are non-Newtonian substances which only start flowing after being subject to shear stress i.e. after certain yield point. The yield point strongly depends on external parameters like temperature and change rate of the acting force. Practical yield point of plastics is determined taking in account the environmental conditions specific for the application. Therefore, for these materials, the measuring mode for determination of relaxation modulus named as Controlled Deformation (CD) have been chosen.

3. Results and discussion

3.1. Linear Visco-elastic Range (LVR)

In the first step the Oscillation Stress Sweep Mode (OSS) was applied in order to determine Linear Visco–elastic Range (LVR) of tested materials. The OSS is to say that the measurement parameters are set in this manner that stress and strain amplitude have a linear relationship which can be described by the following equation:

$$\tau_0 = G' \cdot \gamma_0 \tag{1}$$

A more practical way to indentify the LVR is to look for the region where the material function as e.g. *G'* is independent of shear stress value.

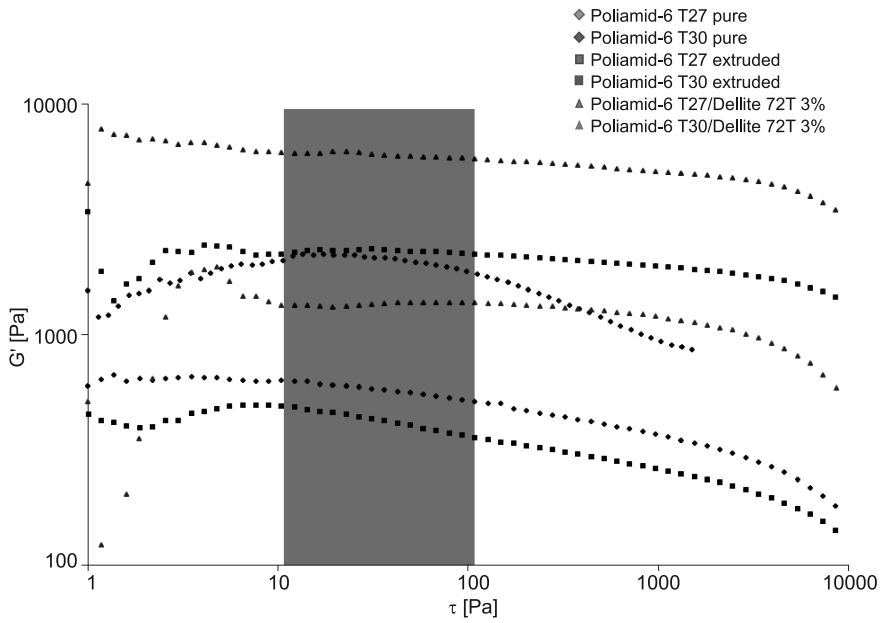

Fig. 1. The determination of material's Linear Visco-elastic Range (LVR)

Rys. 1. Wyznaczanie liniowego zakresu lepko-sprężystego (LVR)

Figure 1 shows the LVR determined for investigated samples. For four of the six samples, linear visco-elastic range was observed from 10 to 100 Pa. For Oscillation Frequency Sweep (OFS) the value of shear stress 50 Pa have been taken.

3.2. Oscilation Frequency Sweep (OFS)

Before the main test, a movable plate was heated in 232°C for 2 minutes. The distance between stationary and movable plate was 0,1 mm. Next, the samples were heated in 232°C for 5 minutes to obtain a melt. When the samples were melted, the structures were pretreated using pre-test in the range of 12–14 Hz. This procedure is necessary to remove stresses remaining in polymer sample after injection moulding and relax polymer chains.

In most cases 0.1 Hz should be a suitable for start frequency, and 14 Hz for end frequency. Lower values require a longer measurement time. Each data point has an estimated test time of the reciprocal of the actual frequency, multiplied by the number of cycles running through. Each data point requires at least 2 cycles – one pre-run and one test run repetition. In this test start frequency and end frequency were 0,01 Hz and 20 Hz respectively.

The OFS test tells about the structural conditions of the sample. Rheological behaviour at high frequencies is normally used to estimate the effect of the filler on processing properties. Low-frequency behaviour is sensitive to the structure of the percolation state of nanofillers within the composite. Fig. 2 and Fig. 3 show an increase in the storage modulus (G') and loss modulus (G''), by the incorporation of 3wt% clay into neat Tarnamid T27 and Tarnamid T30 matrices (Fig. 2 and Fig. 3 respectively).

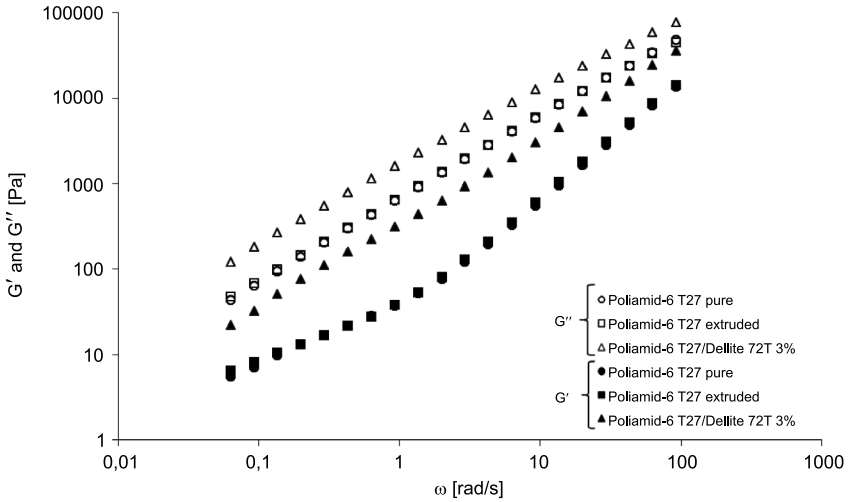

Fig. 2. Frequency dependence of G' and G'' for samples based on PA-6 (T27)
Rys. 2. Zależność ω od G' i G'' dla próbek wytworzonych w oparciu o PA-6 (T27)

This enhancement in the oscilation modulus is significant, in particular, at low frequencies regime. At low frequencies, the degree of dependence of G' on the frequency was sensitive to the effect of clay on visco-elastic properties of the nanocomposites. It was reported

elsewhere that when the clay loading exceeded 3wt% due to degradation process of matrix, the dependency of *G'* of PA-6 nanocomposites on the frequency increased linearly [7]. The results indicates that, when the matrix is degraded, the clay loading exceeded 3wt%, the liquid-like behavior of PA-6/MMT nanocomposites gradually changed to a pseudo-solid like behavior. As shown in Fig. 2 *G′* does not become independent on the frequency at low frequencies because plateau does not appear in the low frequencies regime starting from 0.1 rad/s. This indicates a formation of the intercalative or partial intercalative structure of nanocomposites rather than full exfoliation. The values of loss modulus and storage modulus for polyamide-6/montmorillonite nanocomposite with modified clay increase by many order of magnitude. For example at ω 0,063 rad/s, *G″* of Tarnamid T30/montmorillonite nanocomposite with 3wt% of modified clay is higher by factor about 3,3 times than extruded polymer, and about 3,9 times than pure not extruded Tarnamid T30. For Tarnamid T27/montmorillonite nanocomposite with 3wt% of modified clay, *G″* at ω 0,063 rad/s is higher by factor about 2,5 times than extruded polymer, and about 2,8 times than pure not extruded Tarnamid T27. At the same value of ω, the storage modulus of Tarnamid T30/montmorillonite nanocomposite with 3wt% of modified clay is greater by factor about 5,8 times than extruded polyamide-6, and about 7,3 times than neat polymer. Meanwhile the storage modulus of Tarnamid T27/montmorillonite nanocomposite with 3wt% of modified clay is higher around 3,4 times than extruded polyamide-6, and about 3,9 times than neat polyamide. As shown in Fig. 2 and Fig. 3, the loss modulus was dominant at all range of measurement, so at all range of ω, the viscous properties was dominant over elastic, indeed.

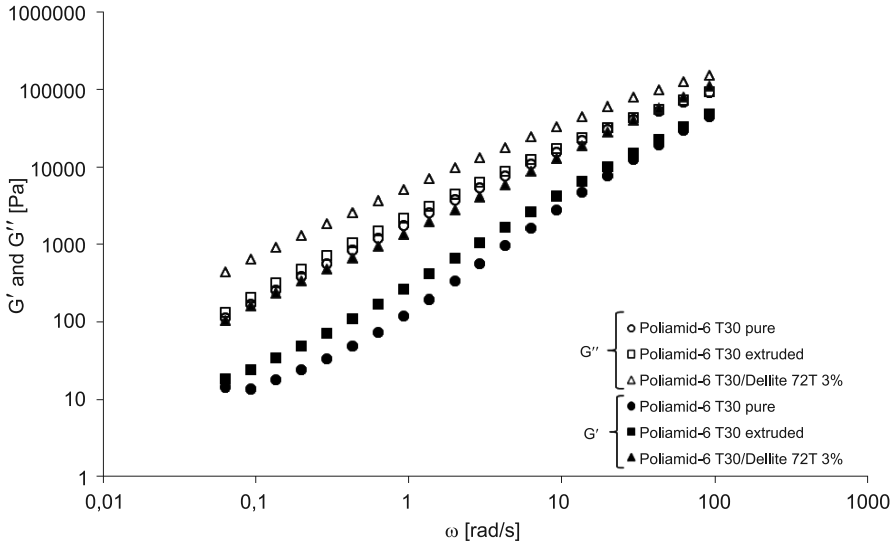

Fig. 3. Frequency dependence of *G′* and *G″* for samples based on PA-6 (T30)

Rys. 3. Zależność ω od *G′* i *G″* dla próbek wytworzonych w oparciu o PA-6 (T30)

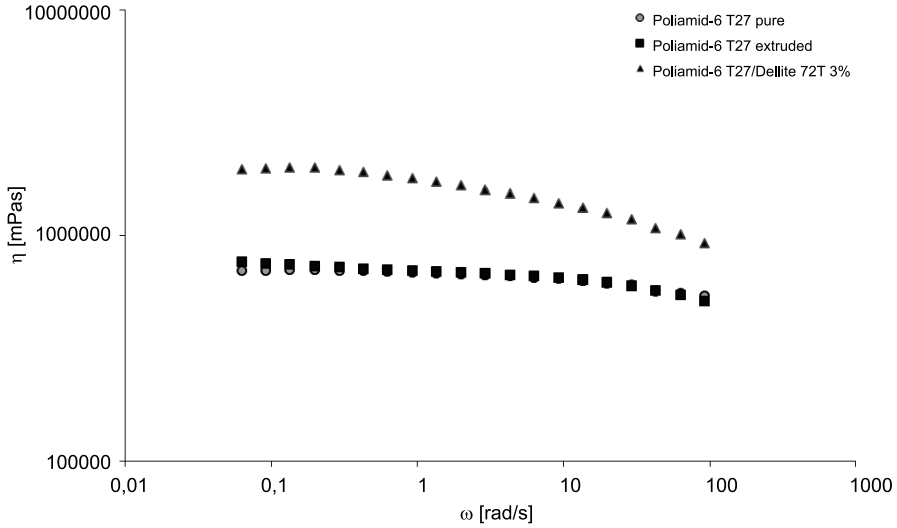

Fig. 4. Frequency dependence of viscosity for samples based on PA-6 (T27)
Rys. 4. Zależność η od ω dla próbek wytworzonych w oparciu o PA-6 (T27)

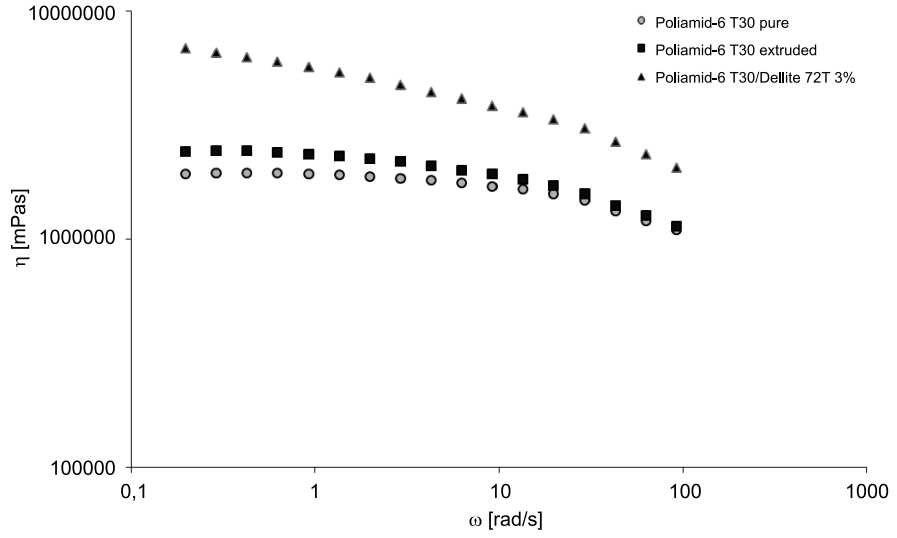

Fig. 5. Frequency dependence of viscosity for samples based on PA-6 (T30)
Rys. 5. Zależność ω od η dla próbek wytworzonych w oparciu o PA-6 (T30)

The viscosity changes with the angular frequency (ω), as can be seen from Fig. 4 and Fig. 5. As shown , the measured viscosity increases by the incorporation of montmorillonite into neat polyamide, particularly, at low frequencies regime. In rheological measurements of polymer melt the viscosity may be influenced by changes in the molecular weight

of polymer, presence of gas bubbles, and the plasticizer effect. Molecular mass of tested polymer may be varied by previous processing operation as well as due to thermal decomposition of polymer during the time of rheological measurement. If the bubbles are present in melt the oscillating deformation changes the surface area of the bubbles, thereby changing the surface Gibbs energy and surface tension.

4. Conclusions

In this work, extruded polyamide, polyamide/clay nanocomposites were prepared by using a co-rotating twin screw extruder. The materials were rheologically characterized.

One can conclude that the visco-elastic properties of PA-6 and PA-6/MMT nanocomposites can be determined using the given procedure to obtain comparable and reproducible results. Measurements of rheological properties under the molten state reveal that nanofiller loading leads to an increase in the shear viscosity, the storage modulus (G') and loss modulus (G'') of nanocomposites. The viscosity increases with the incorporation of montmorillonite into neat polyamide, particularly, at low frequencies regime and may be indicative of the dispersion state of nanofiller.

This work was partially financed by the National Science Centre under decision No. DEC-2011/01/M/ST8/06834.

References

[1] Nevalainen K., Hintze C., Suihkonen R, Eteläaho P., Vuorinen J, Järvelä P., Isomäki N., *Rheological properties of melt-compounded and diluted nanocomposites of atomic-layer-deposition-coated polyamide particles*, Annual Transactions of The Nordic Rheology Society, 2008, 16, 1-9.

[2] Chow W.S., Ishak Z.A.M., Karger-Kocsis J., *Morphological and Rheological Properties of Polyamide 6/Poly(propylene)/Organoclay Nanocomposites*, Macromolecules Material Eng., 2005, 290, 122-127.

[3] Chow W.S., Ishak Z.A.M., Ishiaku U.S., Karger-Kocsis J., Apostolov A.A., *The effect of organoclay on the mechanical properties and morphology of injection-molded polyamide 6/polypropylene nanocomposites*, Journal of Applied Polymer Science, 2004, 91, 175-189.

[4] Kim J.H., Creasy T.S., *Measurement of Sintering Characteristics of Clay-Reinforced Polyamide 6 Nanocomposite*, Polymer Testing, 2004, 23, 629-636.

[5] Majka T.M., Pielichowski K, *Degradacja termiczna nanokompozytów poliamid/krzemian warstwowy*, Czasopismo Techniczne, 2011, 20, 133-142.

[6] Gonza´lez I., Eguiaza´bal J.I., Naza´bal J., *Rubber-toughened polyamide 6/clay nanocomposites*, Composites Science and Technology, 2006, 66, 1833-1843.

[7] Wu D., Zhou C., Hong Z., Mao D., Bian Z., *Study on rheological behaviour of poly(butylene terephthalate)/montmorillonite nanocomposites*, European Polymer Journal, 2005, 41, 2199-2207.

TECHNICAL TRANSACTIONS | CZASOPISMO TECHNICZNE
CHEMISTRY | CHEMIA
1-Ch/2013

PIOTR MIGAS, MARTA KOROLCZUK-HEJNAK, MIROSŁAW KARBOWNICZEK, ANDRZEJ ŁĘDZKI*

RHEOLOGICAL ANALYSIS OF BLAST FURNACE SYNTHETIC SLAG ADMINIXTURES OF Al_2O_3

ANALIZA REOLOGICZNA SYNTETYCZNYCH ŻUŻLI WIELKOPIECOWYCH DOMIESZKOWANYCH AL_2O_3

Abstract

It is common for researchers to believe that liquid slag is a fluid characterized by rheological behavior of ideally viscous Newtonian body. At the same time it is assumed that the fluid is similar to synthetic polymers in terms of its structure. The authors of this paper conducted research into 4-component liquid and solid-liquid synthetic slag system: $CaO–SiO_2–MgO–Al_2O_3$ The research involved graphite measurement systems. A perforated spindle was used for the solid-liquid systems subject to shear stress, whereas a smooth one was used for fully liquid systems. Both measurement systems worked according to Searle's system. This paper presents selected rheological research results concerning oxide solutions in high temperatures and their rheological analysis.

Keywords: *liquid slags*, *rheology*, *non-Newtonian flow*

Streszczenie

Wśród badaczy panuje powszechny pogląd, że ciekły żużel jest cieczą wykazującą zachowania reologiczne ciała doskonale lepkiego Newtona. Zarazem przyjmuje się, że jest on cieczą o podobieństwie strukturalnym do polimerów syntetycznych. Autorzy artykułu wykonali badania czteroskładnikowych ciekłych oraz stało-ciekłych żużli syntetycznych systemu: $CaO–SiO_2–MgO–Al_2O_3$. Do badań wykorzystano grafitowe systemy pomiarowe. Systemy stało-ciekłe poddawano działaniu naprężeń ścinających z wykorzystaniem wrzecion perforowanych dla systemów całkowicie ciekłych użyto wrzecion gładkich. Obydwa układy pomiarowe pracowały w systemie Searle'a. W artykule zaprezentowano wybrane wyniki badań reologicznych roztworów tlenkowych w wysokich temperaturach oraz ich analizę reologiczną.

Słowa kluczowe: *ciekły żużel*, *reologia*, *przepływ nienewtonowski*

* PhD. Eng. Piotr Migas, MSc. Eng. Marta Korolczuk-Hejnak, PhD. Eng. Mirosław Karbowniczek, Prof. PhD. Eng. Andrzej Łędzki, AGH University of Science and Technology, Faculty of Metals Engineering and Industrial Computer Science, Department of Iron Alloys Metallurgy.

1. Introduction

Viscosity is one of the basic physical properties when it comes to metallurgical processes involving liquid slag and metal phases. It has direct influence on the kinetics of reactions taking place between liquid metal and slag as well as on the flow of these phases in metallurgical aggregates. That is why this property is a key parameter mentioned not only in the existing mathematical models but also the ones that are being developed.

The rheological character of liquid slag should be defined not only on the basis of its chemical composition and temperature but also by means of rheological parameters such as: t – time in which the force was applied to the system, τ – shear stress, γ – shear rate [1].

The rheological parameters present in the actual metallurgical processes, which are very difficult to measure, include: dynamics of the arc's influence on the properties of liquid steel and slag, dynamics of the influence of a reduction gas on liquid slag and pig iron in the blast furnace, the phenomena involving the move of semi-liquid and liquid products down the blast furnace in counter-flow with the reduction gas and then their flow down between the pieces of coke.

All these factors influence the liquid slag and pig iron by means of a certain dynamic force. They result in the occurrence of shear stress in the layers of moving slag – changing at the same time its dynamic viscosity coefficient and in some cases its rheological character. It is commonly assumed that fully liquid slag (being a Newtonian fluid) does not change its viscosity under the influence of an applied force. Its viscosity was also influenced by the solid elements content in the liquid – elements which precipitated while the temperature was being decreased, in the course of chemical reactions, as a result of modifying the chemical composition and finally because of solid elements entering slag from the outside, e.g. coal dust, carbides, nitrides insoluble in slag.

Solid-liquid slag systems are present in many metallurgical processes such as: blast furnace process – PCI, the cohesion zone and slag dripping; the arc furnace process – slag foaming, slag in the production of chrome steel; COS – steel casting, casting powder, pig iron and steel refining – 3D technology, desulphurization, dephosphorization, desilicanization. All these processes involve solid elements which precipitated from the solution or which were introduced to the slag system.

The literature contains a significant amount of measurement data concerning the dynamic viscosity of metallurgical slag for fully liquid slag systems [2–5, 15–16]. Their authors did research into the influence of the chemical composition, basicity and temperature on viscosity. Few research centers [6, 7] undertook the complicated research into the changes of the dynamic viscosity coefficient as a rheological property of the liquid or solid-liquid multi-component slag systems.

Rheology is a study of the material deformation and its transition to plastic state. Rheology focuses on such issues as: changing relations between stress and deformation in the function of time, changing viscosity, separation and mixing of substance particles affected by stress [14]. Rheology is a study of two different types of fluids [8]:

– Newtonian fluids – (ideal viscosity) which show a linear relationship between the shear stress and the shear rate,

– Non-Newtonian fluids – which show non-linear relationship between the shear stress and changes in the shear rate.

Newtonian fluids are characterized by a stable viscosity in the course of the flow, the independence of the deformation rate and the repeatability of viscosity value in the course of subsequent identical flows. The viscosity of non-Newtonian fluids is referred to as apparent viscosity. It is independent of the deformation rate, duration and pressure. In reality most fluids are non-Newtonian ones.

The rheological description of fluids includes viscous and elastic features. The viscous features can be determined by defining the flow curve, i.e. the relation between the shear stress (triggered by the shearing fluid) and the shear rate (velocity gradient existing in the flowing liquid). In order to determine the elastic features it is necessary to measure the normal stress in the course of a given viscous flow. Such analysis allows to determine the relationship between the deformation, the shear rate and the shear stress.

Recently researchers have been developing and describing many models used to determine the viscosity of aluminosilicate slag: Urbain's, KTH, Iida, QCV [8–13].

The viscosity (η) of slag is to a large extent dependent on the temperature and the structure of the fluid [14]. It is a measure of the ability of slag to flow when the shear stress is applied. Most slag and metallic fluids show the characteristics of Newtonian fluids, in case of which viscosity is independent of the shear rate [14]. As a result viscosity is defined by the Newton's equation (1) as a constant of the proportional relationship between the shear stress (τ_{xy}) and the normal velocity gradient to the shear stress $\left(\frac{dv_x}{dy}\right)$.

$$\left(\tau_{xy} = \eta \frac{dv_x}{dy}\right) \tag{1}$$

When the layers in the fluid shear, the bonds break. This is a process activated thermally and it is expressed by the Arrhenius equation (2). It is characterized by coefficient A_A and activation energy E_A:

$$\left(\eta = A_A \cdot e^{\frac{E_A}{RT}}\right) \tag{2}$$

Liquid slag consists of, among others, discontinuous ionic structures whose activation energy is closely connected to the type of ions and ionic complexes present in the system as well as to the interionic forces. Due to the fact that the type and size of ions changes with temperature, the activation energy changes significantly with temperature, too.

The Einstein-Roscoe equation (3) is commonly used to describe the viscosity of slag containing dispersed solid phase. The equation below can be used to estimate the viscosity of partially crystallized slag containing up to 30% solid fraction in the volume of the system

$$\eta_S = \eta_L (1 - R\theta_S)^{-n} \tag{3}$$

where η_S refers to the apparent viscosity of the suspension in the fluid and solid elements and η_S to the viscosity of the fully liquid phase, Φ_S is a volume fraction of the solid phase.

For identical size of spherical particles R and n in the equation amount to 1.35 and 2.5 respectively. The reciprocal of the R value in the physical sense refers to the maximum amount of solid phase which the fluid can hold before the viscosity reaches an infinitely large value. The equation was introduced with an assumption that the particles were dispersed evenly in the fluid [6].

The viscosity is a measure of the resistance of the vicious flow and it is to a large extent dependent on the mobility of elements present in the fluid, such as atoms, molecules or ions which respectively reflect: the bond, the size and the configuration of the fluid components. In such a system one can observe a strong relationship between the measured viscosity and the structure. Slag is partially a polymer substance and some of its properties (e.g. viscosity, density, thermal and electric conduction) are dependent on its structure.

A. Shankar and associates [5] conducted research into the dynamic viscosity coefficient taking into consideration the changes in the rotary velocity of the spindle (5 types of rotary velocity ranging from 4 to 80 rpm) for slag systems: $CaO–SiO_2–MgO–Al_2O_3$ and $CaO–SiO_2–MgO–Al_2O_3–TiO_2$ in the basicity range: 0.72–1.23 and in temperature range: 1650 to 1873K. Liquidus temperatures were calculated using Thermo-Calc software so that the systems would be fully liquid. The increase in viscosity value (at the temperature of 1673K) suggested the presence of solid particles in the system. Their amount, however, was not defined. The authors put forward a thesis that viscosity depends to a large extent on the amount and size of solid particles and ions present in the system. The viscosity value is also affected by the degree of slag polymerization, which is in turn dependent on the silica activity – i.e. the possible Si–O–Si bonds as well as free oxygen ions O^2. The change in rotary velocity of the revolving element did not affect the dynamic viscosity of slag.

A. Kondratiev and associates [6] set out to verify the Einstein-Roscoe equation and conducted research into 4 different partially crystallized triple slag systems (among others $Al_2O_3–FeO–SiO_2$) during the cooling process from 1773 to 1633K and the heating process from 1633 to 1723K. In the course of continuous measurements (the value of torque changed with temperature) researchers noticed a sudden increase in viscosity at the temperature of approx. 1668K. That is when solid phase began to precipitate in slag. The parameters adjusted to model (3) are as follows: $R = 1.29$ and $n = 2.04$ and are comparable to the Roscoe model values.

S. Wright, L. Zhang, S. Sun, S. Jahanshahi [7] conducted research into the viscosity of slag ($28\%CaO–10\%MgO–20\%Al_2O_3–42\%SiO_2$) with the addition of solid particles of spinel ($MgAl_2O_4$). The shear rate was changed within the range of 0.5 to $3s^{-1}$ for less than 10% of the solid phase and the range of 0.3 to $1s^{-1}$ for bigger amounts of solid phase. When the content of solid phase was low (up to 10%) the apparent viscosity decreased down to 60%. In the extreme case of 22% of solid phase the viscosity decreased twofold in comparison to the maximum value while the shear rate was increasing. In the case of a 10% or higher content of solid phase the system showed the behavior of the Bigham's type (i.e. the shear stress increased linearly with the grow in the shear rate but there was a residual shear stress for zero shear rate). The residual shear stress suggests the existence of a flow boundary (up to 3Pa depending on the amount and size of solid phase).

S. Seok, S. Jung, Y. Lee, D. Min [3] also studied the viscosity of $CaO–8\%MgO–FeO–Al_2O_3–SiO_2$ in solid-liquid dispersed system saturated with $2CaO·SiO_2$ in a temperature

range of 1673–1873K. They tested viscosity measurements in the temperature of 1873K for 3 different rotary velocities of the spindle (30, 60, 100 rpm). They concluded that the results of viscosity do not depend on the rotary velocity. The apparent viscosity of slag is dependent on the volume fraction of solid phase – estimated on the basis of slag composition.

Despite a significant amount of research conducted into the viscosity of slag systems the data available still seem insufficient to fully understand the structure and to predict the properties of slag commonly used in metallurgical processes. In case of complex slag systems the experimental data are only available for selected temperatures and for a narrow range of concentration. Due to difficult high temperature conditions comprehensive rheological research into slag is conducted in few centers and on a small scale [20, 21]. Each study of this sort brings new results and contributes to a better understanding of the rheological properties of slag

2. Experimental research and results

In order to measure the dynamic viscosity coefficient a force needs to be applied to the liquid system, and as a result the system is set into motion. The application of the force causes one layer of fluid to be transported towards another. Longer chains in fluid and polymerization cause the measurements to be more complicated. The dynamic viscosity is the best property of liquid glass and slag [17] when it comes to analyzing the internal structure of these fluids.

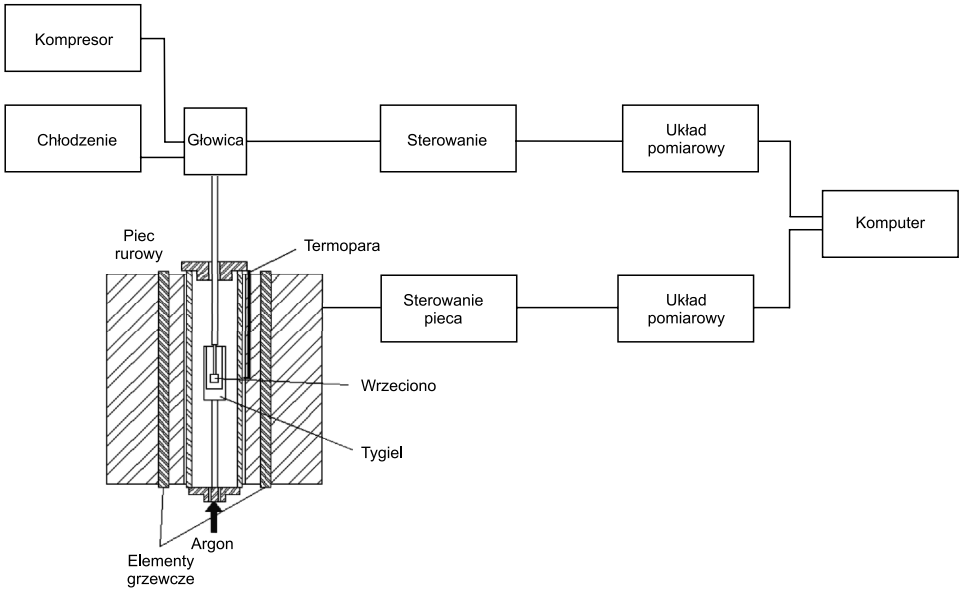

Fig. 1. Scheme of a high temperature rheometer FRS1600

Rys. 1. Schemat reometru wysokotemperaturowego FRS1600

Figure 1 shows a high temperature rheometer scheme, which is a prototype device developed in cooperation with Anton Paar company. Rheometer FRS1600 is equipped with a pipe furnace which makes it possible to obtain temperatures exceeding 1530°C.

The measuring head and the cooling system are the most important parts of the rheometer. Both the head and the furnace are operated remotely using a computer. There is a thermocouple in the furnace, which allows for temperature measurements. The resistance pipe furnace with a mullite pipe is controlled by means of Eurotherm. Inert gas (argon, its purity – 5.0) is introduced into the furnace. It allows to maintain a protective atmosphere in the course of long rheological measurements.

The calibration of the device was performed on a medium with a known value of viscosity coefficient in given temperature. In this case it was model glass Standardglas I der DGG (Kalk-Natron-Glas). Coefficients C_{SS} and C_{RS} were determined. These coefficients characterize the geometry of the measurement system for a shear rate which is possible to reach without causing a turbulent flow in the fissure.

The measurement system in the rheometer consists of concentric cylinders working according to Searle's method. According to this method there is a moving inner cylinder (spindle) and a motionless crucible (outer cylinder).

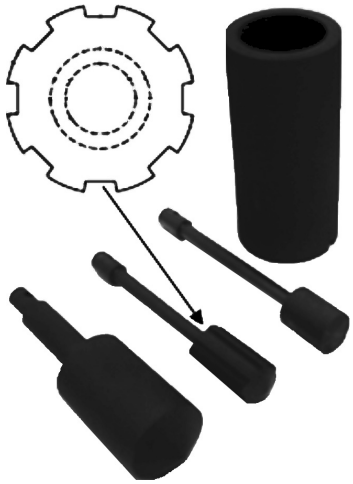

Fig. 2. Measurement systems used

Rys. 2. Stosowane systemy pomiarowe

Figure 2 presents measurement instruments used for rheological research into liquid and solid-liquid slag systems – in this case these were elements made of graphite. In this figure there is one type of crucible and three geometry types of spindles used for rheological research into liquid ionic solutions. The inner diameter of crucible was 30 mm, whereas the diameter of spindle amounted to 16 mm. The spindle which was used for research into solid-liquid systems had a perforated side surface in order to ensure a simple shear of the fluid and the most linear distribution of velocity in the rheological fissure. The fissure was 7 mm, which is a desirable size from the point of view of analyzing the rheological behavior of the fluid.

The rheological research focused on multi-component slag of the blast furnace type in the system $CaO–SiO_2–Al_2O_3–MgO$. This slag was obtained by means of a synthesis of pure components in liquid form: CaO – calcined powder, SiO2 – analytically pure quartz, Al_2O_3 – analytically pure, MgO – analytically pure calcined powder (made by a company called E. Merck). Special attention was paid to weighing the components. Before the components were weighed, they had been dried in the temperature of 120°C for 5 hours. Then they were carefully mixed. Slag was melted in an induction furnace (in a graphite crucible). The chemical compositions of slag samples were analyzed using an XFR spectrometer TWIN-X. The results of this analysis can be found in Table 1.

Table 1

Percentage and mass chemical composition

Components	1		2		3		4		5	
	%	g	%	g	%	g	%	g	%	g
CaO	44.23	22.11	41.61	20.81	40.34	20.17	37.66	18.83	35.56	17.78
MgO	6.46	3.23	6.07	3.04	5.88	2.94	5.49	2.74	5.18	2.59
Al_2O_3	7.07	3.54	12.76	6.38	15.60	7.80	21.29	10.65	25.65	12.83
SiO_2	42.24	21.12	39.55	19.78	38.18	19.09	35.56	17.78	33.61	16.80
B3	1.03		0.91		0.86		0.76		0.69	
B1	1.05		1.05		1.06		1.06		1.06	

Then equillibrium calculations of solid phase precipitation from liquid slag systems were conducted. The chemical composition and temperature of the analyzed slag constituted boundary conditions for which researchers calculated the type and amount of solid particles precipitating from the system. The mass of the sample used for this rheological experiment was 50g – this mass was used to calculate the mass content of particular oxides in the system. The equilibrium calculations were made using FactSage application. The obtained results are shown in table 2.

Thanks to FactSage thermodynamic database it was possible to determine the types and amounts of possible solid precipitations in the analyzed samples: sample 1 – $MgOCa_3O_3Si_2O_4$-merwinite, $CaSiO_3$-pseudowollastonite; sample 4 – $Ca_2Al_2SiO_7$_gehlenite; sample 5 – $Ca_2Al_2SiO_7$-gehlenite. In case of sample 2 and 3 solid particles appear only when the temperature rises over 1270°C or 1250°C respectively. These temperatures are theoretical ones and were not applied in the course of rheological experiments. Due to certain differences in behavior observed for sample 4, only selected samples 1, 2, 3 and 5 were presented in the Table 2.

The behavior and influence of Al_2O_3 on viscosity in liquid silica systems resembles that of SiO_2. This oxide can also behave as a cross-linking element of the fluid structure in systems with higher basicity. Tetrahedral ion AlO_4^{4-} can be produced in such systems. It is characterized by high durability due to a big charge capacity – which is compensated by

the cation (Ca^{2+}). The production of AlO_4^{4-} ion can cause an increase in the resistance of flow. That is why the viscosity models used to estimate the dynamic viscosity coefficient show lower viscosity by approx. 40% than the one obtained in the course of measurements. It is true, however, that there are few experimental data available in literature to explain this discrepancy [18].

Table 2

A comparison of experimental results and calculations

No.	T [°C]	γ [s^{-1}]	η_{measur} [Pa·s]	mass of sol-part. [g]	mass of sol-part. [%]
1	1330	15–150	0.797–0.768	1.88	3.760
	1340	15–150	0.730–0.695	0.83	0.416
	1350	15–150	0.278–0.257	0.00	0.00
	1400	15–150	0.454–0.427	0.00	0.00
2	1330	15–150	1.310–1.140	0.00	0.00
	1340	15–150	1.270–1.020	0.00	0.00
	1350	15–150	1.330–1.140	0.00	0.00
	1400	15–150	0.774–0.598	0.00	0.00
3	1330	15–150	1.863–2.35	0.00	0.00
	1340	15–150	1.207–1.159	0.00	0.00
	1350	15–150	1.081–1.041	0.00	0.00
	1400	15–150	0.705–0.664	0.00	0.00
5	1330	15–150	25.890–4.700	13.62	6.812
	1340	15–150	16.370–12.61	11.46	5.730
	1350	15–150	16.280–10.81	9.14	4.571
	1400	15–150	2.198–1.713	0.00	0.00

Table 3 presents measurements schedules prepared in the course of rheological analysis of the above mentioned slag systems.

Table 3

Chosen schedule of measurement

Measurement stage	$\dot{\gamma}$ [s–1]	T [°C]
Step I	15	cooling/homogenization
Step II	A) 15-150 (log) B) 150-15 (log)	Const.
Step III	A) 15-180 (log) B) 180-15 (log)	Const.
Step IV	A) 30, 60, 80, 120, 80, 60, 30, B) 5, 200, 15, 200, 15, 150, 15, 150,	Const.

Measurement schemes, which are presented in table 3, brought results that were later on used to prepare Fig. 3. The data used include step II and III – useful in describing the course of hysteresis reflecting the changes in shear stress.

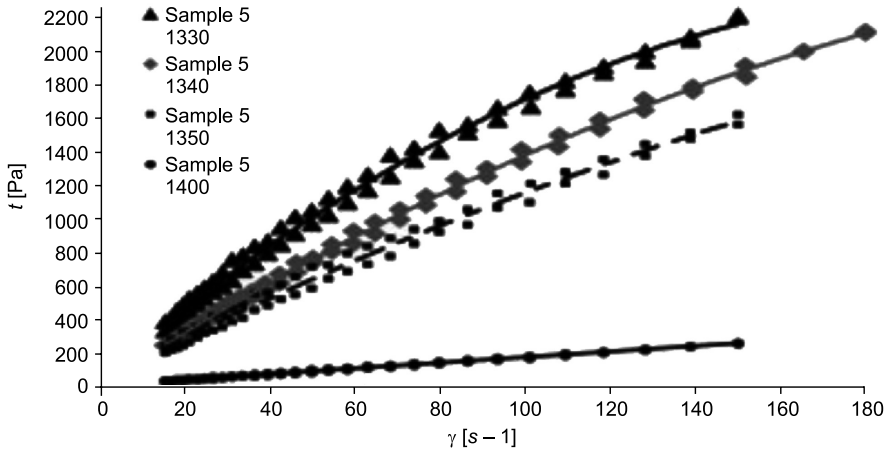

Fig. 3. Flow curves for sample 5 in different temperatures

Rys. 3. Krzywe płynięcia dla próbki 5 w różnych temperaturach

Figure 3 presents the changes in shear stress in the function of shear rate, a standard rheological curve known as – the flow curve. In this case it is a fluid-solvent system in which solid elements precipitated due to a drop in temperature and a change in chemical composition. Sample 5 represents the slag system with the highest content of Al_2O_3 at the level of 25.65 wieght percent.

Table 4 shows function formulas for selected trend lines with the highest regression coefficient R^2 and a set confidence coefficient $\alpha = 0.01$ assuming that the numerousness of each sample is $N = 60$ and the degrees of freedom amount to $n = 58$. The table also shows

Table 4

Function equations for trend lines and τ_0 for sample 5

T [°C]	Sample 5				Solid elements [%]
	Function	R^2	α/n	τ_0 [Pa]	
1330	$-0{,}0507x^2 + 21{,}582x + 65{,}418$	0.994	0.01/58	65.42	13.62
1340	$-0{,}0259x^2 + 16{,}301x + 11{,}461$	0.998	0.01/58	11.46	11.46
1350	$-0{,}0175x^2 + 12{,}904x + 43{,}252$	0.989	0.01/58	43.25	9.14
1400	$1{,}6607x + 7{,}1967$	0.996	0.01/58	7.19	0.00

the calculated value of τ_0 representing a theoretical flow boundary. Each of the calculated regression coefficient was compared to $R_{critical}$ from table 9.2 [22] with a given confidence

coefficient and appropriate degrees of freedom. In case of temperature 1400°C, in which theoretically solid elements are not present, one can observe a change in the function type from a quadratic to a linear one if the criterion of regression coefficient – *R* is assumed.

The results presented in table 4 suggest a change in a rheological character of the system – it becomes very similar to an ideally viscous Newtonian body. It is assumed that this system is fully liquid. A total resemblance of a fully liquid system to an ideal Newtonian body seems to reflect the opinions presented in some of the research papers [2–13].

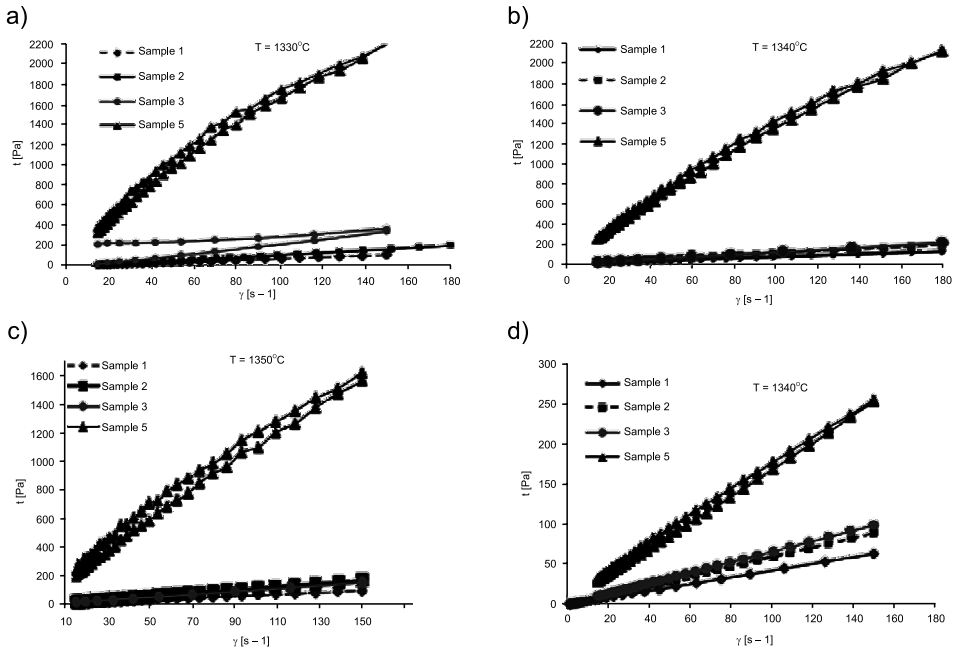

Fig. 4. Flow curves for samples in temperatures a) 1330°C, b) 1340°C, c) 1350°C, d) 1400°C

Rys. 4. Krzywe płynięcia dla próbek w temperaturach: a) 1330°C, b) 1340°C, c) 1350°C, d) 1400°C

Figure 4 presents flow curves for selected samples in the temperature range of 1330––1400°C. Samples 1, 2, 3, 5 represent different chemical composition of slag with admixtures of Al_2O_3. It is clear that slag with the highest concentration of aluminum oxide changes its rheological character as a result of a decrease in temperature. The remaining samples show resemblance to ideally viscous Newtonian flow, in all measured temperatures. Only in case of Fig. 4a for sample 3 the flow curve shows a slight deviation from the similarities to an ideally viscous Newtonian body – it is described by a curve in the form of a slight hysteresis of the flow curve.

Figures 4a, b and d refer to samples which show changes in shear stress depending on the concentration of Al_2O_3 in the system. An increase in aluminum oxide concentration leads to a rise in shear stress (if the shear stress rate values remain constant).

The change in rheological character of the analyzed fluid-solid elements system is caused by the amount of solid elements that precipitated from the system due to a decrease in temperature, to change of shape and size of these elements.

Despite the content of solid elements (calculated theoretically) sample 1 shows similarities to a Newtonian body in temperatures 1330°C and 1340°C (respectively 3,76 and 0,86%). It may be the result of the low mass of the precipitated elements and totally different (in terms of quality) solid elements precipitated in a system with a different chemical composition (described above) in comparison to that of sample 5. In the case of sample 3, however, there are no solid element precipitating in given temperatures according to thermodynamic calculations for a given chemical composition. Despite this fact, there are clear differences between this sample and a Newtonian fluid – it may suggest a significant influence of the internal structure of the fully liquid solution on the rheological character of the fluid.

3. Conclusions and observations

The following can be concluded on the basis of the conducted research and analyses:

- For the slag system $CaO\text{-}SiO_2\text{-}MgO\text{-}Al_2O_3$ (theoretically in a totally liquid state) in the temperatures above 1400°C the analyzed liquid ionic solutions resemble ideally viscous Newtonian fluids;
- In case of the analyzed systems with solid particles the nature of the fluid changes – it is no longer a Newtonian fluid but a system diluted by shearing (a pseudoplastic one) and the shear rate influences the value of the dynamic viscosity coefficient, an increase in $\dot{\gamma}$ causes the viscosity to decrease;
- The amount of solid particles influences the changes in rheological character of the fluid/suspension. Even a small amount of solid particles in the system approx. 11.46-17.55% changes the type of the analyzed fluid from a Newtonian one to a system diluted by shearing. In case of the analyzed system it is not necessary for solid elements to be present in the amount of approx. 40% in order to change its character;
- The type and amount of solid elements in the system and the type of complex anion lattice (in a fully liquid system and also in the remaining liquid part in the solid-liquid system) is an important issue from the point of view of changes in viscosity changes and the rheological character of the fluid. As far as solid-liquid slag systems are concerned, it seems necessary to include shear rate when using Einstein's equation;
- Adding Al_2O_3 to the slag systems causes the amount of solid particles to increase in lower temperatures. It also leads to the polymerization of the viscous part of the system. The slag system changes its character from Newtonian to pseudoplastic.

The question of the internal structure of the strongly polymerized fully liquid slag systems with the addition of solid particles (as presented above) still remains open. So does the influence of the applied shear stress on such a system – this in turn affects the dynamic viscosity coefficient and potentially triggers changes in rheological character of the fluid.

These experiments and studies were conducted as part of statutory research of MEiN number 11.11.110.081.

References

[1] Sasaki Y., Urata H., Iguchi M., Hino M., *Stress Relaxation Behavior with Molten $CaO–SiO_2–Al_2O_3$ Slag*, ISIJ International, vol. 46, 2006, nr 3, pp. 385-387.

[2] Seetharaman S., Mukai K., Sichen D.U., *Viscosity of slags – an overview*, Steel Research Int., vol. 76, 2005, nr 4, pp.267-278.

[3] Seok S., Jung S., Lee Y., Min D., *Viscosity of highly basic slags*, ISIJ Int., vol. 47, 2007, nr 8, pp.1090-1096.

[4] Viswanathan N.N., Ji F.-Z., Sichen D.U., Seetharaman S., *Viscosity Measurements on Some Fayalite Slags*, ISIJ International, vol. 41, 2001,nr 7, pp. 722-727.

[5] Shankar A., Görnerup M., Lahiri A.K., Seetharaman S., *Experimental Investigation of the Viscosities in $CaO–SiO_2–MgO–Al_2O_3$ and $CaO–SiO_2–MgO–Al_2O3–TiO_2$ Slags*, Metallurgical and Mat. Trans. B, vol. 38B, 2007, nr 12, p. 911.

[6] Kondratiev A., Zhao B., Raghunath S., Hayes P.C., Jak E., *New tools for viscosity measurement and modeling of fully liquid and partly crystallised slags*, Proceedings of EMC 2007.

[7] Wright S., Zhang L., Sun S., Jahanshahi S.,*Viscosity of a $CaO–MgO–Al_2O_3–SiO_2$ Melt Containing Spinel Particles at 1646K*, Metallurgical and Mat. Trans. B, vol. 31B, 2000, nr 2, pp. 97-104.

[8] Kondratiev A., Hayes P.C., Jak E., *Development of a Quasi-chemical Viscosity Model for Fully Liquid Slags in the $Al_2O_3–CaO–'FeO'–MgO–SiO_2$ System. Part 1. Description of the Model and Its Application to the MgO, $MgO–SiO_2$, $Al_2O_3–MgO$ and CaO–MgO Sub-systems*, ISIJ International, Vol. 46 (2006), No. 3, pp. 359-367.

[9] Kondratiev A., Hayes P. C., Jak E., *Development of a Quasi-chemical Viscosity Model for Fully Liquid Slags in the $Al_2O_3–CaO–'FeO'–MgO–SiO_2$ System. Part 2. A Review of the Experimental Data and the Model Predictions for the $Al_2O_3–CaO$-MgO, $CaO–MgO–SiO_2$ and $Al_2O_3–MgO–SiO_2$ Systems*, ISIJ International, Vol. 46 (2006), No. 3, pp. 368-374.

[10] Kondratiev A., Hayes P.C., Jak E., *Development of a Quasi-chemical Viscosity Model for Fully Liquid Slags in the $Al_2O_3–CaO–'FeO'–MgO–SiO_2$ System. Part 3. Summary of the Model Predictions for the $Al_2O_3–CaO–MgO–SiO_2$ System and Its Sub-systems*, ISIJ International, Vol. 46 (2006), No. 3, pp. 375-384.

[11] Kondratiev A., Hayes P.C., Jak E., *Development of a Quasi-chemical Viscosity Model for Fully Liquid Slags in the $Al_2O_3–CaO–'FeO'–MgO–SiO_2$ System. The Experimental Data for the 'FeO'–MgO–SiO_2, $CaO–'FeO'–MgO–SiO_2$ and $Al_2O_3–CaO–'FeO'–MgO–SiO_2$ Systems at Iron Saturation*, ISIJ International, Vol. 48, (2008), No. 1, pp. 7-16.

[12] Kondratiev A., Jak E., *Review of Experimental Data and Modeling of the Viscosities of Fully Liquid Slags in the $Al_2O_3–CaO–'FeO'–SiO_2$ System*, Metallurgical And Materials Transactions B Volume 32b, December 2001, 1015.

[13] Mills K.C., Sridhar S., *Viscosities of Ironmaking and Steelmaking Slags*, Ironmaking & Steelmaking, 1999, vol. 26, pp. 262-268.

[14] Ferguson J., Kembłowski Z., *Reologia stosowana płynów*, Wydawnictwo MARCUS, Łódź 1995.

[15] Xie D., Mao Y., Zhu Y., *Viscosity and flow behaviour of TiO_2-containing blast furnace slags under reducing conditions*, VII International Conference on Molten Slags Fluxes and Salts, The South African Institute of Mining and Metallurgy, 2004.

[16] Song M., Shu Q., Sichen D.U., *Viscosities of the Quaternary $Al_2O_3–CaO–MgO–SiO_2$ Slags*, Steel Research Int. 82, 2011, No. 3.

[17] Mills K., *The estimation of slag properties*, Department of Materials, Imperial College, London, UK, Short course presented as part of Southern African Pyrometallurgy 2011.

[18] Boccaccini A.R., Riazc S., Moisescu C., *On the viscosity of glass-crystal systems*, Journal Of Materials Science LETTERS 20, 2001, 1803-1805.
[19] Schramm G., *Reologia- Podstawy i zastosowania*, Haake GmbH, OWN PAN, Poznań 1998.
[20] Migas P., Korolczuk-Hejnak M., Karbowniczek M., *Rheological measurements of selected grades of liquid steels*; Rheology – theory and application, Vol. 2 EKMA, Warszawa 2011.
[21] Korolczuk-Hejnak M., Migas P., *Selected grades of steel as rheologically defined liquid bodies*, No. 2, Vol. 57, 2012.
[22] Volk W., *Statystyka stosowana dla inżynierów*, WNT, 1973.

TECHNICAL TRANSACTIONS | CZASOPISMO TECHNICZNE
CHEMISTRY | CHEMIA
1-Ch/2013

JOANNA PŁOCICA*, BARBARA TAL-FIGIEL, WIESŁAW FIGIEL**

CORRELATION BETWEEN RHEOLOGICAL STUDIES AND ORGANOLEPTIC COSMETIC EMULSION WITH LANOLIN – NATURAL EMULSIFIER

KORELACJA POMIĘDZY BADANIAMI REOLOGICZNYMI I ORGANOLEPTYCZNYMI EMULSJI KOSMETYCZNYCH Z EMULGATOREM NATURALNYM – LANOLINĄ

Abstract

In this paper rheological investigations of cosmetic emulsions, prepared with lanoline as an emulsifier were carried out. The strong influence of emulsifier content and the applicability of rheological measurements to validate cosmetic products were shown.

Keywords: *cosmetic emulsions*, *lanolin mixer*, *rheology*

Streszczenie

W artykule przeprowadzono badania reologiczne emulsji kosmetycznych sporządzonych z wykorzystaniem lanoliny jako emulgatora, za pomocą miksera recepturowego. Wykazano silny wpływ zawartości emulgatora na konsystencję produktu oraz przydatność pomiarów reologicznych do oceny jakości preparatów kosmetycznych

Słowa kluczowe: *emulsje kosmetyczne*, *lanolina*, *reologia*

* MSc. Eng. Joanna Płocica, Krakowska Wyższa Szkoła Zawodowa.
** PhD. Eng. Barbara Tal-Figiel, prof. PK, PhD. Eng. Wiesław Figiel, Institute of Chemical and Process Engineering, Cracow University of Technology.

1. Introduction

The word lanolin comes from the Latin word “lano”, which means wool, since it is obtained from wool fat. When the time for sheeps clipping is approaching, their sebaceous glands secrete a large amount of sebum, which is deposited on the wool. Lanolin is obtained during cleaning of wool since the residual lanolin content of dry, clean wool fibres should not be higher then 2–3%. Surplus fat is collected in form of O/W (oil in water) emulsion, which, after dewatering by centrifugation, is subjected to further purification process. The obtained material is used in cosmetics and pharmacy [1–3].

Pharmaceutical lanolin occurs in the form of golden-yellow sticky mass, with a specific odor, containing no more than 0.25% w/w of water. Chemically it is a complex mixture of esters of high molecular weight aliphatic, steroid and triterpenoid alcohols which does not contain either glycerol or glycerides. It melts in 38–44 °C range [1]. Since the composition of lanolin resembles the intercellular lipids of the stratum corneum, from ancient times it has been used in cosmetics for skin care and presently it is widely used in topical pharmaceutical formulations and cosmetics [4, 5]. As a hydrophobic vehicle, it forms emulsions with water, but due to the presence of polar functional groups it possesses emulsifying properties and can absorb big amount of water; therefore lanolin is used in the preparation of water-in-oil creams, ointments, lipsticks, nail polish remover, hair lotions and deodorants, it ensures the emollient qualities that protect and care for our skin and hair.

Being a natural product with surface active properties, lanolin has many advantages but also some disadvantages, especially from the cosmetic point of view, the most important are: strong smell, high viscosity, yellow color and the poor coating ability. Those negative characteristics can be modified through physical and chemical processes and the resulting derivatives may be better suited to the specific purposes.

The first group of derivatives of the raw lanolin is lanolin modified physically. It is clear, viscous, rubs better on the skin and has a low viscosity. Thus modified it comes in form of liquid, but has all the features of the parent compound. It is used for the manufacturing of face creams, lotions, baby oils, hair preparations and preparations for tanning. The next group of physically modified lanolin may include so-called lanolin wax. It has better W/O emulsifying capabilities than the basic product and also fulfills an important role as a means to maintain the pigment in the skin. Therefore, it is widely used as a thickening agent in hard cosmetic formulations, such as lipsticks. The largest group of lanolin derivatives are its various chemical modifications, which can be performed on raw, physically unmodified product, as well as on liquid lanolin and lanolin waxes. Hydrogenated lanolin is a soft colorless paste. Preparations containing it in its composition are better absorbed through the skin. Acetylated lanolin has a lower melting point and reduced emulsifying properties. It becomes more hydrophobic than the parent product. It is used frequently in sunscreen preparations, especially for children. Also, it rarely causes allergic reaction, and therefore it is used in cosmetics for people with sensitive and injured skin [6].

In this paper three cosmetic type emulsions with various lanolin content were prepared and investigated by sensory and rheological analysis.

2. Experimental

The research part concerned preparation, evaluation and comparison of properties of three lanoline containing cosmetic type emulsions. Different concentrations of pharmaceutical grade lanoline were used according to the recipe. The emulsion compositions are given in Table 1.

Table 1

Cosmetic emulsion formulations.

Sample number	Lanolin [g]	Rice oil [g]	Distilled water [g]	Lanolin concentration [% mas]
1	1.2	14.4	14.4	4
2	1.5	14.25	14.25	5
3	3	13.5	13.5	10

The emulsions were prepared using a pharmaceutical mixer Unguator 2100, by Gako, which became a standard in small scale pharmaceutical preparations. The emulsion+ procedure was used in all cases.

Sensory analysis of emulsions was performed by 50 qualified people (cosmetology students), who were asked to assess their scent, color, texture and spreadability on the skin and complete simple questionnaires.

Table 2

The development of organoleptic tests

Scent	**Color**	**Consistence**	**Spreading on the skin**
unpleasant	colourless	very heavy	very difficult to spread
quite unpleasant	not very intensive	heavy	difficult to spread
middling scent	mid-intensive	mid-heavy	mid-difficult to spread
pleasant	intensive	light	easily spreading
very pleasant	very intensive	very light	very easily spreading

To objectify results for the last two columns, which can bear a highly individual mark, the rheological properties of prepared emulsions were measured using rotational rheometer.

3. The results of the organoleptic tests

Results of organoleptic tests of investigated emulsions are presented graphically below. Fig. 1 shows the results of scent comparison.

Basing on the results of flavor assessment, it can be stated that increase of lanolin concentration makes the scent more pleasant.

The next test covered the consistency of emulsions and its results are shown in Fig. 2.

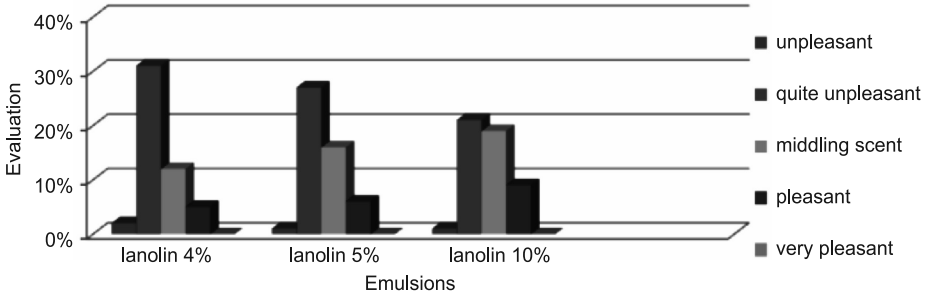

Fig. 1. Rating flavor of three lanoline containing emulsions

Rys. 1. Ocena zapachu trzech emulsji zawierających lanolinę

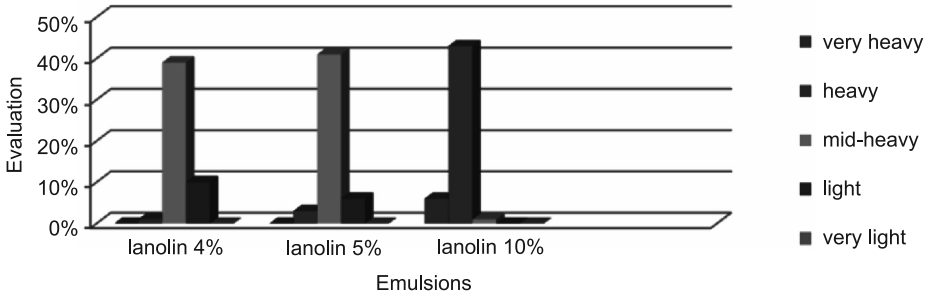

Fig. 2. Consistency rating of three cosmetic emulsions (lanolin-water-rice oil), containing 4%, 5%, and 10% of lanolin

Rys. 2. Ocena konsystencji trzech emulsji kosmetycznych (lanolina-woda-olej ryżowy) zawierających 4%, 5% i 10% lanoliny

The results of consistency assessment can be summarized as: increase of lanolin concentration in the cosmetic emulsion makes it heavier.

The comparison results of emulsion color are presented in Fig. 3.

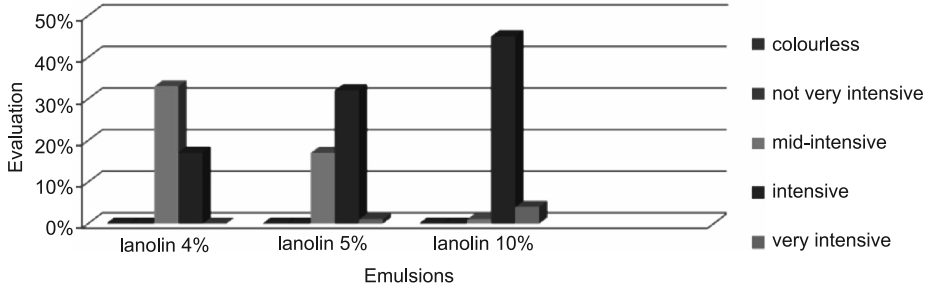

Fig. 3. Assessment of color in three cosmetic emulsions (lanolin-water-rice oil), containing 4%, 5% and 10% of lanolin

Rys. 3. Ocena koloru trzech emulsji kosmetycznych (lanolina-woda-olej ryżowy) zawierających 4%, 5% i 10% lanoliny

Based on the study of color, it can be concluded that the greater the lanolin concentration in emulsion, the more intense the color.

The spreading tests are closely related to consistency. Their results are presented in Fig. 4.

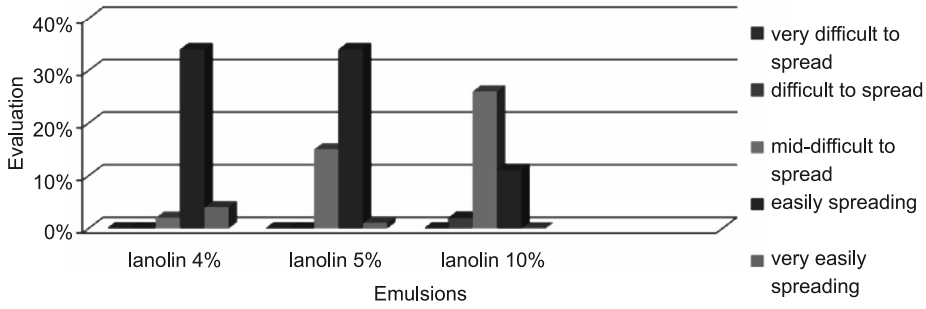

Fig. 4. Assessment of spreading of a cosmetic emulsion (lanolin-water-rice oil) on the skin, with concentrations of 4%, 5% and 10% of lanolin

Rys. 4. Ocena rozprowadzania na skórze emulsji kosmetycznych (lanolina-woda-olej ryżowy) zawierających 4%, 5% i 10% lanoliny

From this figure it can be concluded that the amount of lanolin in the cosmetic emulsion affect its spreading ease. Increasing the concentration of emulsifier in a cosmetic preparation results in difficulties with smearing on the skin.

4. The rheological tests

Along with sensory evaluation, rheological tests were performed. The study of rheological characteristics of cosmetic emulsions was made with rotational rheometer HAAKE RS75, using cone-plate system with 60 mm diameter and 0.5° angle.

Rheological properties were tested at 32 °C and 37 °C. The first one corresponds to skin temperature (direct application temperature), the second to human body temperature (prolonged action). As a basic test, flow curves were determined.

In Figure 5 flow curves representing the cosmetic emulsion (lanolin-water-rice oil), with various lanolin concentrations are shown. It can be seen that increase of lanoline concentration in the emulsion leads to an increase of yield stress, which corresponds to consistence tests results.

The next graph shows viscosity curves of investigated emulsions taken at 32 °C, within the typical shear rate range. The increase in viscosity is proportional to the concentration of emulsifier in the studied emulsions.

Next figures show results of analogous tests performed at 37 °C, which is close to lanolin melting temperature. No qualitative differences can be observed. It which suggests that within the investigated compositions lanolin is completely dissolved in the emulsion.

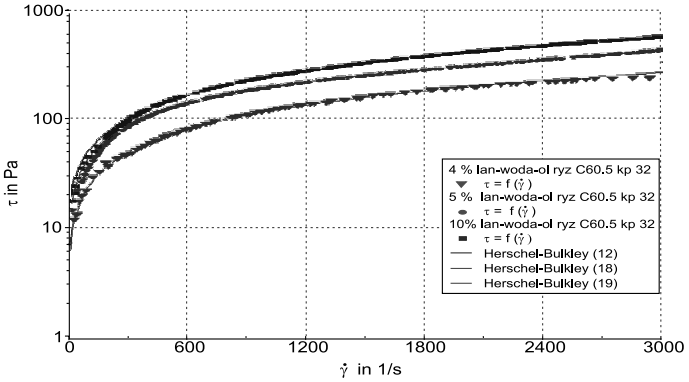

Fig. 5. Flow curves of cosmetic emulsions lanolin-water-rice oil at 32 °C

Rys. 5. Krzywe płynięcia emulsji kosmetycznych lanolina-woda-olej ryżowy w temperaturze 32 °C

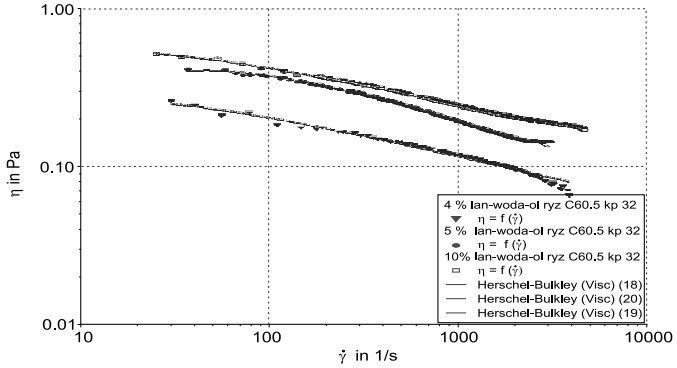

Fig. 6. Viscosity of lanolin-water-rice oil emulsions as a function of shear rate at 32 °C

Rys. 6. Lepkość emulsji w funkcji szybkości ścinania w temperaturze 32 °C

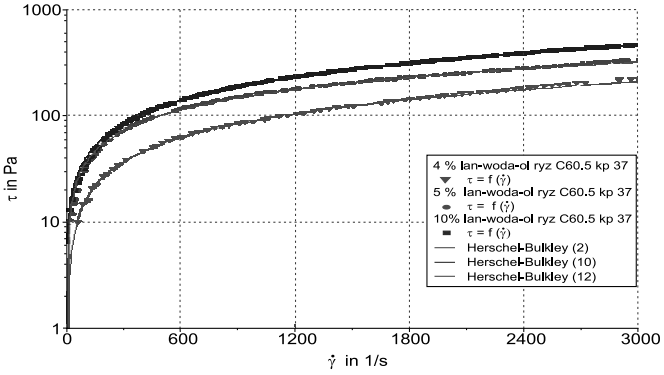

Fig. 7. Effect of lanolin concentration on the flowcurve, for lanolin-water-rice oil at 37 °C

Rys. 7. Wpływ stężenia lanoliny na krzywą płynięcia emulsji kosmetycznej lanolina-woda--olej ryżowy w temperaturze 37 °C

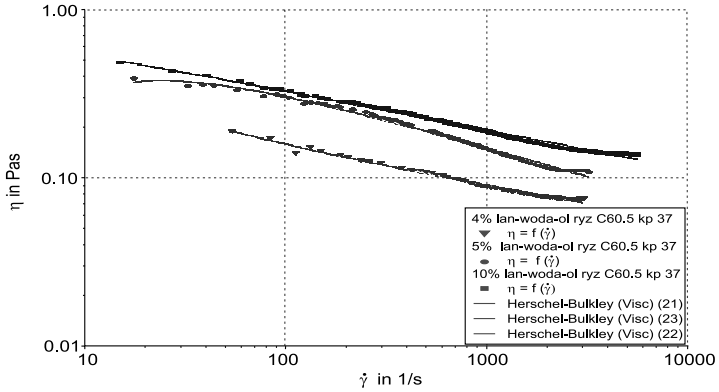

Fig. 8. The viscosity of the cosmetic emulsion lanolin-water-rice oil for various emulsifier concentrations at 37 °C

Rys. 8. Lepkość emulsji kosmetycznej lanolina-woda-olej ryżowy w temperaturze 37 °C

The measurements at different temperatures (32 °C and 37 °C), showed , significant increase in yield stress with increasing concentration of lanolin. The dependence of viscosity on shear stress for the highest lanolin concentration is shown in Fig. 9.

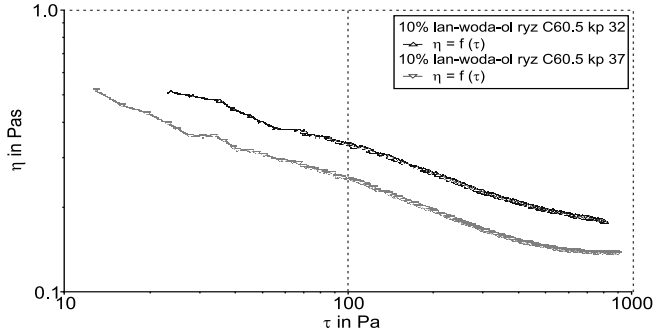

Fig. 9. Effect of temperature on the viscosity as a function of shear stress for 10% lanolin emulsions

Rys. 9. Wpływ temperatury na lepkość 10% emulsji lanoliny w funkcji naprężenia ścinającego

The pattern of all curves indicate that all investigated emulsions are non-Newtonian. Their flow and viscosity curves can be satisfactorily approximated with Herschel-Bulkley rheological model.

5. Conclusions

In this work investigations of cosmetic type emulsions with lanolin acting as an emulsifier as well as rheology modifier, were carried out. Those results can be of some importance, since many synthetic rheology modifiers may lead to allergic reactions, and lanoline as a natural product can be applied instead, giving wide possibilities of controlling the consistency and texture of creams and ointments.

Organoleptic tests revealed that unmodified lanolin can be accepted by majority of testers, even at higher concentrations. Their results, especially those concerning consistency and spreadability, are in a close relationship with rheological properties.

Yield point value is important when testing spreading of emulsion on the skin, and its value affects the subjective assessment of the consistency of respondents. The lowest value of yield stress has an emulsion containing the lowest concentration of lanolin (4%). It corresponds to an organoleptic consistency evaluation results. Viscosity curves presented in Figures 6 and 8 show the highest decrease in viscosity in the case of a cosmetic emulsion containing the lowest concentration used in the system lanolin-water-rice oil. It confirms its high organoleptic assessment of the ease of spreadability.

Theese results confirm that properly conducted rheological measurements allow for a quick and objective emulsion parameters check.

References

[1] Alzaga R., Pascual E., Erra P., Bayona J.M., *Development of novel supercritical fluid extraction procedure for lanolin extraction from raw wool*, Anal. Chim. Acta, 1999, 381, 39-48.
[2] Yao L., Hamond E.G., *Isolation and melting properties of branched-chain esters from lanolin*, JAOCS, 2006, 83, 547-552.
[3] Żmudzińska M., Czarnecka-Operacz M., *Zjawisko paradoksu lanoliny*, Postępy Dermatologii i Alergologii, 2008, XXV, 2, 66-68.
[4] Malinka W., *Zarys chemii kosmetycznej*, Volumed, Wrocław 1999.
[5] Jurkowska S., *Surowce kosmetyczne*, Wydanie IX, Wyższa Szkoła Fizykoterapii, Wrocław 2006.
[6] Mrukot M., *Receptariusz kosmetyczny*, Wydanie I, Wydawnictwo MWSZ, Kraków 2004.

TECHNICAL TRANSACTIONS | CZASOPISMO TECHNICZNE
CHEMISTRY | CHEMIA
1-Ch/2013

MAGDALENA ROSA*, MAGDALENA KWIECIEŃ**, BARBARA TAL-FIGIEL***

RHEOLOGICAL INVESTIGATIONS OF PHARMACEUTICAL EMULSIONS PREPARED WITH MODIFIED LECITHIN

BADANIA REOLOGICZNE EMULSJI FARMACEUTYCZNYCH SPORZĄDZONYCH Z ZASTOSOWANIEM MODYFIKOWANEJ LECYTYNY

Abstract

In this paper the results of rheological investigations of pharmaceutical microemulsions prepared using modern lecithine derived emulsifiers has been prevented out. High stability of obtained systems and wide possibilities of controlling rheological parameters were found.

Keywords: *microemulsion*, *lecithin*, *rheology*

Streszczenie

W artykule przedstawiono wyniki badań reologicznych mikroemulsji farmaceutycznych, sporządzonych z wykorzystaniem nowoczesnych emulgatorów na bazie lecytyny. Stwierdzono wysoką stabilność tych układów oraz duże możliwości regulowania właściwości reologicznych.

Słowa kluczowe: *mikroemulsion*, *lecytyna*, *reologia*

* MSc. Eng. Magdalena Rosa, Koło Naukowe Chemików, Cracow University of Technology.
** MSc. Eng. Magdalena Kwiecień, Lurgi S.A.
*** PhD. Eng. Barbara Tal-Figiel, prof. PK, Institute of Chemical and Process Engineering, Cracow University of Technology.

1. Introduction

Development of modern pharmaceuticals is a complex process, consuming both time and money. In case of topical medications progress made in recent years enabled the elaboration of completely new types of pharmaceutical vehicles which transfer medical substances through the skin or mucosa by means of polymers, gels, emulsions and microemulsions [1]. Those materials exhibit various rheological properties, therefore determination of their flow properties, which are different from those of traditional ointment bases, is necessary when designing new pharmaceutical, as well as cosmetic products. Growing requirements for quality of final products and competition between producers require extended rheologial investigation of raw materials to select optimal process parameters as well as the readymade product, to evaluate its stability and textural characteristics [2].

In this work several medical-type microemulsions, which use modified lecithin as surfactant and rheology modifier, were prepared with the aid of a pharmaceutical mixer – Unguator 2100® by GAKO, and their rheological properties were determined using appropriate measurement procedures. Obtained flow curves confirmed non-Newtonian nature of microemulsions investigated and were interpreted using basic rheological models.

2. Multiphase therapeutic systems

Many of the pharmaceutically active substances have very low solubility in water. In these cases so called vehicle is needed to increase the solubility of active compound [3]. The typical systems which facilitate are:

- solvents which can be mixed with water;
- surfactants forming aggregates;
- complexing agents;
- emulsions.

Unfortunately, these traditional systems have various drawbacks, especially concerning stability. Pharmaceutical products come in form of multiphase systems, usually with high degree of dispersion. The particles can be solid, as in case of suspensions, or liquid as in emulsions. Individual droplet size in typical stable pharmaceutical emulsion is usually below 10 μm. Due to strong interactions of particles, such products usually show features of non-Newtonian fluids. To weaken these phenomena and enhance emulsion stability, various types of surfactants have to be added [4]. When the amount of surfactant is small, the system can be treated as typical oil-water, with lowered interfacial tension. In such systems, there is no direct contact between water and oil phases, because of surfactant molecules being adsorbed at the interphase. When the amount of surfactant in the solution exceeds the critical micellisation concentration, association of surfactant molecules contained in the solvent begins. They combine into larger aggregates, micelles or reverse micelles, depending on the type of solvent. As the amount of surfactant rises further, the system can no longer be treated by this simplified method, and becomes oil-water-Surfactant rather than oil-water. Surplus of surfactants leads to generation of surfactant molecules structures, much more complicated than simple micelles [5]. The interfacial tension in such systems is close to zero, and instead

of typical disperse system consisting of continuous phase and dispersed phase droplets, dispersed structures with periodic order of complex objects are formed. When the amount of surfactant is sufficiently high, the interface becomes disordered and bicontinuous structures emerge. Those systems, known under name of microemulsions, are thermodynamically stable and can be formed with low addition of external energy. They are also transparent, what makes them attractive for pharmaceutical usage.

Winsor classification of such systems takes into account the impact of surfactant with water and oil phases and depending on it, divides microemulsions into four groups:

- Type I, in which the surfactant is soluble both in water and oil in microemulsion O/W. Water phase, which contains a large amount of surfactant coexists with an oil phase containing a small amount of surfactant.
- Type II, in which the surfactant is present mainly in the oil phase in microemulsion W/O. The oil phase coexists with an aqueous phase, in which the surfactant is very low.
- Type III, three-phase arrangement, in which intermediate phase containing large amounts of surfactant exists in parallel with the phases of water and oil.
- Type IV, where there isotropic (single phase) micellar solution occurs.

Presently many pharmaceutical and cosmetic systems come in form of microemulsion. The main difference between microemulsion and common emulsion lies not in size of droplets or degree of cloudiness, but in the fact that they form spontaneously when proper composition is attained, and their properties are independent of production method [6]. Microemulsions can be prepared by mixing the components together in no particular order so to allow the mixture to equilibrate for certain time. The biggest difficulty in their production is that since in case of pharmaceutical systems many components are of natural origin and come from a various sources, the concentrations of the final product have to be optimized for each batch.

Under the influence of increasing concentration of the electrolyte (the ionic surfactants), or increasing temperature (for nonionic surfactants), the phases are subject to change.

There are also other forms of the microemulsions, including [7]:

- combined micelles,
- onion structure with diverse internal structure,
- bubble structure.

The primary factors that influence the structure of microemulsions include the shape of surfactant molecules and such properties of the solvent as ionic strength and pH. Interfacial tension between the aqueous and oil phases in microemulsions attain the value of 10^{-2}–10^{-4} [mNm]. The stability of the microemulsion systems are affected by following physical parameters: density, viscosity, interfacial tension, pH, osmotic pressure, refractive index and particle size [5].

Advantages of microemulsions are very large surface area between the phase and the ability to dissolve components of different polarity. To obtain them, a great amount of surfactant is needed. To avoid usage of synthetic emulsifiers, in pharmaceutical, cosmetic and food products natural-based surfactants are used. One of them is lecithin. Lecithin is the common name for a series of related compounds called phosphatidylcholines combined with various other substances, like fatty acids and carbohydrates. Its name originated from the Greek “Lekithos”, referring to egg yolk, but it is also found in many animal and vegetable sources. Lecithins are prepared by extracting and purifying phospholipids from

naturally occurring products such as soybeans, eggs, sunflower and canola seeds. It is an edible and digestible surfactant and emulsifier. Lecithins also have characteristics that help to control the viscosity of liquids and semi-liquids and disperse and suspend powders into liquids. Compared with its synthetic alternatives, lecithin can be totally biodegraded and metabolised. Therefore, it is is regarded as a well tolerated and non-toxic compound, which is used as an emulsifying and stabilizing agent in the food, pharmaceutical, and cosmetic industries. Lecithins are amphiphilic (they have different affinities for oil and water), and their low production costs make them invaluable in a broad range of manufacturing processes. Commercial sources for lecithin may come from soybeans, egg yolk or brain tissue. Although extensive research in this field has been done, there is still disagreement about lecithin based emulsion structure and the influence of the emulsifier. Therefore, it is essential to understand the behaviour of lecithin in order to understand the behaviour of emulsions stabilised with it. The rheological measurements can give some insight in this matter. In the experimental part the pharmaceutic type microemulsions were prepared using three types of commercial lecithin's: deoiled phosphatidyl choline enriched lecithins Epikuron™ 170 and Epikuron™ 200 and hydrogenated phosphatidyl choline enriched lecithin Epikuron™ 200 SH.

3. Experimental

The following basic components were used:

The oil phase:

- oleic acid,
- IPM (isopropyl myristate),
- Epicuron 200 SH,
- Epicuron 200,
- Epicuron 170.

The aqueous phase:

- buffer – PBS (stable solution of 0.85% NaCl, pH = 7.4).

The surfactant:

- Span 80.

Co-surfactants:

- Ethanol,
- Isopropanol (water solutions).

The compositions of systems investigated are given in Table 1.

Microemulsions were prepared at room temperature (20 °C). The first step was preparation of the oil phase (Epicuron, oleic acid, IPM) with co-surfactant (isopropanol, ethanol). These components had been preliminarily mixed using a magnetic stirrer. In the next step aqueous phase (PBS) and surfactant (Span) were added, and mixing was continued for 30 minutes. Prepared premixes were finally processed with UNGUATOR mixer, using "emulsion" program. It is a factory programmed procedure lasting two minutes while the rotational frequency changes within 250–2500 [min^{-1}] range [8].

Table 1

Composision of systems investigated

Emulsion	Recipe	Ingredient	Amount [g], [ml]
A	1	Epicuron 200SH	5,0 g
		IPM	5,0 ml
		Isopropanol 25 %	5,0 ml
		PBS	5,0 ml
	2	Epicuron 200SH	5,0 g
		IPM	5,0 ml
		Isopropanol 30%	5,0 ml
		PBS	5,0 ml
	3	Epicuron 200SH	5,0 g
		IPM	5,0 ml
		Isopropanol 50%	5,0 ml
		PBS	5,0 ml
B	4	Oleic acid	38,5
		Span 80	7,7
		Ethanol 96%	38,5
		PBS	15,4
C	5	Epicuron 200	5,0 g
		IPM	5,0 ml
		Isopropanol 25 %	5,0 ml
		PBS	5,0 ml
	6	Epicuron 200	5,0 g
		IPM	5,0 ml
		Isopropanol 30%	5,0 ml
		PBS	5,0 ml
	7	Epicuron 200	5,0 g
		IPM	5,0 ml
		Isopropanol 50%	5,0 ml
		PBS	5,0 ml
D	8	Epicuron 170	5,0 g
		IPM	5,0 ml
		Isopropanol 25 %	5,0 ml
		PBS	5,0 ml
	9	Epicuron 170	5,0 g
		IPM	5,0 ml
		Isopropanol 30%	5,0 ml
		PBS	5,0 ml
	10	Epicuron 170	5,0 g
		IPM	5,0 ml
		Isopropanol 50%	5,0 ml
		PBS	5,0 ml

Obtained mixtures were translucent and did not show any heterogeneities under optical microscope, so it was assumed, that they were microemulsions. Additonally they did not show any signs of deterioration during two months.

Rheological investigations were conducted using a rotational rheometer HAAKE RS75. Measurement system uses a cone-plate (titanium cone with a diameter of 20 mm and an angle of 0.3 °). Measurements were taken at three temperatures: 6 °C – typical refrigerator storage temperature, 20 °C – temperature of microemulsions preparation and 32 °C – temperature of formulations application on human skin. The temperature was controlled by HAAKE K15/DC5 circulator. Tests were performed using two measurement modes: flow curve and thixotropy.

4. Results

The results of measurements are presented graphically. All tested microemulsions are non-Newtonian fluids. Figure 1 shows temperature dependence of D-type microemulsion obtained with isopropanol as co-surfactant at concentration of 50%. With increasing temperature noticeable decrease of yield stress can be observed.

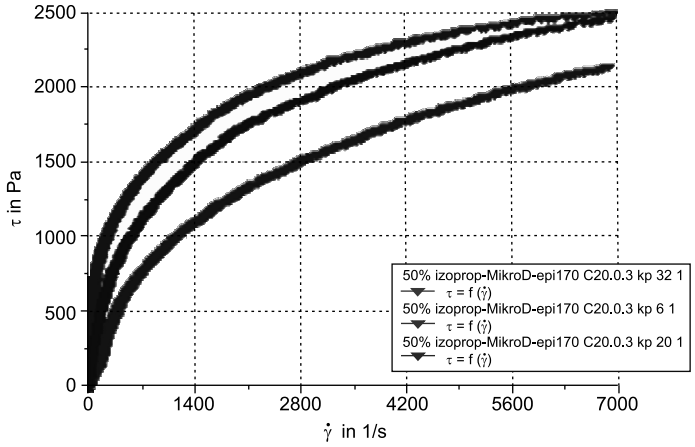

Fig. 1. Flow curves of microemulsion D with 50 % of isopropanol as a temperature function

Rys. 1. Krzywe płynięcia mikroemulsji D z 50% stężeniem izopropanolu w funkcji temperatury

Hysteresis loops shown in Figure 3 have different surfaces depending on the temperature of measurement. At 6 °C microemulsion structure is more compact, thus there is no change in the structure of the preparation.

For the analysis of measurements, two basic rheological models, Ostwald-de Waele and Herschel-Bulkley were used.

The Ostwald-de Waele model is a relatively simple mathematical expression. Although it does not allow for the interpretation of yield stress, it gives satisfactory results for the practical, non zero, range of shear rates (Fig. 3).

Herschel-Bulkley model gives similar results (Fig. 4), but the yield stress value estimate is not always reliable (negative values frequently appear).

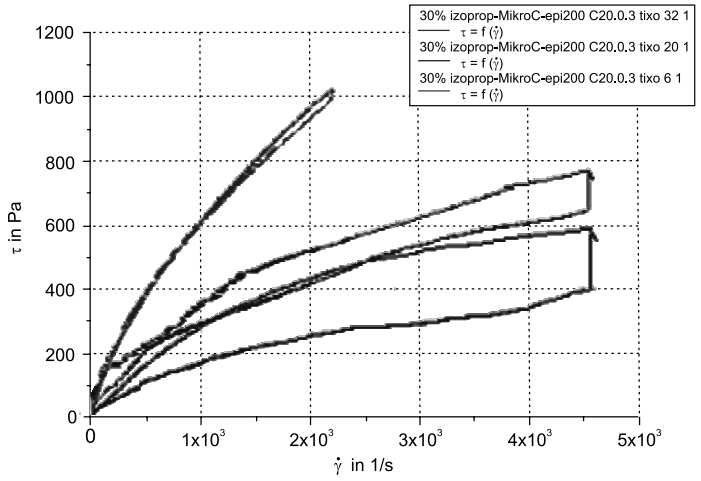

Fig. 2. Thixotropy of microemulsion C with 30% of isopropanol as a temperature function
Rys. 2. Tiksotropia mikroemulsji C z 30% stężeniem izopropanolu w funkcji temperatury

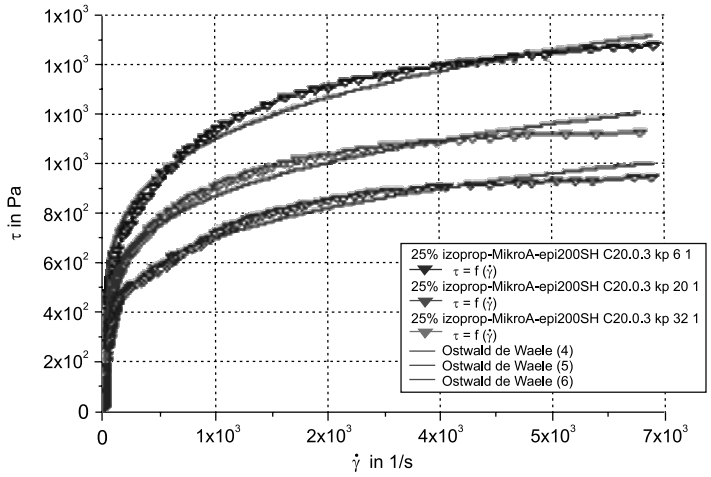

Fig. 3. Approximation of flow curves microemulsion A (25% of isopropanol) by using Ostwald de Waele rheological model
Rys. 3. Aproksymacja krzywych płynięcia mikroemulsji A (25% stężenie izopropanolu) modelem reologicznym Ostwald de Waele

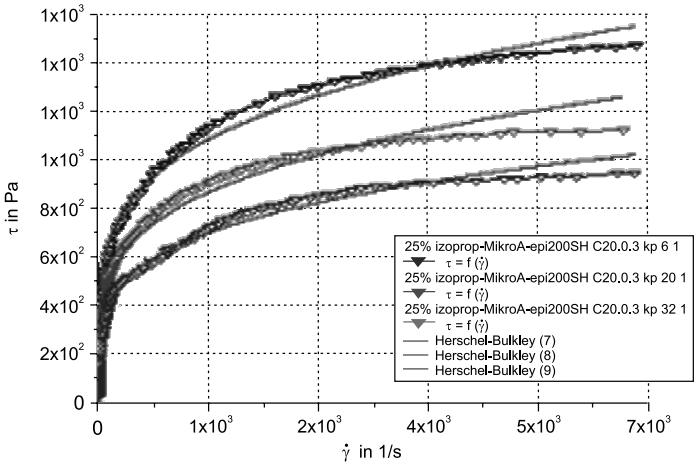

Fig. 4. Approximation of flow curves microemulsion A (25% of isopropanol) by using Herschel-Bulkley rheological model

Rys. 4. Aproksymacja krzywych płynięcia mikroemulsji A (25% stężenie izopropanolu) modelem reologicznym Herschel-Bulkley

5. Conclusions

Microemulsions are peculiar dispersions that in recent years gained great importance in many industries, especially in pharmacy, as a substrate and drug carriers, helping to increase the bioavailability of therapeutic agents and the effectiveness of drugs. Their rheological investigations are important to get complete physical tests.

Investigated microemulsions were found to be non-Newtonian fluids with yield point. With increase of temperature the measured values of yield stress and viscosity decreased, it can therefore be concluded that at 32 °C, the temperature of human skin, the pharmaceutical microemulsions exhibit improved properties, which makes their application easier.

For the analysis of experimental results of the flow curves, approximations using rheological model of Ostwald-de Waele and Herschel-Bulkley'a models were performed. Fitting with these models delivered good results- within the practical shear rate range, the regression line practically coincides with the experimental flow curves.

References

[1] *Mechanisms of Transdermal Drug Delivery*, Potts R.O., Guy R.H. [eds.], Marcel Dekker Inc, New York 1997.

[2] Tal-Figiel B., Figiel W., *Micro-and Nanoemulsions in Cosmetics and Pharmaceutical Products*, Journal of Dispersion Science and Technology, 2008.

[3] Mollet H., Grubernann A., *Formulation Technology*, Wiley-VCH, Weinheim, 2001.

[4] Malmsten M., *Surfactants and Polymers in Drug Delivery*, Marcel Dekker Inc, New York 2002.
[5] Fanum M., *Microemulsions Properties and Applications*, CRC Press, Boca Raton 2009.
[6] Tal-Figiel B., *Emulsions in cosmetics and medicine*, Inż. Chem. Proc., 27, 403-419, 2006.
[7] Chai J.L., Gao Y.H., Zhao K.S., Li G.Z., Zhang G.Y., *Studies on the Phase Properties of Winsor I-III Type Microemulsions with Dielectric Relaxation Spectroscopy*, Chin. Chem. Lett., **16**, No. 9, 1263-1266, 2005.
[8] Maciejewska A., *Unguator 2100-Practical User's Guide*, Eprus-B 2009, Version 1.0.

TECHNICAL TRANSACTIONS | CZASOPISMO TECHNICZNE
CHEMISTRY | CHEMIA
1-Ch/2013

BARBARA TAL-FIGIEL, AGNIESZKA KULAWIK-PIÓRO*

RHEOLOGICAL PROPERTIES OF PRIMARY PHARMACEUTICAL EMULSIONS OBTAINED BY HOMOGENIZATION

WŁAŚCIWOŚCI REOLOGICZNE EMULSJI PIERWOTNYCH O POTENCJALNYM ZNACZENIU FARMACEUTYCZNYM WYTWORZONYCH TECHNIKĄ EMULGOWANIA PRZY UŻYCIU HOMOGENIZATORA

Abstract

The paper presents the results of rheological examinations of primary emulsions with the potential for pharmaceutical applications, created through emulsification using a homogeniser. The water phase of the examined emulsions was made up of water solutions of hydrocolloids, the fatty phase was the pharmaceutical oil Miglyol 812N and canola oil, sunflower seed oil, olive oil. For the determination of relations between the structural parameters of the emulsions and their viscous properties flow curves and viscosity curves were obtained for the examined systems. The obtained results were processed through regression of experimental points by rheological equations, using the own software of the rheometer.

Keywords: *emulsion*, *rheology*, *flow and viscosity curve*

Streszczenie

W artykule przedstawiono wyniki badań reologicznych emulsji pierwotnych o potencjalnym znaczeniu farmaceutycznym, wytworzonych techniką emulgowania z użyciem homogenizatora. Fazę wodną badanych emulsji stanowiły wodne roztwory hydrokoloidów, fazę tłuszczową faza farmaceutyczna Miglyol 812N oraz olej rzepakowy, słonecznikowy, olej oliwkowy. Do określenia zależności pomiędzy parametrami strukturalnymi emulsji a ich właściwościami lepkimi wyznaczono krzywe płynięcia i lepkościowe dla badanych układów. Uzyskane wyniki badań opracowano drogą regresji punktów doświadczalnych za pomocą równań reologicznych, z użyciem oprogramowania firmowego reometru.

Słowa kluczowe: *emulsje*, *reologia*, *krzywe płynięcia i lepkościowe*

* PhD. Eng. Barbara Tal-Figiel, prof. PK, MSc. Eng. Agnieszka Kulawik-Pióro, Institute of Chemical and Process Engineering, Faculty of Chemical Engineering and Technology, Cracow University of Technology.

Designations

HPMC – hydroxypropylmethylcellulose
$\dot{Z}$ – gelatine solution
n – homogeniser rotational speed [s^{-1}]
t – emulsification time [s]
ϕ_{mas} – percentage of mass of dispersed phase in emulsions
τ – shear stress [Pa]
η – dynamic viscosity coefficient [Pa·s]
$\dot{\gamma}$ – shear rate [s^{-1}]
τ_0 – yield stress [Pa]
η_p – elastic viscosity [Pa·s]
n – characteristic flow coefficient [–]
K, η_∞, η_b – correlation equation factors

1. Introduction

Tablets quickly dissolving in the mouth are a modern form of medicine, which is a solution to the common problem of swallowing of a traditional form of medicine – a tablet [1–3]. Such systems are manufactured using techniques such as: lyophilisation, spray drying, granulation, sublimation, direct compression. In lyophilisation and spray drying, the substance subjected to drying is the so-called primary emulsion, which turns into a dry emulsion [4–15]. In this case, the properties of a tablets quickly dissolving in the mouth such as disintegration time, reconstruction ability and bioavailability, are closely related to the physical and chemical properties of primary emulsions.

According to the Polish Pharmacopoeia 7th Edition, tablets quickly dissolving in the mouth are systems for which the disintegration time is lower than three minutes [16]. Literature data shows that the lower the viscosity of primary emulsions, the shorter the disintegration time, because excessively high viscosity of primary emulsions may, according to authors, [4, 6, 7, 17] lower the ability of a porous structure, which determines the disintegration times, to be formed.

The rheological research described in literature concerning rheological properties of primary emulsions is not complete. It do not allow the description of general properties which would enable a quantitative, and not only qualitative, description of these systems. It thus seems purposeful to conduct complete examinations of prime emulsions, which should encompass an analysis of the flow and viscosity curves, and a verification of the obtained results through theoretical models.

2. Materials and research methods

The subject of the research were oil-in-water primary emulsions obtained through emulsification using a homogeniser. The emulsions were manufactured using the Miccra D-9

homogeniser, with a rotational speed range of n = 183.3–650 s^{-1}. The emulsification time was t = 60–300 s.

The water phase of the emulsions was made up of liquid solutions of hydrocolloids, i.e. a 2% by mass water solution of HPMC, a 1.5% by mass water solution of *Ż*, and their mixture. The mass ratio of *Ż*/HPMC was 44:1.

Miglyol 812N pharmaceutical oil, olive oil, canola oil and sunflower seed oil were used as the oil phase of the primary emulsions. The content of the fatty phase was ϕ_{mas} = 0.1–0.3.

The produced primary emulsions were subject to rheological examinations, which entailed the determination of flow and viscosity curves of the primary emulsions.

The flow and viscosity curves were obtained using the RS 75 rotational rheometer from Haake. The rheometer was controlled through a PC connected to the rheometer, using the RheoWin 3.61 specialist rheometer control application.

The examinations were carried out using a cone-plate set-up, angle 0,5°C; diameter 20 mm. Measurement temperature was 293 K, working mode CS, volume of examined sample – 1 cm^3.

Using the proprietary software of the rheometer a regression of the examination points was conducted. The flow curve equations presented in table 1 were used for this purpose.

Table 1

Mathematical equations describing the rheological behaviour of fluids

Item	Authors	Flow curve equation	Viscosity curve equation
1.	Bingham	$\tau = \tau_y + \eta_p \dot{\gamma}$	$\eta = \frac{\tau_y}{\dot{\gamma}} + \eta_p$
2.	Ostwald de Waele	$\tau = K\dot{\gamma}^n$	$\eta = K\dot{\gamma}^{n-1}$
3.	Herschel Bulkley	$\tau = \tau_y + K\dot{\gamma}^n$	$\eta = \frac{\tau_y}{\dot{\gamma}} + K\dot{\gamma}^{n-1}$
4.	Casson	$\tau = \sqrt[n]{\tau_y^n + (\eta_\infty \dot{\gamma})^n}$	$\eta = \sqrt[n]{\left(\frac{\tau_y}{\dot{\gamma}}\right)^n + (\eta_\infty)^n}$
5.	Windhab	$\tau = \tau_y + \eta_\infty \dot{\gamma} + (\tau_1 - \tau_y)(1 - e^{-\dot{\gamma}/\gamma^*})$	$\eta = \frac{\tau_y}{\dot{\gamma}} + \eta_\infty + (\tau_1 - \tau_y)(1 - e^{-\dot{\gamma}/\dot{\gamma}^*})$
6.	Tscheuschner	$\tau = \dot{\gamma}(\eta_\infty + \tau_y / \dot{\gamma} + \eta_b / (\dot{\gamma} / \dot{\gamma}_b)^n)$	$\eta = (\eta_\infty + \tau_y / \dot{\gamma} + \eta_b / (\dot{\gamma} / \dot{\gamma}_b)^n)$

3. Examination results, discussion

Own research had shown that the primary emulsions belonged to a group of non-Newtonian liquids – shear thinning, showing a yield stress (Fig. 1). The type of water phase used did not alter the characteristics of the flow curve, however it influenced the value of the

yield stress. Low yield stress values showed that the examined primary emulsions have weak flow abilities.

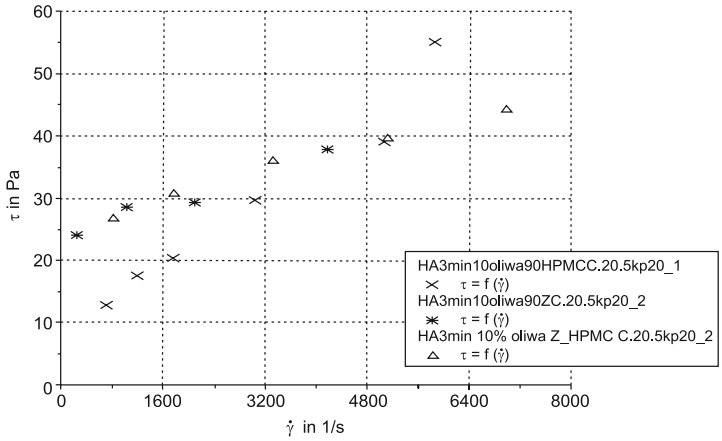

Fig. 1. Flow curves for primary blank emulsions, oil phase olive oil $\phi_{mas} = 0.1$, water phase water solutions of thickening agents 90% by mass: x – 2% HPMC by mass, ∗ – 1.5% *Ż* by mass., Δ – 1.5% *Ż* by mass, 2% HPMC by mass (mass ratio *Ż*/HPMC 44:1), $n = 183.3$ s^{-1}, $t = 180$ s

Rys. 1. Przebieg krzywych płynięcia dla emulsji pierwotnych blank, faza tłuszczowa olej oliwkowy $\phi_{mas} = 0{,}1$, faza wodna wodne roztwory zagęstników 90% mas.: x – 2% mas. HPMC, ∗ – 1,5% mas. *Ż*, Δ – 1,5% mas. *Ż*, 2% mas. HPMC (stos. mas. *Ż*/HPMC 44:1), $n = 183{,}3$ s^{-1}, $t = 180$ s

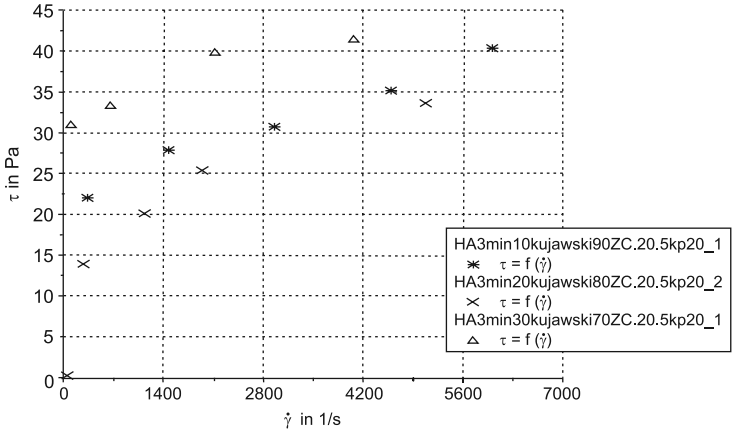

Fig. 2. Flow curves for primary blank emulsions, oil phase 'Kujawski' cooking oil, ∗ – $\phi_{mas} = 0.1$; x – $\phi_{mas} = 0.2$; Δ – $\phi_{mas} = 0{,}3$; water phase 1.5% by mass *Ż* water solution, $t = 180$ s, $n = 183.3$ s^{-1}

Rys. 2. Przebieg krzywych płynięcia emulsji pierwotnych blank, faza tłuszczowa olej Kujawski, ∗ – $\phi_{mas} = 0{,}1$; x – $\phi_{mas} = 0{,}2$; Δ – $\phi_{mas} = 0{,}3$; faza wodna 1,5% mas. wodny roztwór *Ż*, $t = 180$ s, $n = 183{,}3$ s^{-1}

Own research had shown that with an increase in the share of the fatty phase in the blank primary emulsion preparation, the value of the flow limit tended to increase (Fig. 2).

In the analysed range of emulsification times the flow curves of the primary emulsions blank overlapped (Fig. 3).

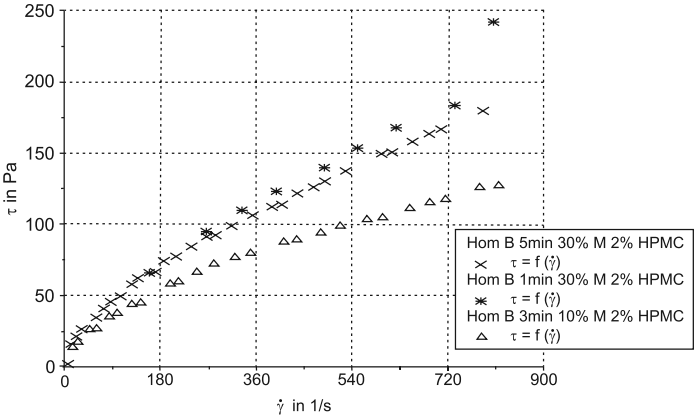

Fig. 3. Flow curves for primary blank emulsions, water phase 70% by mass 2% HPMC by mass, oil phase Miglyol 812N $\phi_{mas} = 0.3$; $n = 266.6\ s^{-1}$, emulsification time: $* - t = 60$ s, $x - t = 180$ s, $\Delta - t = 300$ s

Rys. 3. Krzywe płynięcia emulsji pierwotnych blank, fazę wodna 70% mas. 2% mas. HPMC, faza tłuszczowa Miglyol 812N $\phi_{mas} = 0{,}3$; $n = 266{,}6\ s^{-1}$, czas emulgowania: $* - t = 60$ s, $x - t = 180$ s, $\Delta - t = 300$ s

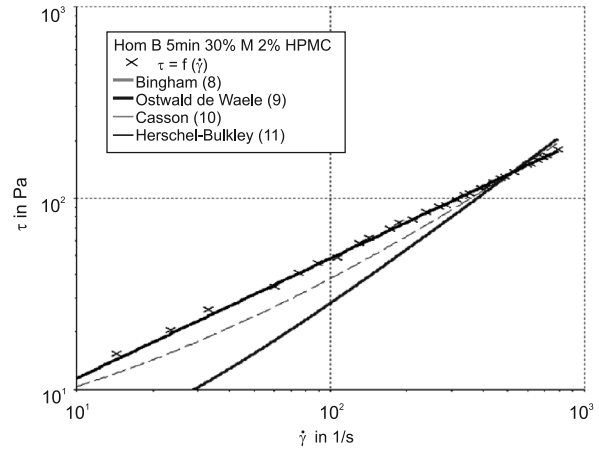

Fig. 4. Flow curves with adapted rheological models, primary blank emulsion, fatty phase Miglyol 812N $\phi_{mas} = 0{,}3$, water phase 70% by mass HPMC water solution 2% by mass, $n = 266{,}6\ s^{-1}$, $t = 300$ s

Rys. 4. Krzywe płynięcia wraz z dopasowanymi modelami reologicznymi, emulsja pierwotna blank, faza tłuszczowa Miglyol 812N $\phi_{mas} = 0{,}3$, faza wodna 70% mas. 2% mas. wodny roztwór HPMC, $n = 266{,}6\ s^{-1}$, $t = 300$ s

Good correlation of experimental with calculation data from models available in literature was shown by the models of Widhab, Ostwald de Waele, Herschel-Bulkley, Casson, lowest correlation was obtained for the model of Bingham. Despite high correlation factors for some models, negative values for certain parameter models were obtained, which is contrary to physical possibility. Sample results of own research were presented in Fig. 4. Parameters of the individual models were presented in Table 2.

Table 2

Rheological models and their parameters for blank primary emulsion: fatty phase Miglyol 812N ϕ_{mas} = 0.3; water phase 70% by mass 2% by mass HPMC water solution, t = 300 s, n = 266.6 s^{-1}

Rheological model	Model parameters	R^2 correlation factor
Bingham	τ_0 = 25,83 η_p = 0,2128	0,9826
Ostwald de Waele	K = 1,697 n = 0,7056	0,9820
Herschel-Bulkley	τ_0 = 16,37 K =0,5697 n = 0,8580	0,9836
Casson	τ_y =8,552 η_p = 0,500 n = 0,1500	0,9840

From the practical point of view, the most important rheological property of primary emulsions is their viscosity.

Obtaining low viscosity values for emulsions with high coagulation speeds stemmed from ordered grid structures. At high coagulation speeds de-aggregation of the grid begins, with ordering of the individual macromolecules aiming at coagulation (Fig. 5). Comparing the viscosity of primary emulsions at the same coagulation speeds it was shown that the lowest viscosity was found in primary emulsions containing a 2% by mass HPMC water solution as the water phase.

The conducted research shows that the viscosity of the primary emulsions is influenced by the content of the fatty phase (Fig. 6). The higher the content of the fatty phase, the higher its viscosity, whereby the value of the viscosity depended on the utilised fatty phase and thickening agent. This is caused by an increase of the number of drops of the fatty phase per volume unit of the primary emulsion. An increase of the drop count of the dispersed phase is accompanied by a decrease of the distances between the drops. As the force of interactions between the drops increases, collision processes become more frequent, which may consequently lead to the creation of agglomerates or floccules.

Similarly as for the flow curves, the obtained results of analyses of viscosity curves were processed via regression of analytical points using the equations shown in Table 1, using the proprietary software of the rheometer. Based on the obtained correlation factor values it was determined that in the examined range of concentrations and emulsification process parameters, the viscosity models describing blank primary emulsions containing as the water phase water hydrocolloid solutions and as the fatty phase Miglyol 812N or sunflower seed oil, castor or olive oil well, were: the Bingham model, the Ostwald de Waele model and the Herschel-Bulkley model.

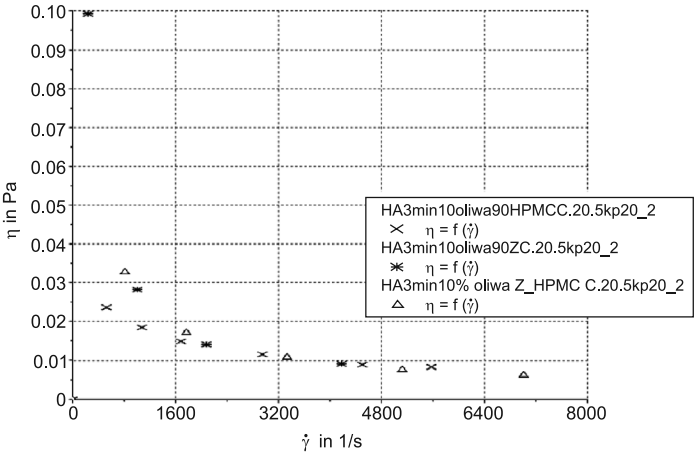

Fig. 5. Viscosity curves of primary blank emulsions, oil phase – olive oil $\phi_{mas} = 0.1$; water phase 90% by mass: Δ – 1.5% by mass *Ż* water solution *Ż*, 2% by mass HPMC water solution (mass ratio *Ż*/HPMC 4:1), *x* – 2% by mass HPMC water solution, ∗ – 1,5% by mass *Ż* water solution, *t* =180 s, *n* = 183.3 s^{-1}

Rys. 5. Przebieg krzywych lepkościowych emulsji pierwotnych blank, faza tłuszczowa olej oliwkowy $\phi_{mas} = 0,1$; faza wodna 90% mas.: Δ – 1,5% mas. wodny roztwór *Ż*, 2% mas. wodny roztwór HPMC (stosunek mas. *Ż*/HPMC 4:1), *x* – 2% mas. wodny roztwór HPMC, ∗ – 1,5% mas. wodny roztwór *Ż*, *t* =180 s, *n* = 183,3 s^{-1}

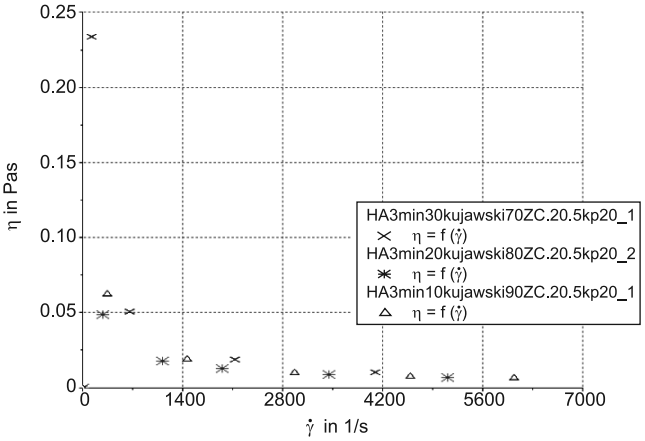

Fig. 6. Viscosity curves for primary blank emulsions, oil phase 'Kujawski' cooking oil: Δ – $\phi_{mas} = 0.1$; ∗ – $\phi_{mas} = 0.2$; *x*– $\phi_{mas} = 0.3$; water phase 1.5% by mass *Ż* water solution, *t* = 180 s, *n* = 183.3 s^{-1}

Rys. 6. Przebieg krzywych lepkościowych emulsji pierwotnych blank, faza tłuszczowa olej Kujawski: Δ – $\phi_{mas} = 0.1$; ∗ – $\phi_{mas} = 0.2$; *x*– $\phi_{mas} = 0.3$; faza wodna 1,5% mas. wodny roztwór *Ż*, *t* = 180 s, *n* = 183,3 s^{-1}

Sample examination results for viscosity curves, verified through viscosity models, were presented in Fig. 7 and Table 3.

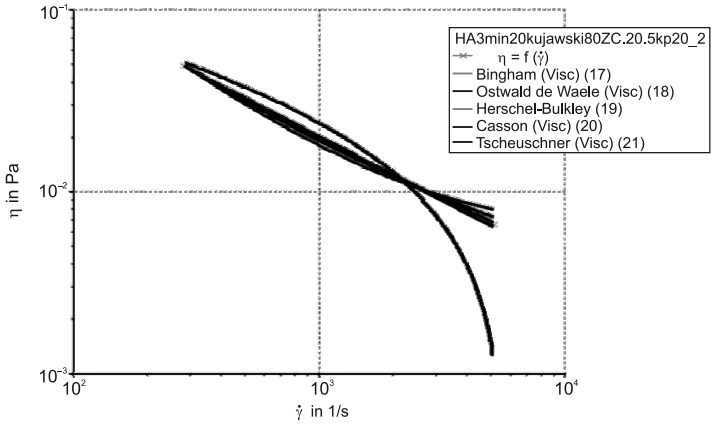

Fig. 7. Viscosity curve for primary blank emulsions with adapted viscosity models, water phase 90% by mass 1.5% *Ż* water solution, oil phase 'Kujawski' cooking oil ϕ_{mas} = 0.2; *t* = 180 s, *n* = 183,3 s^{-1}

Rys. 7. Krzywa lepkościowa emulsji pierwotnej blank wraz z dopasowanymi modelami lepkościowymi. Faza wodna 90% mas. 1,5% wodny roztwór *Ż*, faza tłuszczowa olej Kujawski ϕ_{mas} = 0,2; *t* = 180 s, *n* = 183,3 s^{-1}

Table 3

Parameters of viscosity models (η=f(γ̇)), blank primary emulsion water phase 90% by mass 1,5% *Ż* water solution, fatty phase 'Kujawski' cooking oil ϕ_{mas} = 0.2; *t* = 180 s, *n* = 183.3 s^{-1}

Rheological viscosity model	Model parameters	R^2 Correlation factor
Bingham	τ_y / γ̇ = 0,005573 η_p = 12,50	0,9979
Ostwald de Waele	*K* = 2,619 *n* – 1 = 0,2959	0,9997
Herschel-Bulkley	τ_y / γ̇ = 6,961 *K* = 0,4735 *n* – 1 = 0,4769	0,9999
Casson	τ_y / γ̇ = 9,102 η_p = 0,500 *n* = 0,001852	0,9996
Tscheuschner	η_∞ = –0,03220 τ_y / γ̇ = 0,04892 η_b = 0,5000 γ̇ / $\dot{\gamma}_b$ = 1,000 *n* = 0,3169	0,9750

4. Conclusions

Primary emulsions with potential pharmaceutical applications containing hydrocolloid water solutions as the water phase in the examined concentration range belonged to the non-Newtonian group of liquids shear thinning, showing a yield stress.

The execution of complete rheological research encompassing the determination of flow and viscosity curves for primary emulsions allows the determination of the most favourable formulations for these systems. Assuming their lowest possible viscosity as a criterion of quality for primary emulsions, the rheological analyses supply guidelines enabling the selection of a water phase, and the determination of the type and content of the oily phase to be used for this purpose.

Scientific work financed from national budgetary resources for science in the period 2010–2012 as a supervised research project no. NN 209 415139.

References

[1] Singh S.K., Mishra D.N., Jassal R., Soni P., *Fast disintegrating combination tablets of omeprazole and domperidone*, Asian J. Pharm. Clinic Reserch, 2009, 2, (3), 74.

[2] Abdelbary G., Prinderre P., Eouani C., Joachim J., Reynier J.P., Piccerelle Ph., *The preparation of orally disintegrating tablets using a hydrophilic waxy binder*, Inter. J. Pharm. 2004, 278, 423.

[3] Dobetti L., *Fast-Melting Tablets: Developments and Technologies*, Pharm. Techn. Europe 2000,12,(9), 32.

[4] Ahmed I., Aboul-Einien M., *In vitro evaluation of fast disintegrating lyophilized dry emulsion tablet containing griseofulvin*, Eur. J. Pharm. Sci., 2007, 32, 58.

[5] Takeuchi H., Sasaki H., Niwa T., Hino T., Kawashima Y., Uesugi K., Ozawa H., *Redispersible dry emulsion systems as novel oral dosage form of oily drugs: In vivo studies in Beagle dogs*, Chem. Pharm. Bull., 1991, 39, (12), 3362.

[6] Corveleyn S., Remon J.P., *Formulation and production of rapidly disintegrating tablets by lyophilisation using hydrochlorothiazide as a model drug*, Inter. J. Pharm. 1997, 152, 215.

[7] Corveleyn S., Remon J.P., *Formulation of a lyophilized dry emulsion tablet for the delivery of poorly soluble drugs*, I. J. Pharm., 1998, 166, 65.

[8] Christensen K.L., Pedersen G.P., Kristensen H.G., *Physical stability of redispersible dry emulsion containing amorphous sucrose*, Eur. J. Pharm. Biopharm., 2002, 53, 147.

[9] Vyas S.P., Jain C.P., Kaushnik A., Dixit V.K., *Preparation and characterization of griseofulvin dry emulsion*, Pharmazie 1992, 47, (6), 463.

[10] Dollo G., Le Corre P., Guerin A., Chebanne F., Burgot J.L., Leverge R., *Spray-dried redispersible oil-in-water emulsion to improve oral bioavailability of poorly soluble drugs*, Eur. J. Pharm. Sci., 2003, 19, 273.

[11] Christensen K.L., Pedersen G.P., Kristensen H.G., *Technical optimisation of redispersible dry emulsions*, Inter. J. Pharm. Biopharm., 2001, 212, 195.

[12] Christensen K.L., Pedersen G.P., Kristensen H.G., *Preparation of redispersible dry emulsion by spray drying*, Inter. J. Pharm. Biopharm., 2001, 212, 187.

[13] Lladser M., Medrano C., *The use of supports in the lyophilization of oil-in-water emulsions*, J. Pharm. Pharmacol., 1986, 20, 450.
[14] Richter V.A., Steiger-Trippi K., *Untersuchungen über die zerstäbungstrocknung von emulgierten arzneizubereitungen*, Pharm. Acta Helv., 1961, 36, 322.
[15] Corveleyn S., Remon J.P., *Bioavailability of hydrochlorothiazide: conventional versus freeze-dried tablets*, Int. J. Pharm., 1998, 173, 145.
[16] Farmakopea Polska VII.
[17] Kiekens F., Vermeire A., Samyn N., *Optimisation of electrical conductance measurements for the quantification and prediction of phase separation in o/w-emulsions, containing hydroxypropylmethylcelluloses as emulsifying agents*, Int. J. Pharm., 1997, 146, 239.

TECHNICAL TRANSACTIONS | **CZASOPISMO TECHNICZNE**
CHEMISTRY | CHEMIA
1-Ch/2013

JAROSŁAW WASILEWSKI*, KRYSPIN MIROTA**, TOMASZ KILJAŃSKI***

BIOMECHANICAL ASPECTS OF A ATHEROSCLEROSIS

BIOMECHANICZNE ASPEKTY MIAŻDŻYCY

A b s t r a c t

Pathogenesis of atherosclerosis is a complex multifactorial process of vascular wall injury. It is widely accepted that the local hemodynamic factors, in particular, disturbed flow and low/oscillatory shear stress leads to the plaque development. We present a consistent concept of atherosclerosis aetiology, taking into consideration the four main components contributing in the atheroma formation: geometric, hemodynamic, hemorheological, and mechanical risk factors. Exemplary illustrative flow simulation results for formulated concept have been presented. It assumes the pulsatile non-Newtonian fluid flow and uses realistic coronary artery geometry based on medical imaging and segmentation.

Keywords: *atherosclerosis pathogenesis*, *shear stress*, *computational fluid dynamics*

S t r e s z c z e n i e

Przyczyna miażdżycy jest złożona i wieloczynnikowa. Uważa się, że czynniki hemodynamiczne, a w szczególności przepływy zaburzone, gdzie na ścianę naczynia działają małe i oscylacyjne naprężenia ścinające, odgrywają kluczową rolę w powstawaniu zmian. W artykule przedstawiono spójną koncepcję etiologii choroby, która uwzględnia cztery główne jej komponenty: parametr geometryczny, hemodynamiczny, hemoreologiczny i mechaniczny. Przytoczono przykłady symulacji jako ilustrację do sformułowanej koncepcji. Zakładają one pulsacyjny przepływ płynu nie-Newtonowskiego oraz stosują realistyczny model geometrii tętnicy wieńcowej bazujący na obrazowaniu i segmentacji naczyń.

Słowa kluczowe: *patogeneza miażdżycy*, *naprężenia ścinające*, *numeryczna mechanika płynów*

* Dr Jarosław Wasilewski, Śląski Uniwersytet Medyczny, III Katedra i Kliniczny Oddział Kardiologii w Zabrzu, Śląskie Centrum Chorób Serca w Zabrzu.

** Dr Kryspin Mirota, Katedra Podstaw Budowy Maszyn, Wydział Budowy Maszyn i Informatyki, Akademia Techniczno-Humanistyczna w Bielsku-Białej.

*** Dr hab. inż. Tomasz Kiljański, Katedra Inżynierii Chemicznej, Wydział Inżynierii Procesowej i Ochrony Środowiska, Politechnika Łódzka.

1. Introduction

In developed countries every fifth death is caused by coronary artery disease (CAD). Despite tremendous progress in cardiology, biology and basic sciences, atherosclerosis remains an unsolved health and social problem. Atherosclerosis is diffused disease, with predominate location restricted mainly to the aorta, proximal segments of the arteries which originate from the aorta, and both saphenous vein and radial artery aorto-coronary by-passes. The atherosclerotic process is uncommon or almost never occurs in the internal mammary arteries (IMA) even when they are used as conduit for a coronary artery by-pass graft [1]. 10% of remaining IMA graft failure, so-called "string phenomenon" (the narrowing of the whole length of the artery), is attributed to competitive flow in the native artery, and low wall shear stress in the anastomosis [2, 3].

State of the art, routine diagnostic methods are not capable of determining the course of the atherosclerotic process and prediction of when (if ever) acute coronary syndromes will occur, or which lesions will progress into vulnerable plaque or significant hemodynamic stenosis (stable angina). In each individual person, it requires many years to follow the course of the disease. We find about coronary artery atherosclerosis when plaque ruptures or when the plaque restricts the coronary flow during exercise (stable CAD). Plaque visualization at the coronarography allows determination of the status quo only and does not indicate both, when the disease emerged or whether lesion will cause future cardiac events. Therefore, angiography presents the plaques distribution, but does not answer key questions about both the history of the disease and the prognosis. Computational Fluid Dynamics (CFD) seems to be a promising tool, which will efficiently reduce limitations regarding atherosclerosis progression due to the possibility of computer simulation of atherosclerotic plaque growth [4].

2. The biomechanical forces acting on the vessels and atherosclerosis

The vascular wall is exposed to two biomechanical forces. The first one is tensile stress. It is directed perpendicular to the wall and affects all layers of the artery, which causes smooth muscle cell hypertrophy. The second force, much more essential in atherosclerosis, is tangential to the endothelium (endothelial shear stress, ESS). ESS is related to blood viscosity, while tensile stress is relates to arterial blood pressure. ESS depends on velocity gradient (shear rate) and blood viscosity.

On the basis of clinical studies and follow-up coronary angiography, it has been proven that plaque progression relates particularly to those lesions that are exposed to low and oscillatory shear stresses, which clearly implies that biomechanical forces have significant impact on atheroma formation. For example Gibson et al [5] conducted a study to assess the rate of change in coronary arterial diameter in patients over three years. They found a significant correlation between the low shear stress and an increased rate of atherosclerosis progression.

After aorto-coronary by-pass graft surgery, in the native artery segment that had been by-passed the progression of atherosclerosis is rapid. It is caused by the emergence

of reverse flows and oscillatory shear stresses in the by-passed artery [1]. Experimental data confirms that it is possible to reduce the formation of atherosclerotic lesions by lowering the tendency to formation of secondary flows. In animals, adding drag reducing polymers to the blood inhibits the development of atherosclerotic plaques in the mechanism of flow stabilization [6, 7]. Those results support the notion that hemodymamics play the important role in atherogenesis.

The pathogenesis of atherosclerosis is a complex multifactorial process of vascular wall injury. There are four main components involved in the atheroma formation: geometric, hemodynamic, hemorheological, and mechanical [8]. Table 1 presents the importance and contribution of each.

Table 1

The main components involved in the atheroma formation

Risk components	The role in atherosclerotic process
GEOMETRIC	Obtuse angle of bifurcation, unequal cross-sectional area of vessels after bifurcation. Periodic changes of coronary artery curvature due to heart deformation in each cardiac cycle.
HEMODYNAMIC	High flow velocity and centrifugal effect of the flow leads to skewness of the velocity profile, flow separation and oscillatory flow. Formation of disturbed and secondary flows generates regions of low and oscillatory endothelial shear stress.
HEMORHEOLOGICAL	In areas of disturbed flows, non-Newtonian properties including shear-thinning and yield-stress, prolong residence time of blood borne atherogenic particles (LDL, macrophage) and facilitates their penetration to the arterial wall.
MECHANICAL	In the aging process, systemic factors i.e. hypertension, renal insufficiency and diabetes, change the stiffness of arterial wall, and leads to reduced artery compliance, with resulting increase in systolic pressure and decrease in diastolic pressure and hence facilitate generation of the secondary flows.

Despite the fact that the classic risk factors are systemic in nature, arterial lesions are restricted to the points which are exposed on disturbed flow and low and oscillatory ESS. The evidence that blood flow plays a key role in atheroma formation is not at random plaque distribution. Preferred location are lateral walls of the bifurcations, areas near to the side branches and branch ostia (Fig. 1) [9, 10].

Atherosclerotic plaques, particularly at the early stage, are eccentric, and in segments where vessels have no side branches, they emerge from the inner curvature (Fig. 2). That is why, in coronary arteries lesions usually emerge from the epicardial surface (inner curvature). Such plaques localizations indicate their relationship with flow conditions, which are largely determined by complex arterial geometry.

From fundamental mechanics, both the fluid dynamics and the shear stress distribution are dependent on the vessel geometry (Fig. 3).

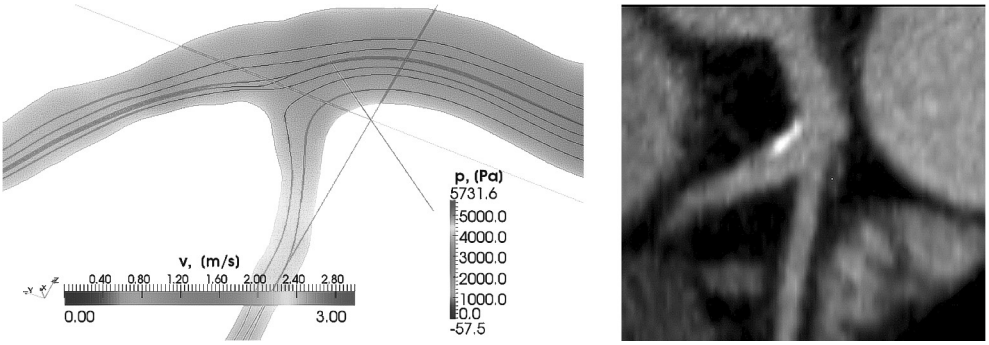

Fig. 1. Plaque formation typically develops at the lateral walls of the bifurcation, as blood tends to separate and form regions of oscillating ESS. Left panel. Calcified plaque at left anterior descending artery (lateral wall). Right panel, schematic representation of calculated stream lines in secondary flow region at the artery bifurcation

Rys. 1. Blaszki miażdżycowe typowo powstają na bocznych ścianach podziałów naczyniowy, czyli miejscach w których dochodzi do oderwania warstwy przyściennej, gdzie ściana naczynia narażona jest na oscylacyjne naprężenia ścinające. Panel lewy. Uwapniona blaszka miażdżycowa przy ścianie bocznej gałęzi przedniej zstępującej. Panel prawy, schematyczne przedstawienie wyznaczonych linii prądu, regionie powstawania przepływu wtórnego w podziale naczyniowym

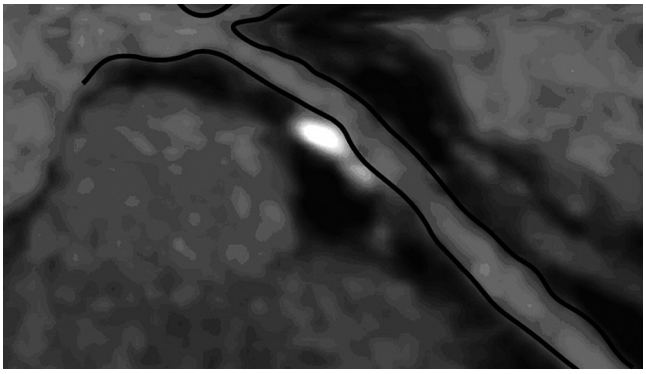

Fig. 2. Left anterior descending artery (imaging with multislice computed tomography). Partially calcified plaque located on epicardial surface of the coronary artery (inner curvature). Human coronary arteries enlarge in relation to plaque area and that functionally important lumen stenosis may be delayed

Rys. 2. Gałąź przednia zstępująca (obrazowanie za pomocą wielowarstwowej tomografii komputerowej) częściowo uwapniona blaszka miażdżycowa na powierzchni nasierdziowej (krzywizna wewnętrzna). Na wczesnym etapie, formowanie się blaszek odbywa się w błonie wewnętrznej, bez zawężenia światła naczynia

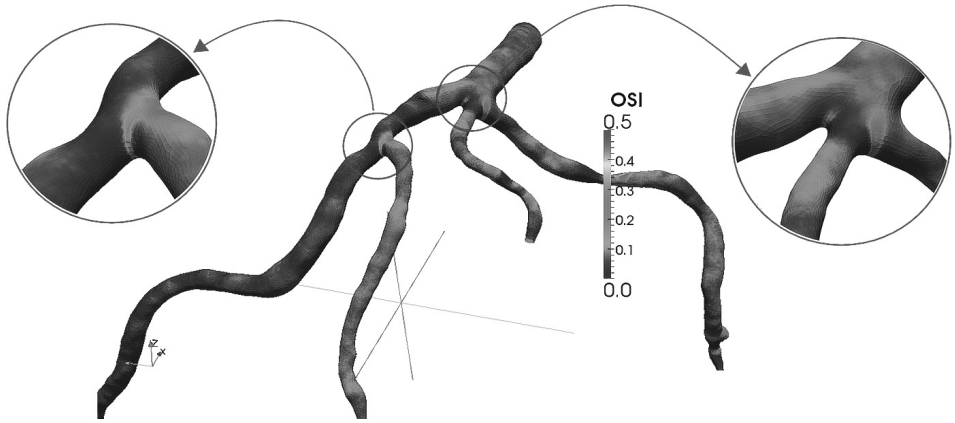

Fig. 3. The numerical simulation (CFD) of oscillatory shear stress distribution in the left coronary artery. The risk points of plaque formation are distributed in segment 6 of the left descending artery, vicinity of the diagonal branch and in the middle segment of circumflex artery – the regions of highest value of the oscillatory shear stress index value, OSI

Rys. 3. Rozkład wskaźnika oscylacyjnego naprężenia ścinającego w anatomicznej geometrii lewej tętnicy wieńcowej zamodelowany za pomocą numerycznej mechaniki płynów (CFD). Miejsca ryzyka powstania zmian miażdżycowych znajdują się w segmencie 6 gałęzi przedniej zstępującej, ostium gałęzi diagonalnej pierwszej oraz w środkowym odcinku gałęzi okalającej – miejscach występowania największych wartości oscylacji przepływu, OS

3. Mechanotransduction

The science that deals with forces associated with biological response of, for example, vessel wall to the flow is mechanobiology. The phenomenon of endothelium sensing ESS and transferring it to biochemical signals is called mechanotransduction [14]. The precise molecular mechanisms remain unknown however, it is believed that mechanoreceptors of cell membrane are involved. Mechanical signals from the flow are being transformed into biochemical signals with the use of transcription factors, like Nuclear Factor kappa B (NF-kB) and Activator Protein 1 (AP-1). It is estimated that hundreds of gene activity depends on the flow velocity profile and ESS distribution [15–17]. Those genes are called shear regulated.

Laminar flow with axially symmetric, fully developed flow velocity profile, activates atheroprotective genes and increases expression of atheroprotective particles. Therefore high ESS is a critical factor in maintaining normal endothelial function. Physiological shear stress stimulates the vascular endothelium to produce mediators of vasodilatation (nitric oxide, prostacyclin, endothelial hyperpolarizing factor) exerting a critical impact in maintaining normal endothelial structure and function. The physiological ESS can be characterized as: anti-inflammatory, antithrombotic, antiproliferative and antioxidant [18–20].

Low and oscillatory ESS tiger unfavorable gene expression and biomechanical response. Reorganisation of endothelial cells and disruption of intercellular connections at the area of low/oscillatory shear stress, facilitates the transport of particles including low density lipoproteins, monocytes, fibrin and other blood-borne atherogenic particles into the intima. It is believed that mechanoreceptors of cell membrane are involved in this process (membrane integrins, ion channels, receptors for tyrosine kinase, protein G, caveolae). Low and oscillatory ESS leads to endothelial dysfunction, which manifests i.e. with increased synthesis of oxygen free radicals, prothrombotic factors, expression of adhesion proteins and chemotactic factors. Disturbed flows facilitate macrophages, leukocytes, and platelets recruitment to the vessel surface. These, in turn, get into intima and release cytokines and growth factors. Increased permeability of the endothelial barrier and reduced thickness of the glycocalix allows infiltration of lipids, fibrinogen, fibrin and other atherogenic particles into the intima. Uncontrolled uptake of oxidized lipids by macrophages leads to formation of foam cells, which become an integral part of plaque. An increase in production of platelet-derived and endothelium-derived growth factors, stimulates smooth muscle cell migration from media to intima. As a response to numerous cytokines and oxidative stress, smooth muscle cells of the vessel wall transform into osteoblasts participating in the plaque calcification process.

In experimental studies low ESS at inner curvatures are being related to the formation of the vulnerable plaque with thin fibrous cap, rich in cholesterol, but poor in smooth muscle cells [21]. This phenomenon is explained by increased inflammation caused by low ESS compared to oscillatory shear stresses [21]. This means that type of shear stress has an impact on plaque metabolism and its susceptibility to rupture. Hence flow modeling methods in vitro may be extremely useful in studies on the pathogenesis and course of the atherosclerotic process [22].

Multislice Computed Tomography (MSCT) evaluation of coronary artery anatomy, and developments in rheometrics, allows us to apply the more robust CDF technology in cardiology applications. It is assumed that computed simulation of flow conditions should take into account viscoelastic properties of arteries, the variable artery geometry, pulsatile nature of flow and blood non-Newtonian properties. The significant progress of CFD technology and improvement in methods for arteries segmentation based on MSCT dataset mean that modeling of the artery blood flow can be the new research tool in cardiology [23, 24].

The aim of using CFD in cardiology is to create a computational model of the cardiovascular system in order to improve the quality of predicting the progression of atherosclerosis (answer on key question plaque stability, progression and hemodynamic significance).

4. Graft failure

Patients with symptomatic CAD require revascularisation, including implantation of coronary artery by-pass grafts. Over the years, since by-pass grafting there is increasing problems of grafts patency. The key risk factors of graft anastomosis patency is too large width of the by-pass graft and type of anastomosis, which determined shear stress distribution.

Clinical practice shows that graft failure is caused not only by plaque formation at the site of anastomosis but very often by atherosclerotic lesions forming along the course of coronary by-pass graft. There are no differences in failure rate between saphenous vein and radial artery grafts [25, 26].

This phenomenon may be related to the appearance of atherogenic flow (secondary disturbed flows) in the aorto-coronary by-pass similar to that which occurs in the native coronary artery originating from sinus of Valsalva. Unlike by-passes outgoing from the aorta, the IMA conduits are resistant to atherosclerosis and are rarely the subjects of closure [27].

In comparison to aorto-coronary by-pass, flow velocity profile in IMA is more stable. It can be assumed that lack of secondary flows and high shear stress are the reason why IMA by-passes are resistant for atherosclerosis [28].

Within aorto-coronary vein by-passes the flow velocity profile is far different. In protodiastolic phase, blood velocity reaches maximum velocity, while at its ending it suddenly slows down, which contributes significantly to forming atherogenic secondary flows in the late diastole.

It may be assumed that venous by-pass implanted for example to subclavian artery instead of aorta, will reveal more stable flow, and it can prevent atheroma formation [1] This type of vascular conduits may be an alternative for by-passes implanted to the aorta, however, there is no experimental or CFD research data revealing benefits of such surgical technique. Coronary by-passes imaging with MSCT and CFD technology may significantly contribute to the understanding of, why aorto-coronary by-passes are atherosclerotic-prone and IMA by-passes are atherosclerotic-resistant.

5. Hemorheology

Hemorheology plays an important role in atherosclerosis. Rheology research allows for determining an appropriate rheological model of blood for its use in computer simulation. Non-Newtonian properties of blood become significant in the zones of disturbed flows, which should be considered in the CFD simulations [29, 30].

Blood rheology has been more difficult to accurately study than other risk factors for cardiovascular disease, explaining why it may be an overlooked factor in our understanding of cardiovascular disease. Rheology of blood depends largely on fibrinogen concentration and hematocrit [31].

The increase in blood viscosity is not relevant at laminar flow (high shear stress), but at risk vascular points of disturbed and oscillatory flow, rheological properties of blood (in particular shear-thinning and yield-stress) hemorheological abnormalities increases the blood residence time near by the vessel wall. Therefore increases in fibrinogen concentration favor the retention and penetration of blood borne atherogenic particles into arterial wall. This phenomenon plays an important role in vascular biology and is an important mechanism in the atheroma formation. Measurement of fibrinogen concentration, hematocrit value and blood viscosity as a function of shear rate must be taken into account when modeling the flow.

A number of researchers measured blood viscosity in patients with CAD, diabetes and myocardial infarction [32–36]. They found that the viscosity of whole blood might be associated with CAD. The hemorheology is now entering a new phase of acceptance with the development of new instruments which, unlike conventional rheometers, easily and accurately determine whole blood viscosity as a function of shear rate, as well as red blood cells deformation and aggregation by laser light scattering technique [37].

6. Conclusions

The initiation and progression of atherosclerosis are determined by a complex interplay between the main risk components: geometric, hemodynamic, hemorheological, and mechanical. The participation of each of them has an impact on plaque progression, stability or vulnerability. CFD is a well-established tool for the simulation of flow fields existing in real complex vascular geometries. The high image quality (MSCT), excellent contrast opacification of the coronary arteries makes CFD as excellent tool for the ESS noninvasive evaluation. The growing understanding of the biomechanical processes responsible for atherosclerosis might allow CFD to aid early identification of a high-risk coronary plaque and thereby provide a rationale for innovative diagnostic and/or therapeutic strategies for the management of coronary patients and prevention of acute coronary syndromes, and planning revascularisation procedures (stent implementation or coronary artery by-pass grafting).

References

[1] Wasilewski J., Kiljański T., Głowacki J., Miszalski-Jamka K., *Znaczenie zaburzeń przepływu w utrzymaniu drożności pomostów wieńcowych*, Kardiochirurgia i Torakochirurgia Polska, 2011, 8:117-120.

[2] Kolozsvari R., Galajda Z., Ungvari T., Szabo G., Racz I., Szerafin T., Herzfeld I., Edes I., Peterffy A., Koszegi Z., *Various clinical scenarios leading to development of the string sign of the internal thoracic artery after coronary bypass surgery: the role of competitive flow, a case series*, J Cardiothorac Surg, 2012, 7:12.

[3] Madaric J., Mistrik A., Riecansky I., Vulev I., Pacak J., Verhamme K., de Bruyne B., Fridrich V., Bartunek J.I., *Left internal mammary artery bypass dysfunction after revascularization of moderately narrowed coronary lesions. Colour-duplex ultrasound versus angiography study*, Eur J Echocardiogr, 2008, 9:273-277.

[4] Liu B., Tang D., *Computer simulations of atherosclerotic plaque growth in coronary arteries*, Mol Cell Biomech, 2010, 7:193-202.

[5] Gibson C.M., Diaz L., Kandarpa K., Sacks F.M., Pasternak R.C., Sandor T., Feldman C., Stone P.H., *Relation of vessel wall shear stress to atherosclerosis progression in human coronary arteries*, Arteriosclerosis and Thrombosis, 1993, 13:310-315.

[6] Sawchuk A.P., Unthank J.L., Dalsing M.C., *Drag reducing polymers may decrease atherosclerosis by increasing shear in areas normally exposed to low shear stress*, J Vasc Surg, 1999, 30:761-764.

[7] Ertepinar H., Süzen B., Ozoran A., Ozoran Y., Ceylan S., Yeginoglu G., Uremek G., *Effects of drag reducing polymer on atherosclerosis*, Biorheology, 1999, 27:631-644.

[8] Wasilewski J., Kiljański T., *Biomechaniczna przyczyna miażdżycy*, Wydawnictwo Politechniki Łódzkiej, Łódź 2011.

[9] Wasilewski J., Kiljański T., Głowacki J., *Geometryczny czynnik ryzyka i zaburzenia przepływu w procesie miażdżycowym*, Kardiochirurgia i Torakochirurgia Polska, 2010, 7:325-330.

[10] Wasilewski J., Miszalski-Jamka K., Głowacki J., *Topografia zmian miażdżycowych w badaniu angio-TK tętnic wieńcowych*, Kardiochirurgia i Torakochirurgia Polska, 2010, 7:458-461.

[11] Caro C.G., Fitz-Gerald J.M., Schroter R.C., *Atheroma and arterial wall shear: observation, correlation and proposal of a shear dependent mass transfer mechanism for atherogenesis*, Proc Ro. Soc, London B, 1971, 177:9-159.

[12] Gnasso A., Carallo C., Irace C., Spagnuolo V., de Novara G., Mattioli P.L., Pujia A., *Association between intima-media thickness and wall shear stress in common carotid arteries in healthy male subjects*, Circulation, 1996, 94:3257-3262.

[13] Jiang Y., Kohara K., Hiwada K., *Low wall shear stress contributes to atherosclerosis of the carotid artery in hypertensive patients*, Hypertens Res, 1999, 2:203-207.

[14] Wasilewski J., Kiljański T., Miszalski-Jamka K., *Rola naprężeń ścinających i mechanotransdukcji w procesie miażdżycowym*, Kardiologia Polska, 2011, 69:717-720.

[15] García-Cardeña G., Comander J.I., Blackman B.R., Anderson K.R., Gimbrone M.A., *Mechanosensitive endothelial gene expression profiles: scripts for the role of hemodynamics in atherogenesis?*, Ann N Y Acad Sci, 2001, 947:1-6.

[16] Cheng C., de Crom R., van Haperen R., Helderman F., Mousavi Gourabi B., van Damme L.C., Kirschbaum S.W., Slager C.J., van der Steen A.F., Krams R., *The role of shear stress in atherosclerosis: Action through gene expression and inflammation?*, Cell Biochem Biophys, 2004;41:279-294

[17] Wasserman S.M., Topper J.N., *Adaptation of the endothelium to fluid flow: in vitro analyses of gene expression and in vivo implications*, Vasc Med, 2004, 9, 35-45.

[18] Resnick N., Yahav H., Shay-Salit A., Shushy M., Schubert S., Zilberman L.C., Wofovitz E., *Fluid shear stress and the vascular endothelium: for better and for worse*, Prog Biophys Mol Biol, 2003, 81:177-199.

[19] Won D., Zhu S.N., Chen M., Teichert A.M., Fish J.E., Matouk C.C., Bonert M., Ojha M., Marsden P.A., Cybulsky M.I., *Relative reduction of endothelial nitric-oxide synthase expression and transcription in atherosclerosis-prone regions of the mouse aorta and in an in vitro model of disturbed flow*, Am J Pathol, 2007, 171:1691-1704.

[20] Chien S., *Role of shear stress direction in endothelial mechanotransduction*, Mol Cell Biomech, 2008, 5:1-8.

[21] Cheng C., Tempel D., van Haperen R., van der Baan A., Grosveld F., Daemen M.J., Krams R., de Crom R., *Atherosclerotic lesion size and vulnerability are determined by patterns of fluid shear stress*, Circulation, 2006,113:2744-2745

[22] Malek A.M, Alper S.L., Izumo S., *Hemodynamic shear stress and its role in atherosclerosis*, JAMA, 1999, 282:2035-2042.

[23] Rikhtegar F., Knight J.A., Olgac U., Saur S.C., Poulikakos D., Marshall W. Jr, Cattin P.C., Alkadhi H., Kurtcuoglu V., *Choosing the optimal wall shear parameter for the prediction of plaque location – A patient-specific computational study in human left coronary arteries*, Atherosclerosis, 2012, 221:432-437.

[24] Frauenfelder T., Boutsianis E., Schertler T., Husmann L., Leschka S., Poulikakos D., Marincek B., Alkadhi H., *In-vivo flow simulation in coronary arteries based on computed tomography datasets: feasibility and initial results*, Eur Radiol, 2007, 17:1291-1300.

[25] Crusco F., Antoniella A., Papa V., Menzano R., Di Lazzaro D., Di Manici G., Ragni T., Giovagnoni A., *Midterm follow-up of patients receiving radial artery as coronary artery bypass grafts using 16-detector-row CT coronary angiography*, Radiol Med (Torino), 2007, 112:538-549.

[26] Khot U.N., Friedman D.T., Pettersson G., Smedira N.G., Li J., Ellis S.G., *Radial artery bypass grafts have an increased occurrence of angiographically severe stenosis and occlusion compared with left internal mammary arteries and saphenous vein grafts*, Circulation, 2004, 109:2086-2091.

[27] Hayward P.A., Buxton B.F., *Contemporary coronary graft patency: 5-year observational data from a randomized trial of conduits*, Ann Thorac Surg, 2007, 84:795-799.

[28] Fujiwara T., Kajiya F., Kanazawa S., Matsuoka S., Wada Y., Hiramatsu O., Kagiyama M., Ogasawara Y., Tsujioka K., Katsumura T., *Comparison of blood flow velocity waveforms in different coronary artery bypass grafts. Sequential saphenous vein grafts and internal mammary artery grafts, Circulation*, 1988, 78:1210-1217.

[29] Mejia J., Mongrain R., Bertrand O.F., *Accurate prediction of wall shear stress in a stented artery: newtonian versus non-newtonian models*, J Biomech Eng, 2011, 133:074501.

[30] Liu B., Tang D., *Influence of non-Newtonian properties of blood on the wall shear stress in human atherosclerotic right coronary arteries*, Mol Cell Biomech, 2011, 8:73-90.

[31] Wasilewski J., Poloński L., *Znaczenie fibrynogenu i właściwości reologicznych krwi w miażdżycy i chorobie wieńcowej*, Choroby Serca i Naczyń, 2010, 7:62-71.

[32] Jax T.W., Peters AJ., Plehn G., Schoebel F.C., *Hemostatic risk factors in patients with coronary artery disease and type 2 diabetes – a two year follow-up of 243 patients*, Cardiovasc Diabetol, 2009, 7,8:48.

[33] Cecchi E., Liotta A.A., Gori A.M, Valente S., Giglioli C., Lazzer I.C., Sofi F., Gensini G.F., Abbate R., Mannini L., *Relationship between blood viscosity and infarct size in patients with ST-segment elevation myocardial infarction undergoing primary percutaneous coronary intervention*, Int J Cardiol, 2009, 134:189-194.

[34] Junker R., Heinrich J., Ulbrich H., Schulte H., Schönfeld R., Köhler E., Assmann G., *Relationship between plasma viscosity and the severity of coronary heart disease*, Arterioscler Thromb Vasc Biol, 1998, 18:870-875.

[35] Wasilewski J., Turczyński B., Słowińska L., Kowalik V., Osadnik T., Poloński L., *Haemorheological factors and myocardial reperfusion in patients with ST-elevation myocardial infarction undergoing primary coronary intervention*, Kardiol Pol, 2007, 65:778-785.

[36] Wasilewski J., Podolecki T., Turczyński B., Kowalik V., Głowacki J., *The relationship between plasma viscosity and the degree of coronary artery calcification in the multislice computed tomography*, MEDIMOND-Monduzzi Editore International Proceedings Division, 2010.

CONTENTS

TREŚĆ